Characterization of a murine TCR specific for HLA-A2.1 restricted non-mutated MDM2 peptide for cancer immunotherapy

Dissertation

for the award of the degree

“Doctor rerum naturalium” (Dr. rer. nat.)

in Chemistry

Faculty of Chemistry, Pharmaceutical Sciences and Geosciences

of the Johannes Gutenberg-University Mainz

Eva Amann

Born in Würzburg

Mainz, December 2017

Dean:

1st correspondent:

2nd correspondent:

Day of oral exam: February 27th, 2018

Financial support

Affidavit

Summary

Adoptive cell therapies are promising immunotherapeutic approaches in the field of cancer treatment. To target tumor-associated/specific antigens autologous T cells redirected with T cell receptor (TCR) or chimeric antigen receptor (CAR) were used for adoptive T cell transfer (ACT). The tumor-associated antigen (TAA)-specific TCR described here is a murine TCR recognizing the human protein murine double minute 2 (MDM2) in a CD8-restricted and HLA-A2.1-dependent manner. This TCR has been generated by immunizing $A2k^b$ transgenic mice with the MDM2(81-88) peptide, a naturally processed non-mutated peptide which allows the use of MDM2(81-88)-specific TCR for the treatment of multiple cancer types overexpressing MDM2, including melanoma, glioblastoma, liposarcoma or multiple myeloma (MM).

First we modified the sequence encoding for the wild type (wt) MDM2-specific TCR to enhance the TCR expression levels and to prevent mispairing of natural and transgenic TCR chains thus increasing the safety and the efficacy of the TCR. The whole TCR sequence was codon-optimized, an additional disulfide-bond was introduced between the constant domains of TCR α- and β-chains and the TCR α- and β-encoding genes were cloned in a 2A self-cleaving peptide-based bicistronic retroviral expression vector. We could show that after optimization, TCR expression was enhanced while the affinity of the TCR remained unchanged compared to the wt TCR. This optimized TCR was recognizing and specifically lysing various MM and melanoma cell lines *in vitro*. First *in vivo* studies using a MM cell line in a xenograft mouse model however showed no antitumor response most likely due to tumor antigens` expression modulation and up-regulation of inhibitory molecules on the tumor and tumor-infiltrating T cells. By targeting the tumor with a second TAA-specific TCR and immune-checkpoint inhibitors (ICIs) using nivolumab or pembrolizumab the overall survival of mice could be prolonged.

In this thesis we demonstrated the anti-cancer efficacy of ACT using dual TAA-specific TCR approach to overcome tumor-antigen escape in combination with ICI which resulted in prolonged overall survival in preclinical mouse studies. To achieve a complete response the combination with additional monoclonal antibodies or ICIs might be necessary. Targeting MDM2 in a TCR-based immunotherapy is a potentially new approach for the treatment of MM and melanoma.

Zusammenfassung

Adoptive Zelltherapien stellen im Bereich der Krebstherapie vielversprechende immuntherapeutische Ansätze dar. Für den adoptiven T-Zell-Transfer (AZT) wurden autologe T-Zellen verwendet, welche mit T-Zellrezeptoren (TZR) oder chimären Antigenrezeptoren (CAR) modifiziert wurden, um gezielt Tumor-assoziierte und Tumor-spezifische Antigene zu erkennen. Der hier beschriebene TZR, spezifisch für ein Tumor-assoziiertes Antigen (TAA), ist ein muriner CD8-restringierter und HLA-A2.1-abhängiger TZR, welcher das humane Protein murine double minute 2 (MDM2) erkennt. Dieser TZR wurde durch Immunisierung von $A2k^b$-transgenen Mäusen mit dem MDM2(81-88)-Peptid generiert. Dieses Peptid ist ein natürlich prozessiertes, nicht mutiertes Peptid, so dass es sich für die Behandlung vieler Tumorentitäten eignet, welche MDM2 überexprimieren, wie zum Beispiel Melanom, Glioblastom, Liposarkom oder multiples Myelom (MM).

Zuerst haben wir die für den MDM2-spezifischen Wildtyp (wt) TZR codierende Sequenz modifiziert, um die TZR-Expression zu erhöhen und um eine Fehlpaarung von endogenen und transgenen TZR-Ketten zu verhindern und um dadurch Sicherheit und Effizienz des TZR zu erhöhen. Die vollständige Sequenz wurde Codon-optimiert, eine zusätzliche Disulfidbrücke zwischen den konstanten Regionen der α- und β-Ketten des TZR wurde eingebracht und die für die α- und β-Ketten codierenden Bereiche wurden in einen bicistronischen retroviralen Vektor kloniert, welcher ein selbstschneidendes 2A Peptide enthielt. Wir konnten zeigen, dass nach Optimierung die TZR-Expression erhöht war, verglichen mit dem wt TZR, wobei die Affinität des TZR unverändert blieb. Der optimierte TZR erkannte und lysierte spezifisch verschiede MM und Melanom Zelllinien *in vitro*. Erste *in vivo* Versuche mit einer MM Zelllinie in einem xenograft Mausmodel hingegen zeigten keine antitumorale Antwort, was vermutlich einer veränderten Antigenexpression und einer erhöhten Expression von inhibitorischen Strukturen auf T-Zellen und Tumorzellen geschuldet war. Das Gesamtüberleben der Mäuse konnte durch einen zweiten TAA-spezifischen TZR und durch die Verwendung der Immun-Checkpoint-Inhibitoren (ICIs) Nivolumab oder Pembrolizumab verlängert werden.

In dieser Arbeit haben wir die Antitumor-Effizienz des AZT Verfahrens mittels dualer TAA-spezifischer TZR demonstriert und konnten, in Kombination mit ICIs, das Gesamtüberleben in präklinischen Mausmodellen verlängern. Um eine komplette Remission zu erreichen, wären die Kombination von AZT mit zusätzlichen monoklonalen Antikörpern oder ICIs notwendig. Die auf TZR-basierende und gegen MDM2 gerichtete Immuntherapie ist ein neues potenzielles Verfahren für die Behandlung des MM oder Melanoms.

Table of Content

List of Figures

List of Tables

Abbreviations

^{51}Cr	Radioactive Sodium Chromate 51 isotope ($Na_2{}^{51}CrO_4$)
A2.1	HLA-A2.1
ACT	Adoptive cell transfer
Amp	Ampicillin
APC	Antigen presenting cell
APC	Allophycocyanine
Aqua dest.	Bidistilled water
BM	Bone marrow
bp	Base pair
BSA	Bovine serum albumin
CD	Cluster of differentiation
CDR	Complementary-determining region
CTL	Cytotoxic T lymphocyte
CTLA-4	Cytotoxic T lymphocyte antigen 4
dc	Double chain
DC	Dendritic cell
DMEM	Dulbecco`s Modified Eagle Medium
DMSO	Dimethyl sulfoxide
EDTA	Ethylenediaminetetraacetic acid
FACS	Fluorescence-activated cell sorting
FCS	Fetal calf serum

FITC	Fluorescein isothiocyanate
h	Hour
HEPES	4-(2-hydroxyethyl)-1-piperazineethanesulfonic acid
HLA	Human leucocyte antigen
ICI	Immune-checkpoint inhibitor
i.p.	Intraperitoneal
i.v.	Intravenous
IFN	Interferon
IL	Interleukin
IRES	Internal ribosomal entry site
IU	International unit
kb	Kilo base
kDa	Kilo Dalton
LB	Luria-Bertani
mAb	Monoclonal antibody
MACS	Magnetic-activated cell sorting
MDM2	Murine double minute 2 protein
MHC	Major histocompatibility complex
min	Minute
MM	Multiple myeloma
NaCl	Sodium chloride
Neo	Neomycin

NFM	Nonfat milk
Nod/scid	Nonobese diabetic/severe combined immunodeficiency
NSG	Nod/scid IL-2 receptor gamma chain knockout
OD	Optical density
O/N	Overnight
Opt.	Optimized
PBMC	Peripheral blood mononuclear cell
PBS	Phosphate-buffered saline
PD-1	Programmed cell death protein 1
PD-L1/2	Programmed cell death-ligand 1/2
PE	Phycoerythrin
PFA	Paraformaldehyde
Puro	Puromycin
PVDF	Polyvinylidene difluoride
RPMI 1640	Roswell Park Memorial Institute 1640 medium
RT	Room temperature
s.c.	Subcutaneous
Sc	Single chain
SDS	Sodium dodecyl sulfate
SDS-PAGE	SDS-polyacrylamide gel electrophoresis
sec	Second
SN	Supernatant

SOB-medium	Super optimal broth-medium
TAA	Tumor-associated antigen
TAE buffer	Tris-acetate EDTA buffer
TALEN	Transcription activator-like effector nuclease
TBS	Tris-buffered saline
TCR	T cell receptor
TEMED	N,N,N`,N´-Tetramethylethylenediamine
TfB I/II buffer	Transformation buffer I/II
Tg	Transgenic
TIL	Tumor infiltrating lymphocyte
TNF	Tumor necrosis factor
U	Unit
Wt	wild type

1 Introduction

1.1 Cancer immunotherapy

The history of immunotherapy started already in 1891 when William Coley treated the first time soft tissue sarcoma patients with *Streptococcus pyogenes* to induce erysipelas which was reported to lead to remission in cancer patients. Since it was difficult to cure patients from the streptococcal disease, he went on injecting a mixture of heat-killed *Streptococcus pyogenes* and heat-killed *Bacillus prodigious* and achieved a long-term cure for his patients [1]. Because it was dangerous to treat patients with pathogenic bacteria, radiotherapy combined with surgery was the standard therapy approach for cancer treatment in the beginning of the 20th century. In 1976 Morales at al. published the successful treatment of patients with bladder tumor with a tuberculosis vaccine called Bacillus Calmette-Guerin (BCG) [2]. BCG-therapy is still used as intravesical immunotherapy in patients with early-stage bladder cancer [3]. The same year, interleukin-2 (IL-2) was found to be a crucial T lymphocyte growth factor [4] and since the 1990s IL-2 has been approved by the Food and and Drug Administration (FDA) in the United States of America (USA) for the treatment of metastatic renal cancer [5] and treatment for metastatic melanoma [6].

Monoclonal antibodies (mAbs) have achieved tremendous success in cancer therapy in the last few years [7]. These molecules were first generated in the 1970s by Köhler and Milstein by fusing lymphocytes and myeloma cell lines resulting in hybridomas secreting mAbs of a predefined specificity [8]. Rituximab, an anti-CD20 antibody, was one of the first mAbs used in therapy for the treatment of B cell lymphomas and autoimmune diseases [9],[10]. Antibody-drug conjugates or bispecific mAbs, designed to attach cancer cells and attract T cells have emerged as novel immunotherapeutic treatment approaches for leukemia and solid tumors. A well characterized BiTE (Bispecific T cell Engager) molecule is blinatumomab, a drug approved for the treatment of ALL [11].

Vaccination is an immunotherapeutic approach for induction of an immune response for cancer treatment. The first cancer-related antigen which induced a response of cytotoxic T cells was MZ2-E and was identified in melanoma patients. This antigen showed no similarities to known sequences and was not expressed in normal tissue [12]. However the breakthrough of cancer vaccines as cancer therapy was later in 2010 [13]. There are different vaccination strategies for cancer therapy like using tumor-associated antigens as

protein/peptide-based cancer vaccines or use of dendritic cells as antigen-presenting cells for vaccination [14]. Another approach with impressive results is the RNA-based vaccination with neoantigens for the treatment of melanoma as recently published by Kranz et al. [15] and Sahin et al. [16]. Ott et al also showed the safety, feasibility and immunogenicity of a vaccine which targets up to 20 predicted personal tumor neoantigens [17].

The adoptive cell therapy (ACT) was used the first time by Rosenberg and colleagues in 1988 using autologous tumor-infiltrating lymphocytes (TILs) to treat melanoma patients [18] after they demonstrated that TILs isolated from tumors can be expanded *ex vivo* by stimulation with IL-2 [19]. Clinical studies have reported that ACT of autologous *ex vivo*–expanded TILs can result in 50% objective responses in patients with metastatic melanoma among which 22% achieved a complete tumor regression, and 19% have ongoing complete regressions beyond 3 years [20]. Recent works analyzing patient cancers TILs indicated that T cells targeting mutated or neo-antigens may be central in mediating effective tumor regression seen in response to ACT [21]. ACT of CD4 positive TILs that recognize a mutant tumor-specific neoantigen ERBB2 protein demonstrated a sustained tumor regression in a patient with metastatic cholangiocarcinoma [22] and transfer of CD8 positive TILs targeting mutant KRAS mediated effective antitumor response in a patient with mutant KRAS G12D metastatic colorectal cancer [23]. Despite promising clinical responses reported with TILs-based ACT, the challenge in generating therapeutic numbers of tumor-reactive TILs within a short time remains the main hurdle in the development of a successful TILs therapy, in particular in patients with rapid disease progression. Furthermore, this approach is not always successful [24] and not applicable to non-solid tumors. Therefore genetically engineered T cells expressing antigen-specific T cell receptors (TCRs) or chimeric antigen receptors (CARs) were used for ACT. Unlike TCR, CARs could target a wide range of extracellular tumor antigens independently of MHC molecules, including proteins, glycolipids or carbohydrates. CARs are composed of an extracellular single-chain variable fragment (scFv) of a monoclonal antibody fused to an intracellular TCR CD3zeta-signaling moiety [25]. Several CAR scaffolds (or CAR generation), incorporating one or more intracellular co-stimulatory domains have been generated to enhance the efficacy and persistence [26] of CAR-T cells. First clinical trials using TCR engineered T cells for ACT was in metastatic melanoma patients [27] and T cells expressing a CD19-CAR showed impressive remission rates, of up to 90% most notably in patients with advanced B cell malignancies [28],[29] leading to the recent FDA approval of

CD19 CAR T-cell therapy for the treatment of children and young adults with B-cell acute lymphoblastic leukemia.

One common challenge in ACT using TCR- or CAR-redirected T cells in solid tumors is the tumor microenvironment and its immune-suppressive condition. Beside the inappropriate milieu due to low oxygen- and nutrient-supply, TILs become exhausted due to the presence of suppressor cells and their release of immune-suppressive cytokines [30] and the upregulation of immune inhibitory molecules [31]. In 2010 a new class of mAb blocking these immune inhibitory molecules, named immune-checkpoint inhibitors (ICIs) showed impressive results in clinical trials treating patients with metastatic melanoma. The anti-CTLA-4 (cytotoxic T lymphocyte antigen 4) antibody (ipilimumab) improved the survival in melanoma patients in a phase III clinical trial [32] and was approved for the treatment of metastatic melanoma in the USA in 2011. One year later another antibody (nivolumab) targeting PD-1 (programmed cell death protein 1) exhibited promising results in phase I clinical trials with patients with melanoma, kidney cancer and non-small cell lung cancer [33]. The combination of nivolumab and ipilimumab leads to improved outcomes in patients with advanced melanoma compared to monotherapy [34] and combination therapy was therefore approved as a frontline treatment regimen of advanced melanoma in 2015 in the USA. Today several ICIs are currently tested in melanoma and other cancers, i.e. lung cancer, renal cancer, bladder cancer, kidney cancer or Hodgkin´s lymphoma [35],[36],[37],[38].

1.1.1 TCR engineered T cells based adoptive cell therapy

The concept of adoptive cell transfer goes back to Billingham and colleagues describing immunization experiments in mice by transplanting tissue [39]. The first ACT mentioned above done by Rosenberg and colleagues using TILs showed promising results in patients with metastatic melanoma but beside this cancer type it is not always possible to isolate antitumor-reactive TILs out of tumors [24]. Furthermore the use of TILs for ACT is often cost and time consuming. After isolation of cells there is only a short time for *ex vivo* expansion before TILs can be reinfused back into the patient, therefore it is very challenging to obtain a sufficient number of high quality TILs after *ex vivo* expansion. Most of the tumor-associated antigens (TAAs) are self-antigens and thus also expressed by healthy tissue. Due to self-tolerance the possibility to isolate sufficient high-affinity TCR expressing TILs for TIL-based ACT is virtually low. To overcome this obstacle, lots of efforts were made to modify cells in

vitro by genetic engineering with TAA-specific TCRs. T cell therapy based on TAA-specific TCR redirected T cells is independent on the presence of tumor-reactive T cells and since any TAA of choice can be targeted, this therapy is applicable for a wide range of tumors. The TCR gene therapy relies on the observation that antigen-specificity can be transferred between T cells by introducing genes encoding for TCR α- and β-chains [40]. In the late 1990th T cells were redirected with TAA-specific TCRs [41] and first mouse models were performed analyzing the function of these engineered T cells *in vivo* [42] (summarized in [43]). One of the first clinical trial of ACT with TCR-engineered T cells was published by Rosenberg in 2006 were a TCR against MART-1 showed tumor regression in melanoma patients [27]. Redirected T cells engrafted well in the patients and represented about 10% of peripheral blood mononuclear cells (PBMCs) for at least two months. Since then several trials have been performed targeting different cancer types by TCR-engineered T cells, including melanoma, lung cancer and renal cancer.

1.1.1.1 T cell meditated immune response

The structure of a TCR is a heterodimer composed of either α/β- or γ/δ-chains expressed at the cell surface and responsible for specific recognition of the epitope and the non-variable signaling transduction cluster of differentiation 3 (CD3) complex which contains CD3γ, CD3δ, CD3ε and CD3 ζ subunits [44]. Both α/β and γ/δ TCR chains consist of a variable and constant domain, respectively. The present research work will focus on α/β TCR type. The structure of an α/β TCR/CD3 complex is shown in figure 1.1.

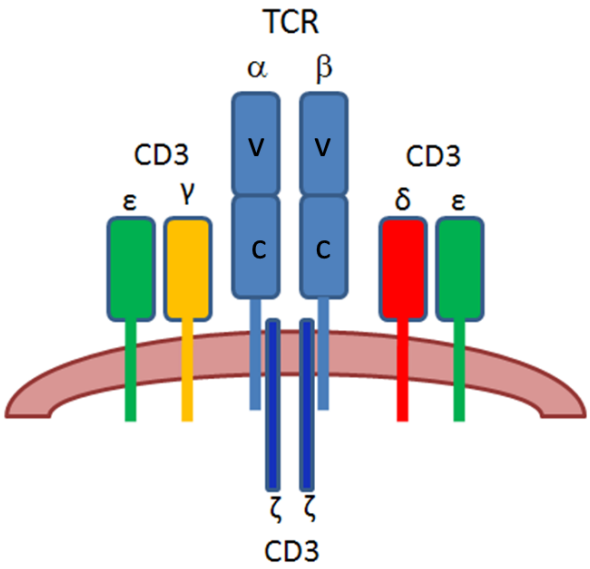

Figure 1.1 Structure of an α/β TCR/CD3 complex expressed on the cell surface. The TCR consists of an α- and β-chain with their constant (c) and variable (v) domains, respectively. The CD3 complex contains four chains called γ-, δ-, ε- and ζ-chain. The γ-, δ- and ε-chains are expressed on the cell surface whereas the ζ-chain is located intracellularly [45].

The variable domains of α- and β-chain build the antigen-specific site of the TCR which recognizes peptides presented by major histocompatibility complex (MHC) molecules, yet MHC-independent α/β T cells have been reported [46]. This antigen-specific site contains the complementarity determining region 1 (CDR1), CDR2 and CDR3. CDR1 and CDR2 are responsible for the first contact of MHC molecule during antigen presentation whereas CDR3 is hypervariable and interacts with the presented peptide [47]. The binding of peptide-MHC complex results in biochemical changes of cytoplasmic parts of the CD3 complex. Cytoplasmic domains of CD3 subunits contain immunoreceptor tyrosine-based activation motifs (ITAMs) which are phosphorylated by kinase LCK and phosphorylated residues are furthermore responsible for activation of downstream molecules involved in TCR signaling cascade. These changes in CD3 complex are referred to as TCR triggering (summarized in [44]). For T cell activation a second signal is provided by interaction of CD28 expressed on T cells and CD80 (B7-1)/CD86 (B7-2) on antigen presenting cells (APCs) [30] and a third signal mediated by cytokines like IL-2. Co-receptors expressed on the T cell surface are also interacting with the MHC molecules expressed on APCs. CD8 coreceptor is expressed on cytotoxic T lymphocytes (CTLs) and is binding to MHC class I molecules whereas CD4 is expressed on T helper (Th) cells interacting with MHC class II molecules. Activated CD8 expressing cells produce and release cytotoxic granules like perforin and granzyme B to induce apoptosis in target cells. CD4 positive T cells are separated in different subtypes:

Th1 cells are involved in the elimination of intracellular pathogens by evoking a phagocyte-based inflammation and produce high levels of interferon-γ (IFN-γ) and IL-2, an essential cytokine for $CD8^+$ T cell proliferation. Th2 cells respond to extracellular pathogens presented by APC like macrophages of dendritic cells (DCs). They provoke an antibody-mediated immune response and an accumulation of eosinophils which combat parasites. But Th2 cells are also involved in the induction and persistence of asthma and other allergic diseases. They secrete mainly IL-4, IL-5, IL-13 and IL-10. Th9 cells are the main $CD4^+$ cells that secrete IL-9 which is found in immune response against parasites and the pathogenesis of allergic diseases like asthma and bronchial hyper reactivity. IL-9 mediates also proliferation of hematologic neoplasias, like Hodgkin´s lymphoma. Th17 cells produce IL-17 and are involved in generation of autoimmune diseases. Regulatory T cells (Treg) express CD25 and the transcription factor FOXP3 and are responsible for the regulation and inhibition of immune responses by secreting immune inhibitory cytokines like IL-10 and tumor necrosis factor β (TGF-β) or by direct cell-cell contact effect. Due to their respective cytokine profile $CD4^+$ T cells influence cells of the innate and adoptive immune system (summarized in [48],[49]).

The variable domain of the TCR α- and β-chain, the antigen-binding site, is highly specific for one single peptide. The diversity of TCRs recognizing different peptide/MHC complexes is caused by rearrangement of gene segments encoding for variable and constant domain including junction segments. The β-chain locus consists of different gene segments called variable (V), diversity (D), junction (J) and constant (C). For rearrangement 50 Vβ, 1 Dβ1 and 1 Dβ2, 6 Jβ1 and 7 Jβ2, 1 Cβ1 and 1 Cβ2 segments are available. The TCR α-chain locus consists of the same segments but is lacking the D segment. For its rearrangement 75 Vα, 60 Jα and 1 Cα segment are available. Since only one segment each is necessary to build a TCR α- or β-chain the possibilities for rearrangements are huge. Geometric recombination, the randomly pairing of α- and β-chains, is even increasing the diversity of TCRs up to more than 10^{15} possible TCR clonotypes.

The rearrangement of TCR chains happens during T cell development in the thymus. Within the thymus microenvironment, a diverse T cell repertoire which is self-tolerant and also self-restricted can be generated. Progenitor cells from the bone marrow enter the thymus medulla and undergo T-lineage specification. These progenitor cells do not express CD4 or CD8 and are therefore called double-negative (DN) cells. They usually express CD2 but lack CD3 and TCR expression. During development, DN cells become TCR expressing CD4 and CD8

double-positive (DP) cells which then develop into CD4 or CD8 expressing single-positive (SP) cells. Within the process from DN to SP, cells are positively or negatively selected in the thymus. DP cells were selected on thymic epithelial cells which express both MHC class I and II molecules and interact with TCR and CD8 or CD4 on the cell surface. If TCR is functional, self-MHC molecules are recognized with a low or intermediate affinity and DP cells are positively selected and protected from apoptosis. In a second selection step, the recognition of self-MHC molecules presenting self-peptides by the cells occurs. Cells which have a high affinity to self-MHC molecules loaded with a self-peptide presented on DCs, macrophages or thymic epithelial cells are negatively selected and undergo apoptosis. The SP cells which finally leave the thymus are able to recognize a self-MHC /foreign-peptide complex (summarized in [50],[51]).

1.1.1.2 Challenges of TCR-based ACT

Important for the successful use of ACT in human cancer is the identification of the ideal antigen which will be targeted by TCR engineered T cells. Ideal antigens for immunotherapy should be specifically expressed on cancer cells and not on normal tissue. Targeting TAA, which are expressed also on normal tissue could result in severe on-target/off-tumor toxicity as reported in patients infused with T cells engineered to express high-avidity MART-1- and gp100-reactive TCRs [52], carcinoembryonic antigen (CEA)-specific TCR [53] or MAGE-A3 TCR [54]. Furthermore, TCR-gene transfer can lead to fatal toxicity due to TCR cross-reactivity as observed in myeloma and melanoma patients treated with affinity-enhanced MAGE A3-TCR [55] and one melanoma patient infused with MART-1 specific TCR [56]. Cancer germline antigens however are expressed by healthy cells only during fetal development and not in adult tissue [57]. To date, two clinical trials of high-affinity TCR-gene transfer with no evidence of severe toxicity were reported with TCR transgenic T cells targeting cancer/testis (CT) antigen NY-ESO-1 in melanoma [58] and multiple myeloma [58]. Tumor antigens can be classified in different categories (summary in[59]):

- Overexpressed or accumulated antigens are expressed by normal and neoplastic tissue whereas expression level in neoplastic tissue is remarkably enhanced like Her2/neu or MDM2 antigens [60],[61].

- Cancer-testis antigens are expressed only in cancer cells and adult reproductive tissue as testis or placenta like melanoma-associated antigen (MAGE)- family or NY-ESO-1 antigens in melanoma and non-small cell lung cancer (NSCLC) [62],[63].
- Lineage-restricted or differentiation antigens are expressed by a single cancer histotype like gp100, Melan A/MART-1 (melanoma antigen recognized by T cells-1) or tyrosinase antigens [64].
- Mutated antigens are expressed by tumors as a result of genetic mutations or modifications in transcription like p53 or Ras [65],[66].
- Oncoviral antigens are encoded by tumorigenic transforming vectors like human papilloma virus (HPV) or Epstein-Barr virus (EBV) [67].
- Oncofetal antigens are expressed in fetal tissue and in adult cancer cells like carcinoembrionic antigen (CEA) in colorectal cancer [68].
- Post-translational altered antigens like MUC1, a transmembrane glycoprotein whose functions are changed after post-translational modifications [69].
- Idiotypic antigens: Individual immunoglobulins exhibit unique V region antigenic determinants called idiotopes. Idiotopes endocytosed and processed by APC or B cells can be recognized as peptide by T cells. Idiotopes are expressed in B cell or T cell lymphomas/Leukemia as a result of clonal aberrancies [70].

In contrast to TAA, cancer-specific mutations (or neoantigens) recognized by TCRs have emerged as better target antigens for cancer immunotherapy, especially for tumors with high mutation rates like melanoma [71]. Neoantigens arise via mutations, including point-mutations, frameshift deletion of insertions, which alter amino acid sequence of proteins. Neoantigens are exclusively expressed by tumor cells what avoids severe on-target/off-tumor toxicities by targeting these antigens with neoantigen-specific TCRs [72]. TCRs specific for neoantigens can be identified by classical approaches since some common mutations, like in BRAF, KRAS and p53 in tumors are well characterized [73],[74],[75]. One approach is the analysis of peptides presented by tumor cells on MHC molecules by mass spectrometry [76]. Based on these mutations, corresponding peptides are synthesized and used to generate/expand neoantigen TCR-specific T cell clone(s) from blood of healthy donors or patients, by repetitive stimulation with the corresponding mutant peptide-pulsed APCs [72]. Another approach to isolate neoantigen TCR-specific T cell clone(s) from blood is

fluorescence-activated cell sorting (FACS) using MHC /peptide multimers coupled with fluorochromes [77]. By using next-generation sequencing (NGS) techniques, including whole-exome/transcriptome sequencing analysis, MHC-binding prediction and peptide-based screening approach, many neoantigens could be identified for antigen-specific TCR T cell therapy, like mutated kinesin family member 2C (KIF2C) antigen, mutated DNA polymerase alpha subunit B (POLA2) [78] or casein kinase 1, alpha 1 (CSNK1A1) [79]. First clinical studies using TILs reactive against mutated neoantigens showed antitumor response, e.g. in a patient with epithelial cancer where therapy with $CD4^+$ TILs reactive against mutated ERBB2 interacting protein achieved a prolonged stabilization in disease [22]. There are currently more than 100 open TCR clinical studies registered (www.clinicaltrials.gov) targeting both solid tumors and leukemia.

The second challenge is the selection of the optimal human T cells subpopulation for TCR engraftment. Preclinical studies in mouse models and also primates have shown that more potent antitumor responses were obtained with T cells in early stage of differentiation like naïve cells or central memory cells [80],[81]. Gattinoni and colleagues have demonstrated that more-differentiated effector T cells are less effective for tumor treatment *in vivo* [82]. Antitumor efficacy is inversely proportional to the differentiation stage of infused T cells. This may influence the objective response in clinical trials as observed in metastatic melanoma patients treated with autologous TILs where the transfer of younger cell was associated with better objective response rates [83].

For a successful outcome of ACT redirected T cells have to express the TCR at a strong level. Transgenic and endogenous TCR chains compete for CD3 complex co-expression which may reduce the expression of the introduced TCR [84]. Moreover, it has been demonstrated that increasing TCR expression has a profound effect on *in vivo* antitumor activity [85].A safety concern of TCR gene transfer is mispairing of endogenous and transgenic TCR chains. Mixed TCR heterodimers not only reduce the expression level of introduced TCR but may also exhibit a new antigen specificity which might be potentially autoreactive [86]. We and other research groups have developed several strategies to reduce the risk of mispairing which will be developed in a separate chapter.

1.1.2 Monoclonal antibodies

Monoclonal antibodies (mAbs) are the fastest growing group of biotechnology-derived molecules used in clinical trials [87] but since the first time they were generated in 1975 by Köhler and Milstein it was a long way of developments until the first mAb was approved for its clinical application. mAbs are produced by a single B lymphocyte clone and recognize the same epitope. In the beginning mAbs were generated using the hybridoma technique where a certain species (e. g. mouse or rabbit) were immunized against a certain epitope and activated B lymphocytes were then fused with immortalized myeloma cells to generate hybridoma cells secreting only antibodies with the same specificity [88]. Further advancement in generating mAbs allowed then the development of specific human mAbs.

1.1.2.1 Mechanism of antitumor functionality and tumor antigens

The mechanism of therapeutic antitumor function of mAb can be divided into two categories of antibodies. mAbs conjugated with radionuclides or, especially for cancer treatment, with chemotherapeutics serve as delivery system for the toxic compounds in predefined target cells. The second category of unconjugated mAbs can induce immune response by binding to their antigen. Antibody-marked cells are then eliminated by complement system activation or antibody-dependent phagocytosis. Unconjugated mAbs can also inhibit the interaction of receptor and ligand by binding to their antigen which results in altered signal transduction of the target cell (summarized in [89] and [90]). Tumor antigens which can be targeted by mAbs can be hematopoietic differentiation antigens like CD20 or CD52, antigens related to growth and differentiation signaling like EGFR (epidermal growth factor receptor) or Her2 (human epidermal growth factor receptor 2) [90].

The first mAb for cancer immunotherapy approved in the USA 1997 was rituximab. It is targeting CD20 and was applied for the treatment of Non-Hodgkin´s lymphoma. Other mAbs for cancer treatment followed like trastuzumab targeting Her2 in breast cancer, alemtuzumab targeting CD52 in chronic lymphocytic leukemia (CLL) or cetuximab targeting EGFR in colon cancer [91].

1.1.2.2 Immune checkpoints and tumor escape

The success of ACT is dependent on a sufficient immune response in cancer patients to achieve an antitumor activity. Therefore the outcome of this approach is limited due to

immune suppressive mediators which often cause an ineffective treatment and tumor outgrowth [31]. The reduced immune response is mediated by tumor immunosuppression and escape mechanisms. Under normal physiological conditions the immune cell functions are tightly regulated by immune checkpoints consisting of a set of cell surface stimulatory and inhibitory molecules. For T cell mediated immune response, T cells need to be activated for further proliferation and migration to secondary lymphatic tissue. Each of these steps is mediated by a balanced activation and inhibition of signaling pathways which are induced by membrane bound (receptors and ligands) or soluble molecules like cytokines. Tumors can take advantage of these regulatory mechanisms and interfere with the expression of immune checkpoint proteins (summarized in [31]) on T cells and APC by triggering the secretion of immunosuppressive cytokines like IL-10 or TGF-β by cells of the tumor microenvironment, e.g. myeloid-derived suppressor cells (MDSCs) to induce inhibitory signaling cascades [92]. MDSCs are not only producing immunosuppressive cytokines but also enzymes like arginase or indoleamine 2,3-dioxygenase (IDO) as well as reactive oxygen species (ROS) and nitric oxide (NO) [31]. Arginase is metabolizing arginine and IDO does so with tryptophan which are both required for T cell function and a lack of these amino acids leads to impaired T cell response[93],[94]. NO has an inhibitory effect on T cell proliferation since it impairs phosphorylation of components of the IL-2 signaling pathway [95]. Moreover, chronic T cell activation in the tumor microenvironment due to persistent exposure to tumor-antigens leads to exhaustion of T cells and consequently up-regulation of inhibitory molecules [96].

A set of mAbs which block interaction of inhibitory receptor and ligand are called immune-checkpoint inhibitors (ICIs). The molecule first targeted by this type of mAb was CTLA-4 which is expressed on T cells and shares the same counterpart as CD28 which is essential for T cells activation. CTLA-4 expression is up-regulated shortly after T cell stimulation via the TCR and CD28-CD80/CD86 interaction. Interaction of CTLA-4 with CD80/CD86 is dampening the T cell response and protects under normal physiological conditions against autoimmune reaction. In cancer situation, CTLA-4 will preferentially bind to CD80/CD86 since it has a higher affinity than CD28 and therefore reduces T cell activity [30]. First clinical trials using the fully humanized anti-CTLA-4 mAb ipilimumab (Yervoy) and tremelimumab were performed in 2000 based on encouraging preclinical tests performed by Allison and colleagues [97]. Ipilimumab was the first checkpoint inhibitor approved in 2011 in the USA

for the treatment of metastatic melanoma. Another immune checkpoint receptor is PD-1. Like CTLA-4, PD-1 (CD279) is expressed on T cells after T cell activation and is reducing their activity in the peripheral tissue [98]. It can be also expressed on other activated immune cell types like natural killer (NK) cells, monocytes, dendritic cells (DCs) or macrophages. PD-1 is binding to programmed cell death-ligand 1 and 2 (PD-L1 and PD-L2). PD-L1 /-L2 expressions are inducible by cytokines like TNF-α, IL-2, IL-7, IL-17 and IFN-γ. PD-L1 is expressed on a broad range of hematopoietic and non-hematopoietic cells like B cells, DCs, macrophages, vascular endothelial cells or epithelial cells. PD-L2 is expressed on B cells, DCs, macrophages and bone marrow-derived mast cells (summarized in [99]). In cancer patients the immunosuppressive influence of the PD-1/PD-L1 and PD-L2 axis is used by the tumor as a mechanism of immune evasion. It was observed that TILs are highly PD-1 positive and also tumor cells up-regulated PD-L1 expression for example in breast cancer or melanoma [100]. Preclinical investigation of PD-1 expressing TILs isolated from melanoma patients showed that these cells were less active, however their cytokine production and proliferation could be increased *in vitro* after blocking of PD-1 [101].

Pembrolizumab (Keytruda) was the first mAb targeting PD-1 approved in the USA for the treatment of advanced melanoma [102]. Nivolumab (Opdivo), a second anti-PD-1 mAb, obtained approval in 2014 for the treatment of metastatic melanoma and showed also good overall response rates in non-small cell lung cancer (NSCLC) and renal cell cancer (RCC) [98]. The combination of nivolumab and ipilimumab is approved for patients with melanoma and showed promising overall response rates in NSCLC. Anti-PD-L1 mAbs like BMS-936559 or MPDL3280A are currently tested in clinical studies for the treatment of metastatic melanoma, NSCLC, renal cancer and other solid tumors with overall response rates of 10% - 38% [98]. The PD-L1 antibody atezolizumab was approved in 2016 in the USA for NSCLC and received EU approval (September 2017) for metastatic lung and bladder cancers. To date ICIs have been approved as single agent for the treatment of multiple cancer types, including solid tumors like NSCLC, squamous cell carcinoma, head and neck cancer, bladder, kidney and renal cancer but also for Hodgkin´s lymphoma or multiple myeloma. Furthermore, ICIs (pembrolizumab or nivolumab) are currently been evaluated in early phase trials in combination with adoptive NY-ESO-1ᶜ259TCR and E7 TCR T cell therapy for multiple myeloma and Human Papillomavirus-associated Cancers and with TILs therapy in patients with metastatic melanoma.

1.2 Tumor-associated antigen MDM2

The murine double minute 2 (MDM2) protein is an ubiquitously expressed E3 ubiquitin-protein ligase. Formerly it was called human double minute 2 (HDM2) since it is the human homolog to the murine protein. Experiments in mice showed that MDM2 is vital for developmental functions since MDM2-deficient mice died early in development. Mice could be rescued by also knocking out p53 demonstrating the determinant role of p53 / MDM2 interaction for development [103].

Full length MDM2 has a molecular weight of 90 kDa and contains 491 amino acids. Analysis of gene sequences in human, hamster, mouse, zebrafish and frog revealed a high similarity in some regions. Based on these similarities a highly related gene was cloned, called MDMX, and alignment of human and mouse MDM2 with MDMX sequence resulted in the identification of three conserved regions called CR1, CR2 and CR3. The N-terminal CR1 binds to the tumor suppressor p53 and inhibits its transactivation function, CR2 codes for a zinc finger domain and CR3 encodes for the RING domain which is responsible for the E3 ubiquitin ligase function [104]. Full length MDM2 is cleaved by caspase 3 during apoptosis after residue 361 resulting in a 60 kDa fragment. The 60 kDa MDM2 isoform is still able to bind p53 but lost its E3 ubiquitin ligase function. In tumor cells MDM2 can be also cleaved in non-apoptotic cells by a caspase distinct from apoptosis-specific caspase 3. The 60 kDa MDM2 isoforms were detected e.g. in breast cancer cells overexpressing MDM2 (summarized in [105]). The structure of MDM2 domains is shown in figure 1.2.

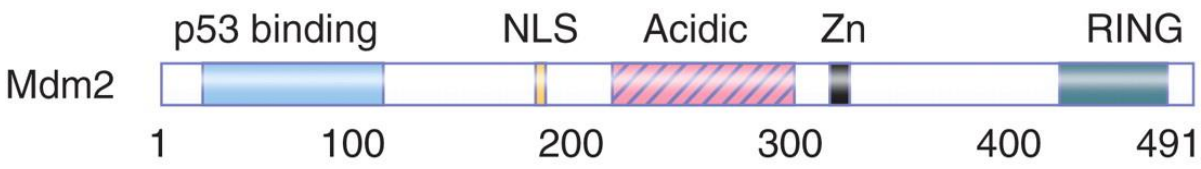

Figure 1.2 Domain structure of MDM2. MDM2 is capable of binding p53 at the N-terminal part followed by the nuclear localization signal (NLS) domain. The acidic domain is required to bind ribosomal proteins. The zinc finger (Zn) and ring domains are located at the C-terminal part of MDM2 [106]. Numbers indicate the amino acid positions.

Ubiquitination of a target protein is a mechanism to control protein function in cells. During this process ubiquitin-like protein modifiers (Ubls) are attached to other proteins and change their characteristics [107]. Ubiquitin is the prototype of the Ubl family and its conjugation to a target protein has different impact on the function of the target. The main known function

of ubiquitination is the tagging of proteins for their efficient recognition and degradation by the proteasome (or lysosomes) [108] but also the transport of a protein to the cell membrane can be regulated by ubiquitin which is acting in this case as a sorting signal on protein cargo [109]. Especially mono-ubiquitination, so the transfer of a single ubiquitin to a target protein, is involved in histone regulation and endocytosis [110]. Ubiquitination is performed in an enzymatic cascade containing ubiquitin-activating enzyme (E1), ubiquitin-conjugating enzyme (E2) and ubiquitin-ligating enzyme (E3). The ubiquitination process can be repeated sequentially which results in a mono- or multi-ubiquitination of proteins [111]. MDM2 belongs to the E3 enzymes and binds to the target protein and E2 enzyme loaded with ubiquitin to allow the transfer of ubiquitin from E2 to the protein. Ubiquitination of proteins by MDM2 leads to their degradation in the proteasome or results in the inhibition on their side of action which is a negative regulation of the target protein by MDM2.

Regarding the project of this thesis we were interested in the tumor suppressor protein p53 as a well-defined target for MDM2. The protein p53 is mainly acting as a transcription factor for different downstream genes and is activated by multiple stimuli. The function of p53 is very complex and it is involved in several processes like control of cell cycle, apoptosis and DNA repair. Especially in cancer the role of p53 as a tumor suppressor gene is relevant because it is inducing autophagy, apoptosis and senescence in tumor cells and inhibiting cell proliferation [112]. The p53 gene (TP53) is the most frequently mutated gene in cancer since mutated p53 is not functional and therefore lost tumor suppressor function [113]. The p53 function in non-cancerous and cancerous cells is tightly regulated by p53 transcription and translation, post-translational modifications, protein stability and its subcellular localization [114]. MDM2 is the master negative regulator for functional p53 since MDM2 is affecting protein stability and leads to p53 nuclear export [115]. MDM2 activity is regulated via the phosphatidylinositol 3 kinase (PI3K) / Akt signaling pathway. Akt phosphorylates MDM2 and leads to its translocation from the cytoplasm to the nucleus where it interacts with p53 [116]. Phosphorylation can also enhance the ubiquitination activity of MDM2 [117]. In both cases p53 function and expression is reduced by MDM2. Therefore MDM2 over-expression and subsequent p53 inactivation is a common observed event in cancer [118],[119].

1.2.1 Tumor oncoprotein MDM2

In normal cells MDM2 is responsible for the regulation of p53 expression at a basal level by ubiquitination and degradation of p53 in the proteasome. Under cellular stress the affinity of MDM2 to p53 is reduced which results in less inhibition and a higher p53 expression in the nucleus. The increased p53 expression is the consequence of enhanced translation rate and less degradation rate [104]. On the other hand MDM2 is also a transcriptional target of p53 which leads to an autoregulatory feedback loop of regulation of p53 activity and function and MDM2 expression level [120]. The effect of MDM2 on p53 protein is dependent on MDM2 expression level. Low levels of MDM2 are sufficient for mono-ubiquitination of p53 which induces its nuclear export and therefore inhibit its transcriptional activity whereas overexpression of MDM2 leads to poly-ubiquitination and degradation of p53 in the proteasome [121].

MDM2 is ubiquitously expressed, however the expression levels varies according to the cell types. MDM2 overexpression in tumors is mediated by gene amplification, increased transcription and enhanced translation [61] and expression levels differs in tumor types. 50%-60% of soft tissue sarcoma and osteosarcoma overexpress MDM2 and a high level of MDM2 was observed in glioblastoma, melanoma and hematological malignancies [122]. A well characterized single-nucleotide polymorphism (SNP) in the MDM2 promotor region, at position 309T>G, causes increased MDM2 expression level and is associated with an earlier onset of tumor formation [123]. By binding and induction of degradation MDM2 can inhibit p53 tumor suppressive function and enables tumor metastasis and disease progression. But observation in cancer patients that harbor mutation in both MDM2 and p53 [124] hypothesized that MDM2 may play a role in tumorigenesis without requiring a functional p53. MDM2 is also involved in p53-independent cell cycle control, DNA repair and can induce apoptosis [125]. These properties make MDM2 an ideal target for cancer therapy [126].

One of the first drugs targeting MDM2 was Nutlin-3a discovered in 2004 by Vassilev et al. [127]. This antagonist binds at the N-terminal domain of MDM2 and prevents its binding to p53. The authors could show that Nutlin-3a exhibited an antitumor activity *in vitro* and *in vivo* in cancer cells harboring a wild type (wt) p53. Nutlin-3a however showed a poor bioavailability and a high toxicity which limited its translation into the clinic [128]. Several other small-molecule MDM2 inhibitors, which prevent p53-MDM2 interaction are being

tested in clinical trials, including the MDM2 antagonists RG7112 tested for its use against solid and hematological cancers (summarized in [128]). Other molecules are targeting the C-terminal located E3 ligase domain and thus inhibit ubiquitination of p53 and are currently tested in clinical trials [129]. Another molecule which supports MDM2 in targeting p53 is MDM4 (an MDM2 homolog, also called MDMX) which is also binding p53 at the N-terminal domain but is lacking the E3 ligase activity. MDM4 can interact with MDM2 which results in a higher E3 ligase activity of MDM2 and therefore an increased p53 ubiquitination [130]. Molecules targeting MDM4 and also MDM2/MDM4 interaction can reactivate the p53 function [131]. A small molecule which is inhibiting the MDM2-p53 interaction is RITA (reactivation of p53 and induction of tumor cell apoptosis). It is not binding to MDM2 but to p53 which is changing its conformation and prevents binding by MDM2 [132]. Preclinical test with tumor cell lines showed already growth suppression by RITA in colon carcinoma, lung carcinoma, skin and breast carcinoma, Burkitt lymphoma and multiple myeloma [133],[134].

1.2.2 MDM2 as antigen for TCR-based immunotherapy

Isolating high-affinity MDM2-specific TCR from cancer patient´s blood is hampered by self-tolerance deletion mechanism (as discussed in 1.1.1). Therefore, our group took advantage of transgenic mice to generate a high-affinity CD8-dependent and human leukocyte antigen HLA-A*0201 (A2.1)-restricted murine TCR recognizing the human MDM2(81-88) non-mutated peptide [135].

To get murine CTLs recognizing human peptides in an A2.1-restricted manner transgenic mice expressing CD8 and $A2K^b$ were immunized with 31 MDM2 peptides which were tested (earlier) for strong to intermediate A2.1 binding by computational score models [136]. The MDM2(81-88) peptide is a naturally processed peptide which was derived from cellular MDM2 protein degradation by the proteasome. The antigen-specificity and A2.1-restriction of the isolated CTL clone recognizing this peptide was investigated in cytolytic assays using A2.1-expressing APCs loaded with MDM2(81-88) peptide or irrelevant peptide as targets [135].

The sequence encoding for the murine MDM2(81-88)-specific TCR which was isolated from the murine CTL clone was cloned in a retroviral vector for transduction of human T cells for functional analysis. Human T cells retrovirally redirected with this TCR specifically recognized tumor cell lines overexpressing MDM2, including leukemia, multiple myeloma, malignant

melanoma, renal cancer cells or APCs loaded with MDM2(81-88) peptide whereas MDM2-negative cells and normal healthy cells expressing MDM2 at a basal level were not recognized [135].

Introducing transgenic TCR chains into T cells harboring a native TCR may generate the formation of mixed TCR dimers with potentially harmful (neo)reactivity as mentioned in chapter 1.1.1.2. Part of this thesis was the molecular modification of the original wt sequence encoding for the MDM2-specific TCR to reduce/limit the occurrence of mispaired TCRs to improve the safety use *in vivo*. Mixed TCR heterodimers have also a negative impact on the expression level of transgenic TCR since low TCR expression after transduction is caused by mispairing with endogenous TCR chains [86]. Several approaches have been described to circumvent TCR mispairing including the exchange of human TCR constant chains with their mouse counterparts, generating a chimeric/murinized TCR [137]. Human chimeric TCR chains with a murine constant domain preferentially pair and stabilize the CD3 complex. Also codon-optimization of the TCR sequences is improving the TCR expression [138]. The aim of this approach is to enhance translation of the transgenic TCR mRNA by exchange of rare codons in preferred codons via synonymous mutations. Codon-modified TCRs are functional and recognize tumor cells expressing the specific epitope. We and other have demonstrated that an enhanced pairing of transgenic TCR chains could be observed by introducing an additional disulfide bond between the two constant domains of TCR α- and β-chains [139]. This was achieved by exchanging specific amino acids in cysteine residues in the constant domains (T48C in the α-chain and S57C in the β-chain) and resulted in an enhanced TCR expression of introduced TCR chains. All these modification steps were performed with the MDM2-specific TCR and the impact on TCR expression and TCR heterodimer formation will be discussed in chapter 4.

1.3 Combination immunotherapy

In chapter 1.1 the different immunotherapeutic approaches were discussed for effective cancer treatment. These treatments led to a better outcome for cancer patients and are an effective addition beside the conventional cancer treatment with chemotherapy. A more specific therapy is the targeted therapy which is more restricted to cancer cells than normal chemotherapy. Drugs used in targeted therapy can for example interfere with chemical signaling pathways or change protein expression within the cancer cells like BRAF (B rapidly accelerated fibrosarcoma) inhibitors used for the treatment of metastatic melanoma. Because some patients become resistant using targeted drugs as mono-therapy this approach is usually combined with conventional chemotherapy [140]. The therapeutic effect of immunotherapy can be also limited due to the immunosuppressive microenvironment surrounding the tumor (in particular solid tumors) as described in 1.1.2.2. Combination of different immunotherapeutic approaches with or without chemotherapy might overcome resistance. Combination therapy can enhance the anti-cancer efficacy of the treatment and can also result in a prolonged tumor control. A prominent example for the advantage of combination therapy is the treatment of melanoma with two ICIs ipilimumab and nivolumab which showed an objective response rates of 53% in patients which did not respond to mono-therapy, respectively [141]. In the same line, the combination of ACT and targeted therapy also showed promising results as observed in a small pilot clinical trial published by Rosenberg and colleagues [142]. Patients with metastatic melanoma were injected with autologous TILs and received a high dose of IL-2. In addition they were treated with the BRAF inhibitor vemurafenib, starting at the time of TILs infusion. The combination therapy was well tolerated comparable to mono-therapy. Objective response rates of 64% and a complete response for 3 years in 18% of the patients were reported. Another combination therapy tested so far in mouse models is the treatment with ACT and ICIs. Moon et al. tested an anti-PD-1 antibody in combination with antigen-specific TCR engineered T cell transfer in a xenograft model using immunodeficient mice [143]. The antitumor response against a lung cancer cell line was enhanced in the combination therapy compared to treatment with ACT or antibody alone. Also the combination of nivolumab and lymphocyte transfer showed a stronger antitumor response compared to mono-therapy in preclinical model of colorectal

cancer [144]. The combination of these two promising approaches is now tested in a first clinical trial for the treatment of metastatic melanoma.

Also for the treatment of melanoma the combination of checkpoint blockade and a personalized immunotherapy was tested as recently published [16]. Patients were treated with individualized mutanome RNA-based vaccines which results in the development of a T cell response against multiple vaccine neo-epitopes. In combination with PD-1 blockade a complete response could be achieved.

In conclusion, immunotherapy was a breakthrough in the treatment of many tumor types in addition to conventional chemotherapy and other treatment methods like irradiation and surgery. The knowledge about the interaction of tumor and its environment and the immune system is in the focus of many research groups and this leads to more specific and thus potent approaches for cancer therapy. The combination of immunotherapeutic approaches, especially with ACT, will improve the outcome of cancer treatment since single approach has its limitations and harbor the risk of resistance developed by patients to mono-therapy. The final goal is to establish high efficient therapies with low toxicity to cure cancer patients and a promising way to achieve this is combining new targeted/tailored immunotherapeutic treatments.

2 Aim of the study

The murine MDM2-specific wt TCR which recognizes the MDM2(81-88)-peptide in a CD8-dependent and A2.1-restricted manner was used in this study for analysis of its antitumor reactivity *in vitro* and in xenograft models of melanoma and multiple myeloma. Overexpression of MDM2 protein and non-functional p53 is observed in several types of tumors and is associated with enhanced proliferation and survival of tumor cells with resistance to standard therapy. ACT using genetically modified T cells with antigen-specific TCRs has demonstrated significant clinical response in cancer patients, mainly with metastatic melanoma, however an immunosuppressive tumor microenvironment represent a serious hurdle to the successful application of this therapy approach. We tested the antitumor activity of T cells retrovirally transduced with an optimized MDM2-specific TCR in multiple myeloma and melanoma xenograft mouse models and addressed the following questions:

a) Does the modification of wt MDM2 TCR have any impact on TCR expression, antigen-affinity and specificity?
b) Does these modifications increase TCR pairing and minimize mispairing?
c) How do we address the safety analysis of TCR gene-modified T cells, in particular on-target/off tumor toxicity?
d) Are multiple myeloma and melanoma cells potential cancer types for MDM2 TCR-based therapy?
e) Do tumor antigen escapes occur in our pre-clinical ACT mouse models? If so, is it possible to circumvent tumor escape mechanisms, including antigen down-regulation and intratumoral-associated T cell exhaustion, by using multiple antigen-specific TCRs in combination therapy with checkpoint blockade to enhance T cell activity *in vivo*?

Since monotherapy for cancer patients with conventional chemotherapy or immuno-therapeutic approaches is not sufficiently effective in many patients, this study aims to improve conventional TCR ACT-based therapy by combination with other immunotherapeutic approaches.

3 Material and Methods

3.1 Devices

Table 3.1 Devices used for laboratory work.

Device	Identification	Manufacturer
Balance	L2200S	Sartorius, Göttingen, Germany
Cell irradiating machine	Gammacell 2000	Mølsgaard Medical, Ganløse, Denmark
Centrifuge	5417R	Eppendorf, Hamburg, Germany
Centrifuge	Megafuge 1.0R	Heraeus, Hanau, Germany
Centrifuge	Biofuge fresco	Heraeus, Hanau, Germany
Centrifuge	Omnifuge 2.ORS	Heraeus, Hanau, Germany
Centrifuge	Megafuge 40R	Thermo Scientific, Langenselbold, Germany
CO_2 Incubator	Heracell	Heraeus, Hanau, Germany
CO_2 Incubator	Function line	Heraeus, Hanau, Germany
Electrophoresis power supply	EPS600	Pharmacia Biotech, München, Germany
Electrophoresis power supply	PowerPac HC	BioRad, Hercules (California), USA
Flow Cytometer	Canto II	Becton Dickinson, Heidelberg, Germany
Gamma counter	Cobra II	Canberra Packard, Schwadorf, Austria
Electroporation device System	GenePulser Xcell	BioRad, Hercules (California), USA
Heating block	Thermo Stat plus	Eppendorf, Hamburg, Germany

Imaging system	ChemiDoc MP	BioRad, Hercules (California), USA
Laminar Flow	S2020 1.8	Thermo Scientific, Langenselbold Germany
MACS-Systems	MACS MultiStand	Miltenyi Biotec, Bergisch Gladbach, Germany
Microscope	Wilovert	Hund, Wetzlar, Germany
Microscope	Axiostar	Zeiss, Jena, Germany
PCR Cycler	MasterCycler Gradient	Eppendorf, Hamburg, Germany
PCR Cycler	Gene Touch	Biozym, Hessisch Oldendorf, Germany
pH meter	Knick pH-Meter 766	Calimatic, Zweibrücken, Germany
Photometer	Ultrospec 1000	Pharmacia Biotech, Munich, Germany
Photometer	Gene Quant II	Pharmacia Biotech, Munich, Germany
Shaker	Aerotron	Infors AG, Bottmingen, Switzerland
UV documentation	Transilluminator	Biostep GmbH, Jahnsdorf, Germany
Water bath	1003	Gesellschaft für Labortechnik, Burgwedel, Germany
Water bath	F12	Julabo Labortechnik GmbH, Seelbach, Germany
Western Blotting System Semi-dry	Trans-Blot SD Semi-Dry Transfer cell	BioRad, Hercules (California), USA
Western Blotting System Wet	Trans-Blot cell	BioRad, Hercules (California), USA

3.2 Chemicals and reagents

All buffers were prepared with distilled Millipore water and sterile filtered with Steritop™ Filter Units (Merck Millipore, Darmstadt, Germany).

Table 3.2 Chemicals and reagents used for cell culture and molecular biology.

Reagent	Manufacturer
Cell culture	
5'-aza-2'deoxy-cytidine	Sigma, Deisenhofen, Germany
Anti-FITC microbeads	Miltenyi-Biotec, Bergisch Gladbach, Germany
Anti-PE microbeads	Miltenyi-Biotec, Bergisch Gladbach, Germany
BSA	Sigma, Deisenhofen, Germany
Chromium-51 ($Na_2{}^{51}CrO_4$)	Perkin Elmer, Boston, USA
DMSO	Sigma, Deisenhofen, Germany
DMEM	Lonza, Basel, Switzerland
Dynabeads Human T-Activator CD3/CD28	Invitrogen, Darmstadt, Germany
EDTA	Sigma, Deisenhofen, Germany
FCS	PAA, Linz, Austria
Fugene 6	Promega, Madison, USA
Geneticin (G418)	Gibco, Eggensheim, Germany
HEPES-Buffer	Lonza, Basel, Switzerland
Human IL-2 (Proleukin® S)	Novartis, Basel, Switzerland
L-glutamine	Sigma, Deisenhofen, Germany

Lymphoprep	Stemcell Thechnologies, Vancouver, Canada
Muromonab-CD3 (Orthoclone Okt-3®)	Janssen-Cilag GmbH, Frankfurt/Main, Germany
Nivolumab (Opdivo®)	Bristol-Myers Squibb, New York City, USA
Nutlin-3	Cayman Chemical, Ann Arbor, USA
Opti-MEM™	Life Technologies / Thermo Fisher Scientific, Waltham, USA
1x PBS (sterile)	Sigma, Deisenhofen, Germany
Pembrozilumab (Keytruda®)	Merck, Darmstadt, Germany
Polybrene	Sigma, Deisenhofen, Germany
RPMI 1640	Sigma, Deisenhofen, Germany
Sodium-Penicillin/Streptomycin	Sigma, Deisenhofen, Germany
Trypsin-EDTA	Sigma, Deisenhofen, Germany
Trypan blue	Sigma, Deisenhofen, Germany

Molecular biology

Acrylamid 4K 30% solution	AppliChem, Darmstadt, Germany
Agar	Roth, Karlsruhe, Germany
Agarose	Starlab, Hamburg, Germany
Ampicillin	Sigma, Deisenhofen, Germany
Ammoniumperoxodisulfat	Sigma, Deisenhofen, Germany
Adenosine triphosphate	Epicentre (Madison, USA)

Bactotryptone	Roth, Karlsruhe, Germany
1x BSA	New England Biolabs, Frankfurt/Main, Germany
Brij 96V	Sigma, Deisenhofen, Germany
CutSmart buffer	New England Biolabs, Frankfurt/Main, Germany
Dithiothreitol (DTT)	Invitrogen, Darmstadt, Germany
DNA ladder 100bp and 1kb	New England Biolabs, Frankfurt/Main, Germany
Ethidiumbromide	Merck, Darmstadt, Germany
6x Gel Loading Dye	New England Biolabs, Frankfurt/Main, Germany
Glycine	Sigma, Deisenhofen, Germany
Herculase II Fusion DNA Polymerase	Agilent, Santa Clara, USA
JM109 stock solution	New England Biolabs, Frankfurt/Main, Germany
LB-medium	Roth, Karlsruhe, Germany
Laemmli sample buffer	Sigma, Deisenhofen, Germany
Leupeptin	Sigma, Deisenhofen, Germany
Methanol	Roth, Karlsruhe, Germany
Milk powder	Roth, Karlsruhe, Germany
Neb 3.1 buffer	New England Biolabs, Frankfurt/Main, Germany
Pepstatin	Sigma, Deisenhofen, Germany

PMSF	Sigma, Deisenhofen, Germany
Pfx50 Polymerase	Invitrogen, Darmstadt, Germany
DC™ Protein assay	BioRad, Hercules (California), USA
Protein standard dual color	BioRad, Hercules (California), USA
Restriction endonuclease AfeI	New England Biolabs, Frankfurt/Main, Germany
Restriction endonuclease Bam HI - HF	New England Biolabs, Frankfurt/Main, Germany
Restriction endonuclease BsmBI	New England Biolabs, Frankfurt/Main, Germany
Restriction endonuclease BsaI-HF	New England Biolabs, Frankfurt/Main, Germany
Restriction endonuclease Nco I - HF	New England Biolabs, Frankfurt/Main, Germany
Restriction endonuclease Not I- HF	New England Biolabs, Frankfurt/Main, Germany
Restriction endonuclease StuI	New England Biolabs, Frankfurt/Main, Germany
Rotiphorese Gel 30	Roth, Karlsruhe, Germany
SDS	Sigma, Deisenhofen, Germany
Sodium fluoride	AppliChem, Darmstadt, Germany
Sodium-orthovanadate	Sigma, Deisenhofen, Germany
Stbl3 Chemically Competent E. coli	Invitrogen, Darmstadt, Germany
T4 DNA Ligase	New England Biolabs, Frankfurt/Main, Germany

T7 DNA Ligase	New England Biolabs, Frankfurt/Main, Germany
TALEN kit	Addgene, Cambridge, USA
TEMED	AppliChem, Darmstadt, Germany
Tetracycline	Sigma, Deisenhofen, Germany
Tris	Roth, Karlsruhe, Germany
Tween-20	Roth, Karlsruhe, Germany
Western Lightning® Plus-ECL	Perkin Elmer, Boston, USA
XL-1 Blue stock solution	Agilent Technologies, Santa Clara, USA

3.3 Buffers and cell culture media

3.3.1 Buffer for molecular biology

LB-medium	25g for 1l medium
LB-plates	add to 1l LB-medium 20g Agar

For antibiotic selection 100µg/ml ampicillin were added to LB-medium or LB-plates.

Lysis buffer	10ml 1% Brij 96V solution 100µl Sodium fluoride (1M stock in water) 100µl Sodium orthovanadate (100mM stock in water) 10µl Leupeptin (1mg/ml stock in water) 10µl Pepstatin (1,5mg/ml stock in water) 100µl PMSF (100mM stock in Ethanol)
10x SDS running buffer	30,2g Tris 144g Glycine 100ml 10% SDS solution Add to 1l with aqua dest.

SOB-medium	0,5g NaCl
	20g bactotryptone
	5g yeast extract
	10ml 250mM KCl
	5ml 2M $MgCl_2$
	add to 1l with aqua dest., adjust pH to 7.0
50x TAE buffer	242g Tris base
	100ml 0.5M Na_2EDTA pH8.0
	57.1ml acetic acid
	adjust to 1l with aqua dest.
5xTBS	6g Tris
	44g NaCl
	add to 1l with aqua dest., adjust to pH 8.0
1xTBST	1l 5xTBST
	5ml Tween-20
	add to 5l with aqua dest
TfB I buffer	30mM cobalt acetate
	50mM $MnCl_2$
	100mM $CaCl_2$
	15% Glycerin
	adjust to pH 5.8 with acetic acid, filter sterile
TfB II buffer	10mM Mops-Na pH 7.0
	75mM $CaCl_2$
	10mM KCl
	15% Glycerin
	filter sterile
Lower Tris	91g Tris
	20ml 10% SDS solution
	Add to 500ml with aqua dest., adjust to pH 8,8

Upper Tris	6,05g Tris
	4ml 10% SDS solution
	Add to 500ml with aqua dest., adjust to pH 6,8
Western-Blotting buffer	5,82g Tris
(semi-dry blotting)	2,93g Glycine
	3,75ml 10% SDS solution
	200ml Methanol
	Add to 1l with aqua dest.
Western-Blotting buffer	2,43g Tris
(wet blotting)	11,25g Glycine
	200ml Methanol
	Add to 1l with aqua dest.

3.3.2 Buffer for cell culture

FACS buffer	0,5% BSA
	in 1x PBS
MACS buffer	0,5% BSA
	2mM Na_2EDTA
	in sterile 1x PBS
1% / 4% PFA	10g / 40g PFA
	in 1l 1x PBS and dissolve at 60°C in the water bath
Erythrocyte lysis buffer	174mM NH_4Cl
	10mM $KHCO_3$
	0.1mM Na_2EDTA
	add to 500ml aqua dest., adjust to pH 7.3

3.3.3 Cell culture media

DMEM	10% heat inactivated FCS 1% L-glutamine 1% penicillin-streptomycin 1% HEPES add to 500ml DMEM, filter sterile
DMEM only	DMEM without supplements
Freezing medium	10% DMSO in FCS, heat inactivated, filtered sterile
RPMI1640	10% heat inactivated FCS 1% L-glutamine 1% penicillin-streptomycin add to 500ml RPMI1640, filter sterile
RPMI1640 with AB-serum	10% heat inactivated AB-serum 1% L-glutamine 1% penicillin-streptomycin 2% HEPES add to 500ml RPMI1640, filter sterile

3.3.4 Peptides

MDM2 (8-mer):	$MDM2_{81-88}$	LLGDLFGV
p53 (9-mer):	$p53_{264-272}$	LLGRNSFEV
HIV(9-mer):	HIVpol 9k	KLVGKLNWA

All peptides were purchased from Biosynthan, Berlin, Germany and dissolved to 10mg/ml in sterile DMSO.

3.3.5 Antibodies for Western Blot

Anti-MDM2 #sc-965	Santa Cruz Biotechnology, Heidelberg, Germany
Anti-p53 #sc-53394	Santa Cruz Biotechnology, Heidelberg, Germany
Anti-GAPDH #5174	Cell Signaling Technology, Cambridge, United Kingdom

3.4 Methods

3.4.1 Cloning of MDM2 TCR in pMx-vectors with the following formats: sc opt., dc opt. and wt

DNA encoding for single chain (sc) optimized (opt.) TCR, double chain (dc) opt. TCR and wt TCR was manufactured by GENEART AG (Regensburg, Germany).

3.4.1.1 Retroviral vectors

Following plasmids were used:

pBullet_IRESneo, pBullet_IRESpuro, pMx_chimTRP2, pMx_IRESneo and pMx_IRESpuro.
All vector maps are listed in the annex (chapter 7.1).

pColt-Galv and pHIT60, used as helper plasmids, were already described [145] and [146].

3.4.1.2 Digestion of DNA: sc opt. TCR

sc opt. TCR (DNA template)	5µg DNA
	1x NEB 3
	1x BSA
	1x Nco I
	1x Not I
	Add to 15µl with aqua dest. Incubate for 60 min at 37 °C.

pMx_chimTRP2	5µg DNA
(vector backbone)	
	1x NEB 3
	1x BSA
	1x Nco I
	1x Not I
	Add to 15µl with aqua dest. Incubate for 60 min at 37 °C.

3.4.1.3 Digestion of DNA: dc opt. TCR

dc opt. TCR	5µg DNA
(DNA template)	
	1x CutSmart
	1x Nco I - HF
	1x Not I - HF
	Add to 10µl with aqua dest. Incubate for 60 min at 37 °C.
pMx_IRESneo	5µg DNA
(vector backbone)	
	1x CutSmart
	1x Nco I - HF
	1x Not I - HF
	Add to 10µl with aqua dest. Incubate for 60 min at 37 °C.

3.4.1.4 Digestion of DNA: wt TCR

wt TCR	1µg DNA
(DNA template)	
	1x CutSmart
	1x Bam HI - HF
	1x Not I - HF
	Add to 15µl with aqua dest. Incubate for 60 min at 37 °C.

pMx_IRESpuro	5µg DNA
(vector backbone)	
	1x CutSmart
	1x Bam HI - HF
	1x Not I - HF
	Add to 10µl with aqua dest. Incubate for 60 min at 37 °C.

DNA was incubated with restriction endonucleases to align the 3´ and the 5´ ends.

Digestion products were analyzed in an agarose gel. TCR inserts have a size of 1.8 kb and vector sizes are indicated in chapter 7.1.

3.4.1.5 Agarose gel electrophoresis

Agarose gel electrophoresis was performed to separate digested DNA according to size. For gel electrophoresis a 1% (w/v) agarose gel was prepared using 1x TAE buffer and 0.5mg/ml Ethidium bromide. Gel was stored at RT until polymerization. The digestion products were mixed 1:6 with 6x gel Loading Dye and applied into the wells of the gel. DNA ladder 1kb was mixed 1:10 with aqua dest. and 10µl were also applied as a 1x mix with loading dye on the gel. At 100V samples run for 45min in 1x TAE buffer and was visualized under UV-light.

DNA sizes corresponding to the insert and vector were cut out with a scalpel and purified.

3.4.1.6 Purification of DNA

Purification and extraction of DNA from standard agarose gels in TAE buffer was performed according to the manufacturer protocol (QIAquick Spin Handbook: QIAquick PCR Purification Kit Protocol, QIAGEN, Venlo, The Netherlands). Purified DNA was eluted with 30µl EB-buffer included in the kit.

3.4.1.7 Ligation

For the ligation of MDM2 sc opt. TCR into pMx_chimTRP2, Quick Ligation Kit was used (New England BioLabs, Frankfurt/Main, Germany). An insert:vector ratio of 3:1 was used in 20µl volume adjust with water. 20µl of 2x Quick ligation buffer was added and mixed. 1µl of Quick T4 DNA Ligase was added, mixed and incubated for 10min at RT.

For cloning of the MDM2 dc opt. TCR and the MDM2 wt TCR into pMx_IRES_neo and pMx_IRES_puro, respectively, an insert:vector ratio of 3:1 was used. Both were mixed with 1xT4 ligation buffer and 1µl T4 Ligase in a total volume of 15µl. Ligation was performed for 16h at 16°C in the water bath.

Until transformation, ligation product was chilled on ice or stored in the fridge.

3.4.1.8 Chemocompetent bacteria

Bacteria were grown overnight (ON) in 3ml LB-medium at 37°C in a shaking incubator at 250rpm. LB-medium was containing 1µl bacteria stock solution and 100µg/ml tetracycline (for XL-1 Blue) or 100µg/ml ampicillin (for JM 109). The next day OD_{550} was measured and ON culture was diluted with SOB-medium until OD_{550} was 0,05. Bacteria were cultured at 37°C and 250rpm until OD_{550} was 0,5. Bacteria were harvested in 50ml Falcon tubes and centrifuged at 1363g for 8min at 4°C. After discarding the supernatant, bacteria cells were resuspended in 30ml Tfb I and incubated for 50min on ice. Bacteria cells were centrifuged at 872g and 4°C for 6min and after removing the supernatant, cells were resuspended in 4ml Tfb II. Aliquots of 100µl were frozen at -80°C.

3.4.1.9 Transformation

After cloning the sequences encoding for the different MDM2 TCR formats into pMx-vectors all XL-1 Blue bacteria were transformed with plasmid DNA (100µl aliquots). After confirming the proper insertion into the vector by restriction digestion and agarose gel electrophoresis, JM109 bacteria were transformed with plasmid DNA.
Bacteria were incubated in the presence of 50ng DNA for 30min on ice. Transformation was carried out by performing a heat shock at 42°C for 60sec. Immediately after heat shock bacteria were cooled down on ice for 3min, transferred into falcon tubes containing 800µl LB-medium and incubated for 60min at 37°C (250rpm). Bacteria were harvested by centrifugation for 5min at RT (2400g) and resuspended in 100µl LB-medium. 70µl out of 100µl were plated on LB-ampicillin agar plates and plates were incubated agar up ON at 37°C.

3.4.1.10 Overnight cultures

Bacterial mini-cultures were started from a single colony picked from a LB-ampicillin agar plate and transferred in 5ml LB-medium containing 100µg/ml ampicillin. Incubation was performed ON at 37°C (250rpm).

Bacterial maxi-cultures were started the same way as mini-cultures, picking a single colony and transferred in 100ml LB-medium containing 100µg/ml ampicillin. Bacteria were incubated for 16h at 37°C (280rpm).

3.4.1.11 Plasmid DNA preparation

Plasmid DNA preparation of 5ml ON culture was carried out according to the manufacturer protocol (QIAprep Miniprep Handbook: QIAprep Spin, QIAGEN, Venlo, The Netherlands). Purified DNA was eluted in 30µl EB-buffer.

Plasmid DNA preparation of 100ml ON culture was carried out according to the manufacturer protocol (EndoFree Plasmid Purification Handbook: EndoFree Plasmid Maxi Kit, QIAGEN, Venlo, The Netherlands). Purified DNA was eluted in 200µl TE-buffer. After determining the concentration plasmid DNA was adjusted to 1mg/ml.

Concentration of DNA was analyzed by UV spectrometry determining the absorption at 260nm. For the measurement samples were diluted 1:50 and purity was controlled by analyzing 260/280nm ratio.

3.4.1.12 Sequencing

Sequencing of DNA-encoding TCR constructs was performed by GENterprise GENOMICS (StarSEQ GmbH, Mainz, Germany) according to the 'Homerun' program. Primers used for sequencing are listed in table 7.1.

3.4.2 Isolation of peripheral blood mononuclear cells (PBMCs)

Buffy Coats from healthy donors were obtained from the Transfusion Center of the University Medical Center Mainz.

Peripheral blood mononuclear cells (PBMCs) were isolated from peripheral blood via ficoll density gradient centrifugation. Blood was diluted 1:1 with PBS. 15ml ficoll was provided in 50ml Falcon tubes and 30ml of blood/PBS mixture were carefully pipetted on top. After

centrifugation at 1055g for 10min at RT without brake, PBMCs were isolated from the interphase between blood plasma and ficoll and washed 3 times with PBS.

Cells were either used immediately after isolation or resuspended in FCS containing 10% DMSO, aliquoted and stored at -80°C. For direct use, erythrocytes were removed with erythrocyte lysis buffer (incubation for 3min at 37°C) and washing the cells with PBS. Cells were cultured in 24 well plates in RPMI1640 containing 10% AB-serum (see 3.4.3).

3.4.3 Retroviral transduction of primary human T cells and Jurkat76 T cell line

For retroviral transduction, the packaging cell line Phoenix-Ampho was thawed and cultured in T75 flasks in DMEM. After three days, cells were trypsinized and transferred in 10cm petri dishes with a cell density of 1,2 x 10^6 cells in 8ml DMEM per plate. The next day - four hours before transfection – medium was refreshed with 6ml DMEM. For transfection of Phoenix-Ampho cells, 800µl DMEM per constructs were prepared in 1,5ml Eppendorf tubes, 35µl Fugene 6 were added and incubated 5min at RT. Then helper plasmids (pHIT 60 and pColt Galv, 5µg each) and 10µg TCR plasmid DNA were added, mixed and incubated for 15min at RT. Finally the mixture was dropped on Phoenix-Ampho cells and incubated at 37°C and 5% CO_2. The same day, frozen PBMCs (3.4.2) were thawed and stimulated with Okt-3 and Proleukin for 48h. Briefly, 2 x 10^6 PBMCs in 1ml medium per well were cultured in a 24 well plate in RMPI1640 containing 10% AB-serum, 600U/ml human IL-2 and 30ng/ml Okt-3. One day after transfection culture medium of the petri dishes containing Phoenix Ampho cells was refreshed with 8ml RPMI with 10% AB-serum. The next day, virus-supernatant (SN) was collected from the petri dishes and transferred into 50ml Falcon tubes. SN was centrifuged at 872g for 10min to remove residual Phoenix cells. Activated PBMCs were pooled in a 50ml Falcon tube and resuspended after centrifugation in virus SN at a concentration of 4 x 10^6 cells per ml of SN. Polybrene was added at a concentration of 5µg/ml and cells were distributed in 24-well plates at 0,5ml/well. After centrifugation at 872g at 32°C for 90min without brake, cells were kept in culture at 37°C and 5% CO_2 for at least 16h. Transduction efficacy was determined by flow cytometry.

Jurkat clone 76 is a human T cell leukemia deficient in endogenous TCR expression. This cell line was used as an additional model for TCR expression analysis. Jurkat 76 cells were resuspended in virus SN at a concentration of 1 x 10^6 cells per ml SN, 5µg/ml Polybrene was

added and cells were plated in 12-well plates with 1,5ml per well. Centrifugation was performed as mentioned above.

3.4.4 Restimulation and culture of human T cells

Human T cells were maintained in culture by repetitive antigen-specific stimulated once a week.

T cells were cultured in 24-well plates at 37°C and 5% CO_2. For restimulation the human chronic myelogenous leukemia cell line K562 stably expressing HLA-A2.1 and CD80 molecules was used as antigen-presenting cells (APC). Up to 5 x 10^6 APCs were resuspended in about 100µl culture medium and loaded with 10^{-4} M cognate peptide and incubated for 2h at 37°C. Afterwards 10ml culture medium was added and APCs were irradiated at 10 Gy. T cells were plated in 24-well plates at 0,5 x 10^6 cells per well in RPMI1640 containing 10% AB-serum. Irradiated APCs were added to 0,3 x 10^6 cells per well together with 600U/ml human IL-2 to obtain a final volume of 2ml/well.

3.4.5 Cell lines

Cell lines were cultured in RPMI1640 or DMEM containing 10% heat-inactivated FCS.

Phoenix-Ampho: The packaging cell line Phoenix-Ampho was purchased from Nolan Laboratory, Stanford University, USA.

Jurkat-76: The human T cell leukemia cell line is deficient for endogenous TCR expression and was obtained from Stauss laboratory, London, United Kingdom.

K562_A2 $CD80^+$: The human chronic myeloid leukemia cell line has very low MHC class I and II expression and was transfected using a vector encoding for HLA-A*0201. HLA-A2.1 positive cells were then transfected with a vector encoding for human CD80.

$EA2k^b$: The murine lymphoma cell line EL-4 originally derived from a C57/BL/6 mouse [147] was transduced with a vector encoding for A2.1/Kb chimeric gene and was derived from Sherman laboratory.

U266: The human multiple myeloma cell line has been described elsewhere [148], [149].

RPMI-8226: The human multiple myeloma cell line has been described elsewhere [148].

NCI-H929 A2.1: The human multiple myeloma cell line has been described elsewhere [148], [150]. NCI-H929 cells were transfected with a vector encoding for HLA-A*0201.

OPM-2: The human multiple myeloma cell line has been described elsewhere [148].

IM-9: The human B-lymphoplastoid cell line has been described elsewhere [148], [151].

KMS-12-BM A2.1: The human multiple myeloma cell line has been described elsewhere [148]. KMS-12-BM cells were transfected with a vector encoding for HLA-A*0201.

LP-1: The human multiple myeloma cell line has been described elsewhere [148], [152].

FD50 A2.1: The human multiple myeloma cell line was established from primary cells of a patient. The cell line was named with the initials FD to preserve patient's anonymity. Cells were transduced with a vector encoding for HLA-A*0201.

Melanoma cell lines D28, MZ9, D41 and DO5 clone #6 were kindly provided by Thomas Wölfel, University Medical Center Mainz, Germany.

3.4.6 Chromium-51 (^{51}Cr) release assay

In this assay the cytolytic function of antigen-specific T cells is measured as already described [65]. Briefly, 0,5 x 10^6 target cells were labeled with a radionuclide of a sodium ^{51}chromate salt ($Na_2{}^{51}CrO_4$) for 90min at 37°C and 5% CO_2. T cells were plated in 100µl RPMI1640 per well in 96-well round bottom plate at different effector:target (E:T) ratios: 30:1, 10:1, 3:1, 1:1 and 0,3:1. Duplicates were used for each condition. After labeling target cells were

washed 3 times with 10ml RPMI1640 and resuspended in 10ml culture medium. 100µl of this target cell suspension were added to the T cells in 96-well plates and incubated for 5h 30min at 37°C and 5% CO_2. To quantify the cytolytic activity of the T cells spontaneous and maximum chromium release of the target cells were included as controls. The maximum release was measured directly with 100µl labeled target cells in the gamma counter. Spontaneous release was determined after culturing target cells in the absence of T cells. To determine the chromium release of the samples, 96-well plates were centrifuged for 9min at 368g at RT without brake. 100µl SN per well were transferred in tubes and measured with the gamma counter. The specific lysis of target cell by the effector cells was evaluated using the following formula:

$$\frac{\text{experimental chromium release} - \text{spontaneous chromium release}}{\text{maximum chromium release} - \text{spontaneous chromium release}} \text{ x } 100 = \% \text{ specific lysis}$$

3.4.7 Transfection of multiple myeloma cell lines

Some of the investigated multiple myeloma cell lines included in this study were HLA-A2.1 negative. These cells were genetically modified with A2.1-encoding vectors as described below. Multiple myeloma cell lines NCI-H929 and KMS-12-BM were transfected by electroporation. Cells were washed with PBS and one time with Opti-MEM (490g, 5min, RT). In the meantime 0,4cm-gap electroporation cuvettes were prepared. Cells were resuspended in 120µl Opti-MEM, 10µg A2.1-encoding plasmid (pEF-BOS_puro, a modified pUC19-derived vector) were added and transferred into the electroporation cuvette. Electroporation was performed at 140V and 25ms. Afterwards, cells were cultured in 6-well plates with 3ml RPMI1640. The next day, cells were selected with 1µg/ml puromycin for 24h.

FD50 cell line was transfected by retroviral transduction (see 3.4.3) using 10µg pMx_HLA-A2.1_IRESpuro plasmid. After transduction cells were selected with 5µg/ml puromycin for 24h. Stable transfectants were generated by selection pressure as indicated above. A2.1 expression was determined by flow cytometry.

3.4.8 Western Blot

MDM2 and p53 expression in cell lines was investigated by Western Blot.

3.4.8.1 Cell lysis for protein preparation

A maximum of 5 x 10^6 cells were washed 2 times (490g, 5min, RT) and transferred to a 1,5ml-eppendorf tube. SN was discarded and cells were frozen as cell pellet at -80°C. For lysis cells were resuspended in 150µl lysis buffer (see 3.3.1) and incubated for 30min on ice in which lysates were mixed every 10min. After centrifugation at 13900g for 10min at 4°C, lysates were transferred to a new 1,5ml eppendorf tube, diluted 1:1 with 2xLaemmli Sample Buffer and heated for 5min at 95°C. Lysates were stored at -20°C.

3.4.8.2 Protein concentration measurement

The protein concentration in lysates was determined using DC™ Protein assay kit (BioRad, Hercules (California), USA). BSA standard was titrated down in the following concentrations:

1) 4000µg/ml
2) 2000µg/ml
3) 1000µg/ml
4) 500µg/ml
5) 250µg/ml
6) 125µg/ml
7) 62,5µg/ml
8) blank

2x5µl of standard (duplicates) were pipetted per well in 96-well plate; undiluted lysates were pipetted in triplicates (3x5µl). 1ml of reagent A was mixed with 20µl of reagent S and 25µl mixture A+S were added per well. Next, 200µl of reagent B was pipetted per well and incubated for 20min in the dark. Finally concentration was measured by the ELISA-Reader (540/690nm).

3.4.8.3 SDS-PAGE

Gel electrophoresis for the analysis of MDM2 protein expression was performed with 10% gel, the detection of p53 in 12% gel. Protein lysates were thawed, heated for 5min at 95°C and 20-30µg protein were loaded on the gel. Electrophoresis was performed in 1xSDS-running buffer at 70V for 45min. After samples have passed the stacking gel, voltage was increased to 130V and electrophoresis ran for additional 4h.

3.4.8.4 Blotting

PVDF-membrane was activated for 5min in methanol and afterwards washed in blotting buffer. Filter paper and fiber pads were saturated in blotting buffer. Gel was removed from the chamber and stacking gel was cut off the separating gel. The gel was washed with blotting buffer and all components were put together as a kind of "sandwich" for the wet blotting chamber in the following order:

Positive pole

- 2 fiber pads
- 3 filter papers
- PVDF-membrane
- Gel
- 3 filter papers
- 2 fiber pads

Negative pole

Chamber was filled with 3l of blotting buffer, a magnetic stir bar was added and chamber was placed on a magnetic stirrer. Blotting was performed for 20h and 200mA at 4°C in the cold room.

3.4.8.5 Blocking and visualization

After blotting membrane was washed shortly with 1xTBST and incubated for 2h at RT with 1xTBST containing 5% nonfat milk powder (NFM) powder under shaking to block unspecific binding. Membrane was washed 3 times with 1xTBST and in the meantime primary antibody was diluted 1:200 in TBST containing 5% BSA and 0,1% Tween. Incubation with antibody was performed ON at 4°C under shaking. The next day, membrane was washed again 3 times with TBST and incubated with secondary antibody (diluted 1:2000 in TBST containing 5% NFM) for 1h at RT. MDM2, p53 and GAPDH proteins were visualized with chemiluminescence.

3.4.9 Primary multiple myeloma cells

Primary multiple myeloma cells were obtained from BM aspirates of patients with multiple myeloma after informed consent and authorization by the Ethical Review Committee (under

the number 837.119.10 (7128)). Briefly, multiple myeloma cells were isolated by two different protocols: Ficoll centrifugation (see 3.4.2) and CD138 isolation by MACS separation (MACS Miltenyi Biotec, Bergisch Gladbach, Germany) according to the manufacturer protocol (3.4.10). Alternatively, multiple myeloma cells were isolated from BM aspirate by using EasySep^{TM} Human CD138 Positive Selection Kit (Stemcell Technologies, Vancouver, Canada) according to the manufacturer protocol. After selection primary cells were cultured in 6-well plates in RPMI1640 containing 10% AB-serum. The next day, cells were stained for flow cytometry (3.4.13) or used for western blot analysis (3.4.8).

3.4.10 MACS separation for CD138

Cells which were harvested after Ficoll centrifugation of BM aspirates (3.4.9) were washed one time with PBS and one time with cold FACS buffer. Cells were resuspended in 50µl/ 1 x 10^6 cells FACS buffer and stained with anti-CD138 FITC labeled antibody (5µl/1 x 10^6 cells). After incubation for 20min at 4°C cells were washed with MACS buffer and resuspended in 80µl MACS buffer per 1 x 10^7 cells. Cells were labeled with 20µl anti-FITC MircoBeads for 15min at 4°C. Afterwards cells were washed with MACS buffer and resuspended in 500µl MACS buffer per 1 x 10^7 cells. MACS® LS-columns (MACS Miltenyi Biotec, Bergisch Gladbach, Germany) were placed in the magnetic field of a MACS separator (MACS Miltenyi Biotec, Bergisch Gladbach, Germany) and equilibrated with 3ml MACS buffer. Cells were loaded on the columns to positively select labeled cells while unlabeled cells run through. After washing the columns 3 times with 3ml MACS buffer, beads-selected cells were eluted from the column with 5ml MACS buffer by removing the column from the magnetic field. Positively selected cells were counted and cultured as described in 3.4.9.

3.4.11 Multiplex Immunoassay

Cytokine production of MDM2-specific TCR transduced T cells was measured by Luminex assay. Effector T cells were incubated in presence or absence of antigen-expressing target cells (E:T = 3:1) for 3 days in a 12-well plate. Release of cytokines by T cells was determined in the culture medium by using Human Cytokine & Chemokine Panel 1A (34 plex) kit (eBioscience, San Diego, USA) according to the manufacturer protocol.

3.4.12 Animals

All mice procedures were performed according to the German federal and state regulations and approved by the responsible national authority (National Investigation Office Rhineland-Palatinate, Approval ID: 23 177-07/G16-1-016).
NSG mice were obtained from and maintained by the central animal facility of the Johannes Gutenberg University Mainz, Germany. This strain was housed under normal conditions according to the guidelines for animal care of the Johannes Gutenberg University Mainz. Mice were sacrificed by cervical dislocation.
NSG mice are deficient for T- and B- lymphocytes and natural killer cells and therefore suitable for human cell engraftment.

3.4.13 Xenograft mouse model

3.4.13.1 Tumor inoculation in NSG mice

For *in vivo* studies the multiple myeloma cell line NCI-H929 A2.1 and the melanoma cell line D28 were used. Cells were washed 2 times with PBS and the indicated amount of cells was resuspended in 200µl PBS per injection. NSG mice were shaved at the site of injection (right flank) and tumor cells were inoculated s.c. Tumor size was measured by digital caliper twice a week and calculated as the product of [length x width x width]. Mice were sacrificed by cervical dislocation when tumor size reached a volume of 1,0-1,5cm^3.

3.4.13.2 Adoptive T cell transfer (ACT) *in vivo*

Human PBMCs were stimulated and transduced as mentioned in 3.4.3. At day six after transduction TCR expression was analyzed by flow cytometry. The number of effective cells was calculated and after removing the microbeads (used for stimulation), cells were washed 3 times with PBS. Mice were exposed to red light before injection to dilate blood vessels in the tail. A number of 5 x 10^6 / 10 x 10^6 effective T cells in 100µl PBS was injected i.v. per mouse.

3.4.13.3 Interleukin-2 treatment

A stock solution of 18 x 10^6 IU Proleukin-2 was diluted in 2,5ml PBS to obtain a concentration of 7,2 x 10^6 IU/ml. 100µl of this Proleukin-2 solution were injected i.p. which means a dose of 7,2 x 10^5 IU/mouse. Proleukin-2 treatment was performed with the day of ACT.

3.4.14 Flow cytometry

Fluorescence activated cell sorting (FACS) was performed with a FACS Canto II (BD Bioscience).

3.4.14.1 Staining for flow cytometry

For FACS staining 0,2-0,5 x 10^6 cells were transferred in FACS tubes and washed with PBS containing 0,5% BSA (490g, 5min, RT). Cells were resuspended in the residual volume (~ 50µl) after removing the SN and fluorochrome-coupled antibodies (see table 3.3) were added. After staining for 20-30min at RT in the dark the samples were washed again in PBS and resuspended in 100µl / 0,1 x 10^6 cells PBS containing 1% PFA.

Except indicated anti-mouse antibodies all used FACS-antibodies were directed against human-origin epitopes. The following antibodies were used:

Table 3.3 Overview of antibodies used for flow cytometry.

Name	Fluorochrome	Clone	Company
CD3	APC	UCHT1	BD Pharmingen ™
CD4	FITC	RPA-T4	BD Pharmingen ™
CD8	APC	RPA-T8	BD Pharmingen ™
CD38	APC	HB7	BD Quantibrite ™
CD138	FITC	MI15	BD Pharmingen ™
CD152 (CTLA-4)	PE	BNI3	BD Pharmingen ™
Mouse Vβ3	PE	KJ25	BD Pharmingen ™
Mouse Vβ6	PE	RR4-7	BD Pharmingen ™

Mouse Vβ6	FITC	RR4-7	BD Pharmingen ™
CD273 (PD-L2)	PE	MIH18	BD Pharmingen ™
CD274 (PD-L1)	APC	MIH5	BD Pharmingen ™
CD279 (PD-1)	FITC	MIH4	BD Pharmingen ™
CD319 (SLAMF7)	Alexa Fluor 647	RUO	BD Pharmingen ™
HLA-A2.1	FITC	BB7.2	BD Pharmingen ™

3.4.14.2 Analysis of flow cytometry data

The analysis of flow cytometry data was performed using FlowJo software.

3.4.15 Statistical analysis

Two-tailed Student's t-test was used to compare differences between groups. P value <0.05 was considered significant.

3.4.16 Transcription activator-like effector nuclease (TALEN)

3.4.16.1 TALE construction

TALEN constructs were engineered as described by Sanjana et al. [153]. Target sequences for TALE DNA-binding site of TCR-α2 and TCR-β1 chains were published by Berdien et al. [154].

3.4.16.2 *In vitro* transcription of mRNA

For mRNA transcription plasmids were linearized using restriction enzyme Stu I and linearized DNA was purified using QIAquick PCR purification kit (Qiagen, Hilden, Germany) according to the manufacturer protocol. mRNA transcription was performed using T7mScript Standard mRNA Production System (Biozym, Hessisch Oldendorf, Germany) in accordance with the manufacturer protocol. mRNA was purified with RNeasy Kit (Qiagen, Hilden, Germany) according to the manufacturers protocol "RNA clean up".

4 Results

4.1 Modification and analysis of a TCR targeting the TAA MDM2

The MDM2-specific TCR described here is a full murine high-avidity TCR isolated from a cytotoxic T lymphocyte (CTL) clone of CD8 x A2K^b transgenic mice. This CD8-dependent TCR is recognizing the peptide sequence MDM2(81-88) in the context of A2.1 [135]. Sequences encoding for the TCR αβ chains have been identified and cloned in retroviral vectors for the transduction of human T cells.

The generated wt TCR was further modified to enhance expression level and to reduce the risk of mispairing of transgenic TCR chains with natural chains. The TCR expression of wt and modified TCRs in transduced primary human T cells and a T cell line was analyzed by flow cytometry. We also determined the affinity of the different TCR constructs for the cognate antigen and investigated effector functions of T cells transduced with these TCRs, including cytokine production and antigen-specific killing of target cells.

4.1.1 Modification of MDM2-specific TCR sequence leads to optimized construct

The sequence encoding for the wt MDM2-specific TCR isolated from the murine CTL clone has been initially cloned in retroviral pBullet-vectors. Sequences encoding for the TCR α- and β-chains were cloned in two separate vectors with puromycin or neomycin selection cassettes, respectively (figure 4.1 A). T cells had to be transduced with both plasmids for a functional TCR expression on their cell surface. For a direct comparison of the wt TCR and the modified TCR, both TCR-sequences were cloned into a pMx-vector. An equal expression level of both TCR-chains was ensured by using the virus-derived self-cleaving peptide P2A-based gene expression cassette. A schematic representation of the wt and the modified constructs is shown in figure 4.1.

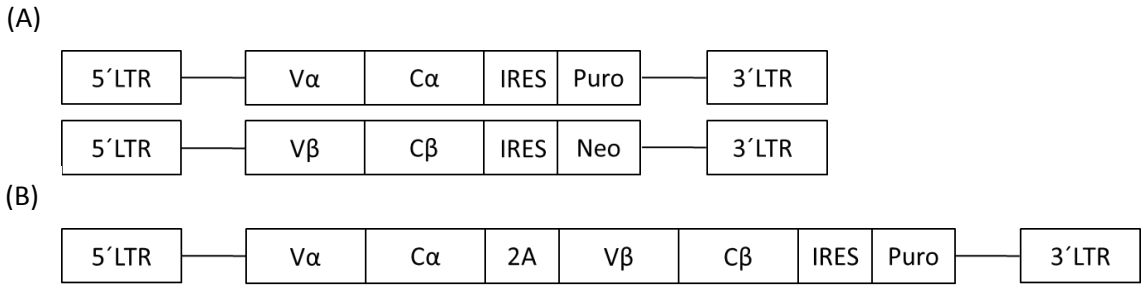

Figure 4.1 Schematic representation of wt and modified sequences encoding for MDM2-specific TCR. (A) Sequences encoding for the wt TCR α- and β-chains were cloned in pBullet-vectors containing an internal ribosome entry site (IRES)-puromycin (Puro) or IRES-neomycin (Neo) cassette. Expression of the TCR genes was controlled by the long terminal repeat (LTR) regions (B) Sequences encoding for the α- and β-chain of the TCR were cloned in 2A-based expression pMx-vector. (V) stands for TCR variable chain and (C) for TCR constant chain.

For selection of MDM2-TCR transduced cells, pMx and pBullet vectors contained a puromycin or neomycin selection sequence downstream an internal ribosome entry site (IRES) (figure 4.1). The sequence of the modified TCR was further codon optimized (opt.) to increase the expression in human T cells. An additional disulfide-bond between the constant α- and β- TCR chains has been generated by mutagenesis of residue 57 of the constant β region from serine to cysteine (S57C) and residue 48 in the constant α region from threonine in cysteine (T48C). This disulfide-bond enhances the stability of expressed TCR and reduces the risk of mispairing of transgenic and naturally expressed TCR-chains.

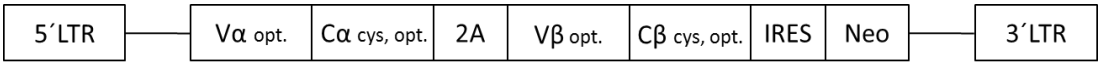

Figure 4.2 Schematic representation of optimized sequence encoding for MDM2 double-chain (dc) TCR. TCR sequence showed in figure 4.1 B was optimized and residues 57 in Cβ and 48 in Cα were exchanged by cysteine (cys.) to generate a second disulfide bond between the constant TCR domains. The TCR sequence was cloned upstream an IRES-neo cassette in a 2A-based expression pMx-vector.

The opt. and cysteine-modified (cys.) double-chain (dc) MDM2-TCR (defined as dc opt.) was cloned into a pMx-vector containing an IRES-neomycin cassette for subsequent selection of TCR-transduced T cells (figure 4.2).

The impact of these different modifications on TCR expression and TCR affinity are described in the following sections.

4.1.2 MDM2-specific TCR expression pattern is improved after optimization

To investigate the effect of TCR sequence modification and expression vector construct on the TCR expression, primary human T cells were retrovirally transduced with wt or dc opt. TCR and TCR expression analyzed by flow cytometry. Expression of MDM2-specific TCR was assessed at day 1, 4 and 11 after transduction (figure 4.3) by staining T cells with anti-murine

TCR vβ6 antibody as the β-chain of MDM2 TCR belongs to the vβ6 subfamily. Because MDM2 TCR is functional on $CD8^+$ T cells only, the TCR expression was gated on $CD8^+$ cells.

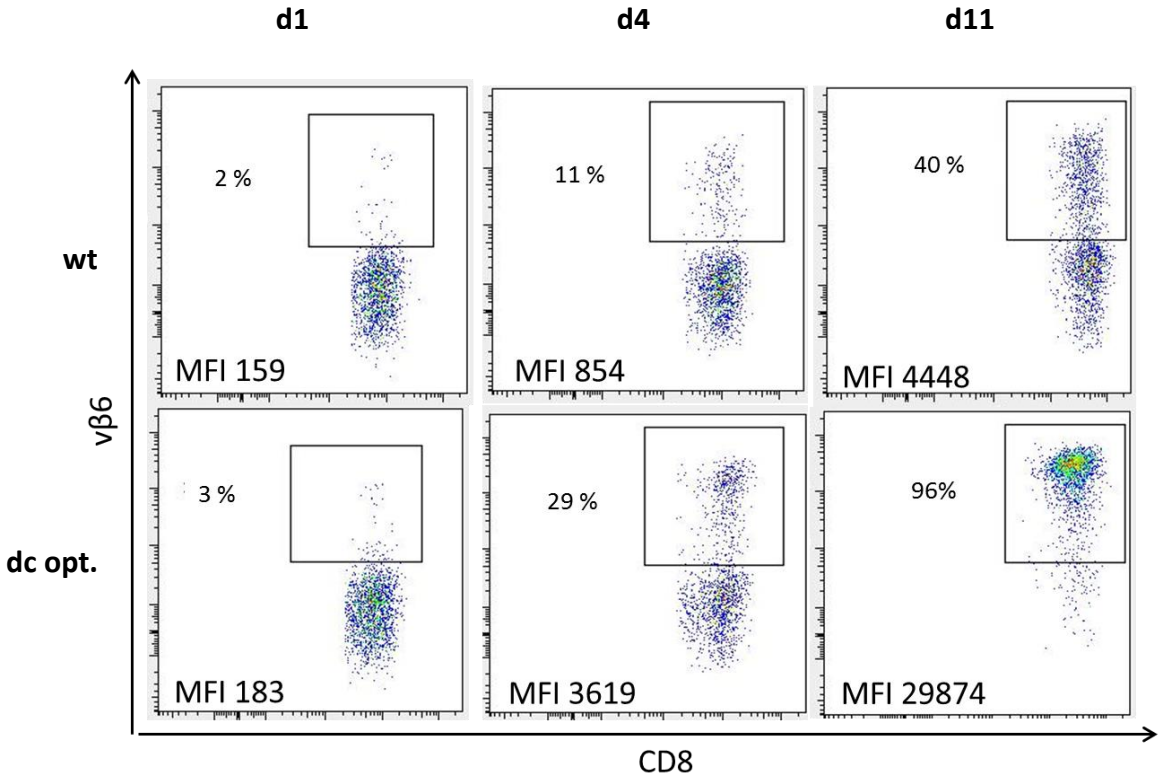

Figure 4.3 TCR expression could be enhanced after optimization of wt TCR-sequence. Flow cytometry data shows the expression of MDM2 wt and dc opt. TCR. Human T cells were retrovirally transduced with wt or dc opt. TCR and stained at day 1 (d1), d4 and d11 after transduction for human CD8- and murine TCR vβ6-expression. Analysis of percentage and mean fluorescence intensity (MFI) were determined with FlowJo software. The percentage of $CD8^+Vβ6^+$ T cells as well as the MFI of the TCR vβ6 expression is indicated.

On day 1 after transduction no difference in TCR expression could be observed between wt and dc opt. construct. But shortly after polyclonal restimulation of T cells at d4 after transduction the frequency (%) of TCR $vβ6^+$ cells obtained with the opt. construct was significantly higher compared to the wt construct (29% and 11% $CD8^+vβ6^+$, respectively). Also a 4-fold increase in the mean fluorescence intensity (MFI) which reflects the expression level of the TCR (here of the vβ6 expression) could be observed with the opt. TCR at d4 after transduction (MFI_{wt} 854 versus $MFI_{dc\ opt.}$ 3619). After selection of transgenic TCR-positive T cells via antibiotic treatment and a second antigen-specific stimulation round, TCR expression was strongly enhanced (d11 after transduction). T cells transduced with the opt. construct were nearly 100% $CD8^+vβ6^+$ whereas wt TCR-transduced T cells showed a TCR expression of about 40% $CD8^+vβ6^+$ only. The MFI of the optimized construct was 6-fold higher than the wt construct (MFI_{wt} 4448 versus $MFI_{dc\ opt.}$ 29874). The expression level of wt

TCR could not be increased in further restimulation rounds as shown in figure 4.4 at day 32 after transduction (47% and 100% $CD8^+v\beta6^+$).

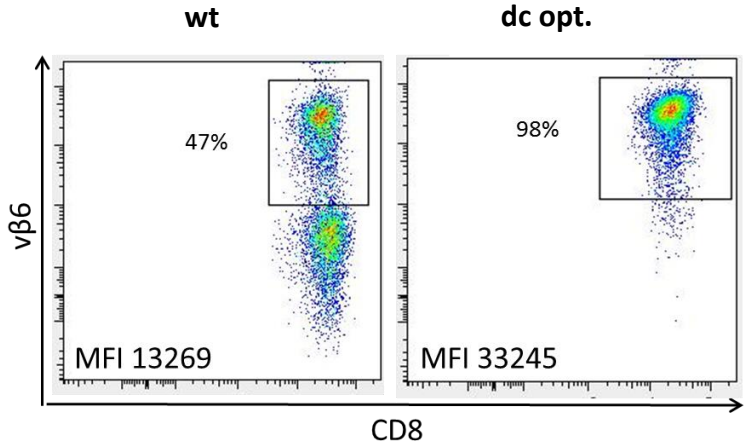

Figure 4.4 Expression level of wt TCR did not increase even after several restimulation. Flow cytometry data shows the expression of MDM2 wt and dc opt. TCR at day 32 after transduction. T cells were retrovirally transduced with wt or dc opt. TCR and stained for human CD8- and murine TCR vβ6-expression. The percentage of $CD8^+V\beta6^+$ T cells as well as the MFI of the TCR vβ6 expression is indicated.

Figure 4.4 shows that the MFI of the wt construct was increasing compared to d11 (MFI_{d11} 4448 versus MFI_{d32} 13269) but did not reach the level of the opt. construct ($MFI_{dc\ opt.}$ 33245).

4.1.3 Difference in TCR expression between wt and opt. construct may be due to mispairing with endogenous TCR chains

Due to the modifications, described in 4.1.1, the TCR expression in T cell retrovirally transduced with the opt. MDM2 TCR construct could be remarkably enhanced. The low TCR expression observed in T cells transduced with the wt construct is probably due to mispairing with naturally expressed TCR chains. To address this question a CD8- and CD4-negative T cell line lacking endogenous TCR (Jurkat 76 (JK76)) was retrovirally transduced with MDM2 wt and dc opt. TCR constructs and expression of vβ6 and CD3 were analyzed by flow cytometry (figure 4.5).

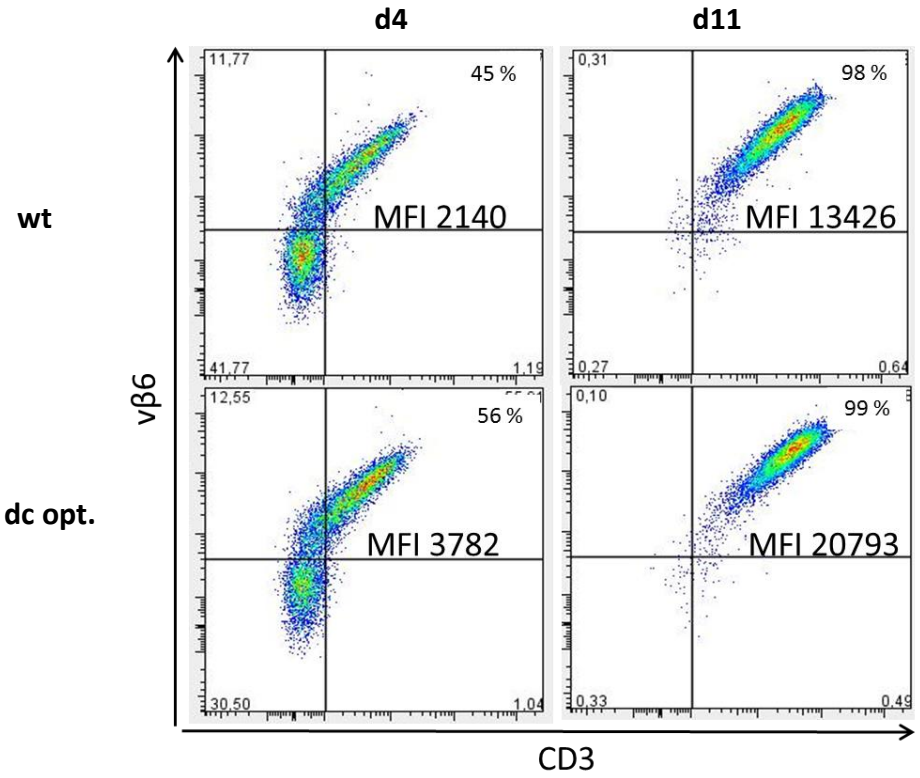

Figure 4.5 Expression of wt and dc opt. TCR are comparable in cells lacking endogenous TCR. Flow cytometry data show TCR expression in Jurkat 76 (JK76) cell line at day 4 and 11 after transduction. JK76 cells were transduced with MDM2 wt or dc opt. TCR and cells were stained for human CD3- and murine vβ6- expression. The percentage of $CD3^{+}V\beta6^{+}$ T cells as well as the MFI of the TCR vβ6 expression is indicated.

Shortly after transduction (day 4) TCR expression, as determined by cell surface expression of CD3 and TCR Vβ6 chain, was slightly higher in JK76 cells transduced with the opt. construct (56% and 45% $CD3^{+}v\beta6^{+}$). Also the MFI of the optimized construct was almost 2 times higher than of the wt construct ($MFI_{dc\ opt.}$ 3782 versus MFI_{wt} 2140). However, after selection with antibiotics TCR expression was comparable in JK76 transduced with the wt or the opt. construct (98% and 99% $CD3^{+}v\beta6^{+}$) whereas the MFI_{wt} was slightly lower than $MFI_{dc\ opt.}$ (13426 versus 20793).

These results suggest that significant mispairing occurs between the wt TCR and endogenous TCR chains resulting in low TCR expression in a competitive setting (human T cells) but high expression levels in T cells lacking endogenous TCR. To further confirm these observations, we also investigated mispairing of wt and opt. TCR directly by knocking out endogenous TCRs in T cells using TALEN (transcription activator-like effector nuclease) as gene-editing approach. Using TALEN constructs targeting sequences in the constant domains of the α- and β-chains, endogenous TCRs expression could be reduced (data not shown). However,

subsequent transduction with MDM2 wt or dc opt. TCR was not successful. We optimized the transduction and electroporation protocol by changing different parameter like stimulation conditions and stimulation period of T cells before and after electroporation, electroporation conditions or MACS separation of CD3 negative cells. Overall, we could achieve a CD3 knockout in 25% of T cells after TALEN treatment. However, these selected CD3 knocked out cells showed resistance to a further transduction with a transgenic TCR.
Another attractive gene-editing method could be the use of CRISPR/CAS9 (clustered regularly interspaced short palindromic repeats/CRISPR-associated protein 9), however for a lack of time this technique could not be set up in the laboratory.

4.1.4 Affinity of the opt. MDM2 TCR is not impaired compared to the wt TCR

After investigating the TCR expression in primary human T cells and the JK76 T cell line, the affinity of these two TCR constructs was analyzed. In a cytolytic assay target cells loaded with titrated amount of MDM2(81-88)-peptide were used. CD8 T cells transduced either with the MDM2 wt TCR or the dc opt. TCR were used as effector cells and incubated with target cells in different effector to target (E:T) ratios between 0,3:1 to 30:1. The level of specific lysis (in the presence of increased peptide concentration) was observed with the wt and dc opt. TCR-modified $CD8^+$ T cells was comparable (figure 4.6).

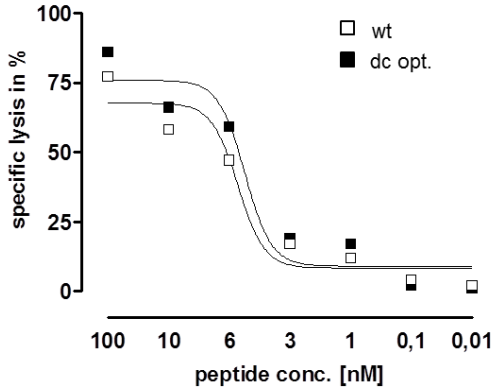

Figure 4.6 Affinity of wt and dc opt. TCR are comparable. ^{51}Cr-release assay shows the cytolytic function of effector T cells transduced with the MDM2 wt or dc opt. TCR. As target cells $EA2k^b$ cells loaded with the MDM2(81-88)-peptide in concentrations (conc.) of 100nM to 0,01nM were used. Target cells were loaded with 100µCi ^{51}Cr for 90min and then co-incubated for 5h30min with effector $CD8^+$ T cells transduced with MDM2 wt or dc opt. TCR at effector:target (E:T) ratio of 1:1. Non-linear regression analysis was performed using Prism software.

The affinities of the TCRs have been determined and defined as the concentration of peptide needed to induce a half-maximum specific lysis (EC50).

In figure 4.6 it is shown that the specific lysis activities of both TCRs were comparable and relatively high, with EC50 values of 6nM for wt TCR and 5nM for the dc opt. construct, indicating high-affinity TCRs. Importantly, performed modifications discussed in 4.1.1 did not impair the affinity of the opt. TCR construct.

4.1.5 MDM2 TCR-modified T cells showed specific lysis of overexpressing tumor cell lines

We next investigated the capacity of these TCRs to lyse tumor cell lines that endogenously process and present MDM2(81-88) peptide in the context of A2.1. A cytolytic assay was performed using an MDM2-overexpressing cell line as target and human $CD8^+$ T cells expressing either the wt or dc opt. TCR as effector cells. Different E:T ratios in the range of 30:1 to 0,3:1 have been tested (figure 4.7).

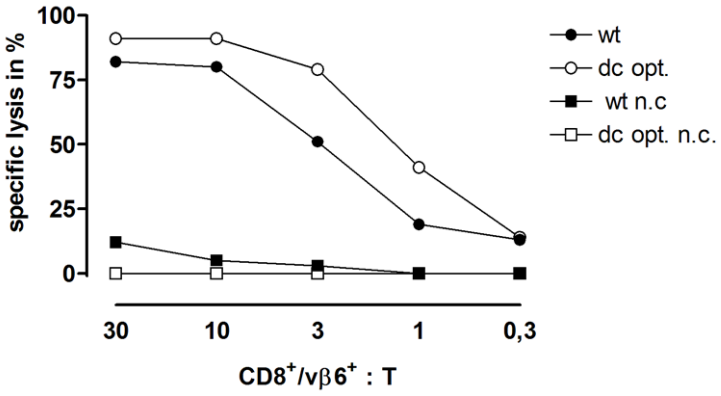

Figure 4.7 T cells transduced with MDM2 wt or dc opt. TCR showed comparable specific lysis of MDM2-expressing target cells. ^{51}Cr-release assay shows the cytolytic function of effector T cells transduced with the MDM2 wt or dc opt. TCR. As target cells (T) the MDM2-overexpressing multiple myeloma cell line NCI-H929 A2.1 was used. EA2k^b cells loaded with an irrelevant HIV-peptide served as negative control (n.c.). Target cells were loaded with 100µCi ^{51}Cr for 90min and then co-incubated for 5h30min with effector T cells ($CD8^+$/v$\beta6^+$) retrovirally at indicated E:T ratios.

Regarding the recognition of an MDM2-expressing target cell line the opt. MDM2-specific TCR showed a higher killing capacity especially at lower E:T ratios, e.g. 3:1 (80% versus 50% specific lysis) and 1:1 (40% versus 20% specific lysis). At higher E:T ratios 30:1 and 10:1 the functionality of wt and opt. TCR were similar (about 80% lysis by the wt and 90% lysis by the opt. TCR). These results show that the opt. MDM2-TCR is functional and antigen-expressing target cells are as good recognized as by the wt TCR.

4.1.6 MDM2 TCR T cells release a wide range of cytokines in response to specific antigen recognition

We also wanted to analyze another effector funtion of cytotoxic T cells and determined their capacity to release cytokines in response to antigen-specific activation. T cells transduced with the opt. MDM2 TCR were co-incubated in the presence or absence of tumor cells expressing MDM2 and A2.1. After 3 days, cytokines released into the culture medium were determined in a bead-based multiplex assay.

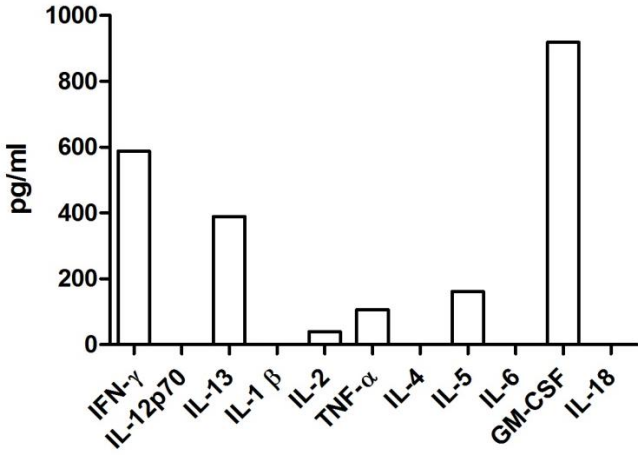

Figure 4.8 MDM2 TCR transduced T cells release different cytokines in response to antigen-specific stimulation. Multiplex assay presents the amount of cytokines produced by T cells after antigen-specific stimulation. T cells were transduced with MDM2 dc opt. TCR (E) and co-incubated with D28 melanoma cell lines (T) overexpressing MDM2 at an E:T ratio of 3:1 for 72h. As negative control T cells were incubated with culture medium only. Shown are mean values of duplicates, n=1.

$CD8^+/v\beta6^+$ T cells which were cultured with medium only without the specific activation by target cells did not release cytokines in a detectable amount. Tumor-specific activated T cells released a set of different cytokines (figure 4.8), in particular high amount of IFN-γ [600pg/ml] and GM-CSF (granulocyte-macrophage colony-stimulating factor) [1000pg/ml]. IL-13 was detected in a concentration of 400pg/ml. TNF-α and IL-5 were released at a low level [<200pg/ml]. IL-2 levels were hardly measurable [< 50pg/ml] and IL-18, IL-6, IL-4, IL-1 β and IL-12 p70 were not detected. We were expecting to see this high amount of INF-γ secretion since it is a cytokine which is released by stimulated $CD4^+$ and $CD8^+$ T cells. IL-2 is mainly produced by $CD4^+$ T helper cells and at a lower amount by $CD8^+$ cytotoxic T cells. In this experiment our antigen-specific T cell population was composed of $CD8^+$ T cells only, which may account for the low IL-2 concentration. IL-4 is also mainly produced by $CD4^+$ T helper type 2 cells, which did not compose the T cell population used in this assay. GM-CSF is a cytokine which is produced by T cells after TCR-stimulation along with the appropriate co-

stimulatory signals. Since T cells were stimulated with MDM2-expressing tumors they produced a high level of GM-CSF. IL-13 and IL-5 are produced by different cell types and also activated T cells. In summary, T cells transduced with opt. MDM2 TCR produce several cytokines after antigen-specific stimulation. All together, these results revealed a selective responsiveness of MDM2-specific CTLs upon antigen-stimulation.

4.1.7 Optimization of an MDM2-specific sc TCR enhances its expression but impairs its affinity

To further reduce any residual mispairing that may occur with the opt. TCR construct, our group has generated a so called single-chain (sc) TCR. Here the variable α and variable β domains are connected via a peptide-linker, whereas the constant α domain is co-expressed. The sequence encoding for the constant α domain and the regions encoding for the remaining TCR were cloned in two separate pBullet-vectors (figure 4.9 A). Since this sc TCR was hardly expressed after transduction of human T cells (data not shown) we decided to optimize it. The TCR sequence has been codon optimized and an additional disulfide-bond was added as well. Finally the sequences encoding for the constant α domain and the Vα-Linker-VβCβ TCR have been cloned in one pMx-vector containing a self-cleaving peptide 2A. Figure 4.9 shows the schematic representations of the sc wt and the sc opt. TCR.

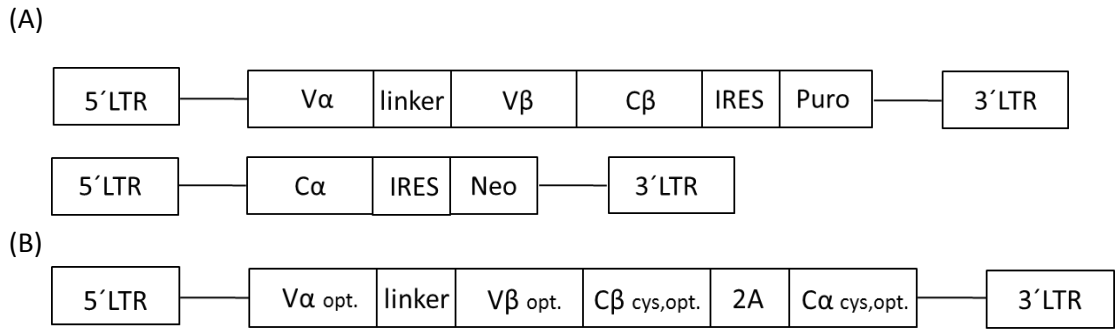

Figure 4.9 Schematic representation of the wt and opt. sequence encoding for MDM2-specific sc TCR. (A) The sequence is encoding for the sc TCR in a pBullet vector containing an IRES-puro element. The coding region of the Cα domain has been cloned in a pBullet-vector containing an IRES-neo element. (B) The sequence encoding for the sc TCR including the 2A element was codon optimized (opt.) and residues 57 in Cβ and 48 in Cα were replaced by cysteine (cys.) to generate an additional disulfide bond between the constant TCR domains. The opt. sequence was cloned in the pMx-vector.

Compared to the sc wt TCR (figure 4.9 A) cells transduced with the sc opt. TCR could not be selected with antibiotics (figure 4.9 B). As already mentioned the sc wt TCR was not expressed on the cell surface. Therefore the effect of optimization steps on TCR expression and function was tested in comparison to the wt TCR construct. As described for the dc opt.

TCR (4.1.2) T cells were transduced and TCR expression was analyzed by flow cytometry at day 1, 4 and 11 after transduction (figure 4.10).

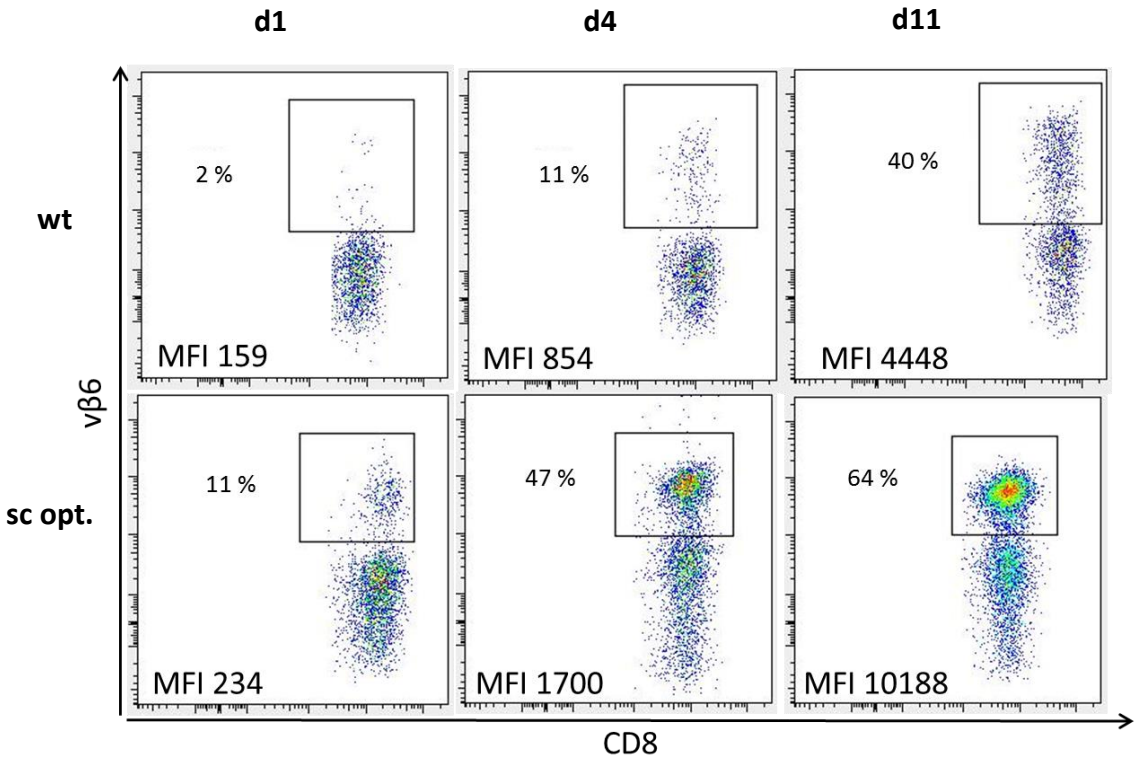

Figure 4.10 MDM2 sc opt. TCR expression is increased compared to wt TCR. Flow cytometry data show MDM2 TCR expression in transduced T cells at day 1 (d1), d4 and d11 after transduction. T cells were transduced with wt or sc opt. TCR and stained at indicated timepoints for human CD8 and murine TCR vβ6 expression. The percentage of $CD8^+v\beta6^+$ T cells as well as the MFI of the TCR vβ6 expression is indicated.

We observed a clear difference in the expression of wt and sc opt. TCRs already at day 1 post transduction. The wt TCR was hardly expressed (2% $CD8^+/v\beta6^+$) whereas the sc opt. TCR was expressed at a level of 11% $CD8^+/v\beta6^+$. At day 4 after transduction sc opt. TCR expression was 4-fold higher than wt TCR expression (47% versus 11% $CD8^+/v\beta6^+$, respectively). At day 11 after transduction sc opt. TCR expression was 64% $CD8^+/v\beta6^+$ and wt TCR expression 40% $CD8^+/v\beta6^+$ and MFI was more than 2-fold higher (MFI_{sc} 10188 versus MFI_{wt} 4448). Modifications performed based on the sc wt TCR did enhance the TCR expression of the sc opt. TCR since this construct was stably expressed whereas the sc wt TCR-construct had a poor expression. Moreover, TCR expression of sc opt. TCR was even improved compared to the wt TCR.

We performed cytolytic assays to determine the affinity of the MDM2 sc opt. and wt TCRs using target cells loaded with the MDM2(81-88)-peptide in a concentration range of 1000nM

to 0,01nM. Also the capacity to recognize and lyse antigen-expressing target cells was evaluated.

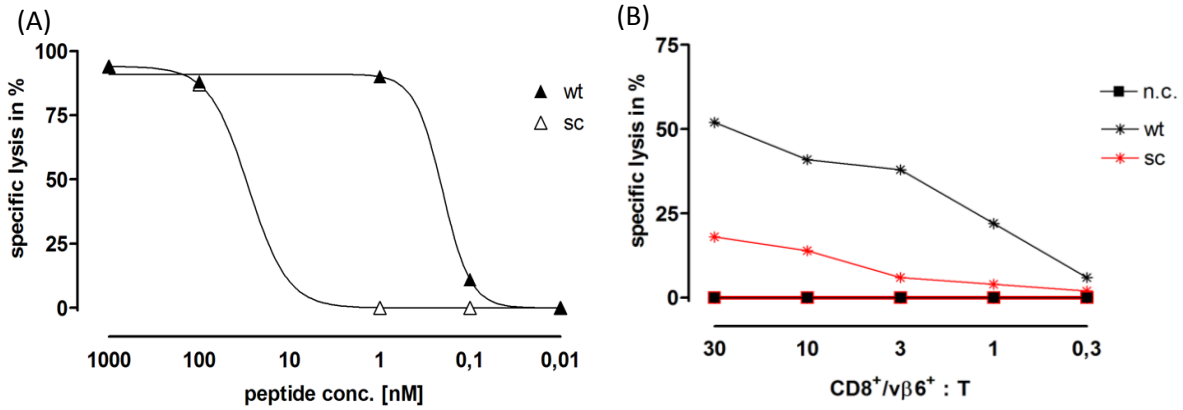

Figure 4.11 Recognition of target cells by the sc opt. TCR is impaired compared to the wt TCR. ^{51}Cr-release assay demontrates the cytoloytic function of effector T cells transduced with the wt TCR or the sc opt. TCR. As target (T) cells (A) EA2k^{b} loaded with the MDM2(81-88)-peptide in concentration of 1000nM to 0,01nM and (B) the MDM2-overexpressing melanoma cell line D28 (* stars) and the A2.1-negative cell line 397mel (n.c.) were used. Target cells were loaded with 100µCi ^{51}Cr for 90min and co-incubated with T cells (CD8^{+}/vβ6^{+}) for 5h30min (A) at an E:T ratio of 3:1 or (B) at indicated E:T ratios.

We observed a much higher EC50 of the sc TCR compared to the wt TCR (figure 4.11 A). The EC50 value for the sc opt. TCR was 47nM whereas the EC_{50} for the wt TCR was 0,3 nM. The reduced TCR affinity (of the sc TCR) was associated with a lower recognition of antigen-expressing target cells (figure 4.11 B). A2.1-negative cells served as a negative control (n.c.). These cells are not recognized by both TCRs. The antigen-expressing target cell line was two times better recognized by the wt TCR than by the sc TCR (about 50% specific lysis versus 20% at a ratio of 30:1). At the ratio 3:1 the difference is even higher (40% specific lysis versus 5%). In summary we observed a clear impairment of TCR affinity and function in T cells transduced with the sc opt. TCR. Probably the modification descibed above to enhance TCR expression changed the three-dimensional structure of the sc TCR which changed the binding site and resulted in a lower affinity. This issue was not observed after modification of the dc TCR.

In conclusion, we could enhance MDM2 TCR expression on T cell surface by optimization and reduce the formation of mispaired TCR heterodimers. The opt. TCR was still able to recognize and kill antigen-specific target cells and showed a similar affinity compared to the wt TCR. TCR expression analysis of a generated sc opt. TCR revealed an improvement compared to the wt TCR whereas TCR affinity was remarkably impaired.

Based on these data all the subsequent experiments were performed with the MDM2 dc opt. TCR.

4.2 Cytotoxic response of the MDM2-specific TCR in multiple myeloma

In chapter 4.1 we showed that we could enhance the TCR expression by modification of the TCR sequence without damping the affinity. In addition we were able to reduce the risk of TCR mispairing. To investigate the antitumor response of the dc opt. TCR *in vitro* and *in vivo*, we focused on multiple myeloma (MM) as a tumor model.

Different MM cell lines were screened for MDM2 and A2.1 expression and recognition of these cell lines by the MDM2 TCR were tested *in vitro*. Finally we analyzed the function of the MDM2 TCR *in vivo* using a xenograft mouse model.

4.2.1 MDM2 is strongly expressed in multiple myeloma cell lines

To determine the expression level of MDM2, cells were lysed and western blot analysis was performed. Figure 4.12 shows the expression of full length MDM2 (90 kDa) and the expression of the house keeping gene GAPDH (glyceraldehyde-3-phosphate dehydrogenase).

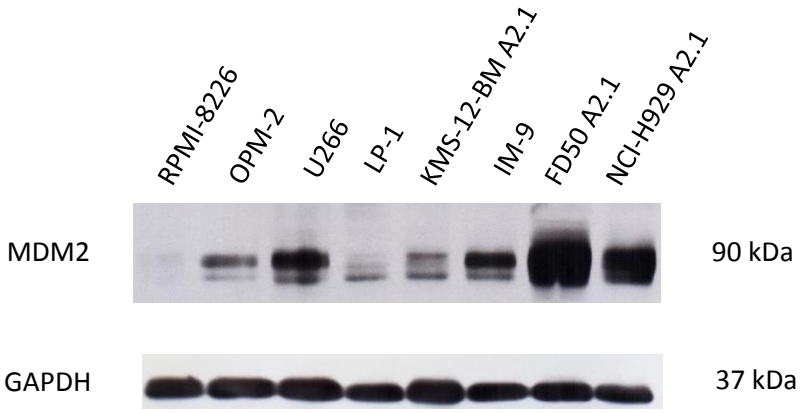

Figure 4.12 MM cell lines show a strong MDM2 protein expression. Western blot analysis shows the MDM2 protein- expression level. MM cells were lysed and 20µg protein was used for SDS-PAGE and wet blotting ON on a PVDF membrane. MDM2 protein showed a specific band at 90 kDa and GAPDH protein used as internal control at 37 kDa.

RPMI-8226 cell line showed almost no expression of MDM2 and served as a negative control (figure 4.12). The cell lines FD50 A2.1 and NCI-H929 A2.1 exhibited a very strong MDM2 expression, U266 and IM-9 a strong expression. In the OPM-2 and KMS-12-BM A2.1 cells a moderate MDM2 protein level could be detected. LP-1 cells as the RPMI-8226 cell line did not express MDM2. In total six out of eight cell lines expressed MDM2 and could serve as potential targets for MDM2 TCR-specific cytotoxicity.

4.2.2 A2.1 expression levels differ between the multiple myeloma cell lines

Since the MDM2-specific TCR is A2.1 restricted also the A2.1 expression profile of the MM cell lines was investigated. FD50, NCI-H929 and KMS-12-BM were originally A2.1 negative and were transfected with A2.1-encoding plasmid. In figure 4.13 the MFI of the A2.1 signal in the different MM cell lines is shown.

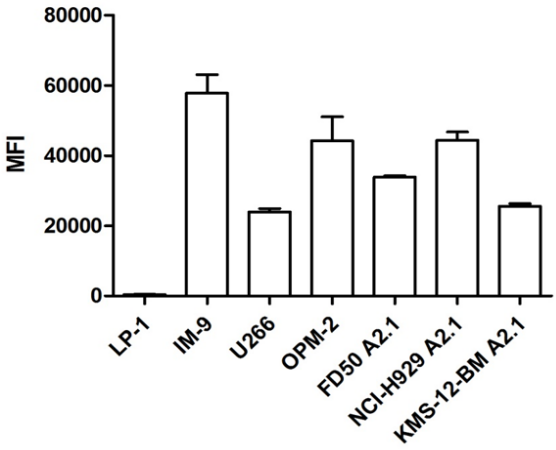

Figure 4.13 A2.1 expression level differs between the A2.1 positive MM cell lines. Flow cytometry analysis determines the A2.1 expression in MM cells. MM cells were stained for A2.1 and expression was measured by flow cytometry. MFI was calculated using FlowJo software. Mean values from three experiments are shown.

The A2.1-negative cell line LP-1 served as a negative control (figure 4.13). The cell line IM-9 has the highest A2.1 expression (MFI 59000). NCI-H929 A2.1 and OPM-2 have an intermediate A2.1 expression (MFI 48000). FD50 A2.1 cells express A2.1 with a MFI of 38000 whereas U266 and KMS-12-BM A2.1 cell lines showed the lowest expression level (MFI in the range of 25000). These results demonstrated that A2.1 expression levels strongly differ among the cell lines, which may have consequences on their recognition by MDM2 TCR-T cells.

4.2.3 A2.1 and MDM2 expression levels determine the susceptibility to lysis by MDM2-specific TCR

After determining MDM2 antigen and A2.1 expression in MM cells, we wanted to know if there is a correlation between antigen-specific recognition and expression levels of both parameters. To assess whether cells with a strong MDM2 and A2.1 expression (IM-9 and NCI-H929 A2.1) are more efficiently recognized than cells with a lower MDM2 and A2.1 expression (KMS-12-BM A2.1) we performed a cytolytic assay. Cell lines tested for MDM2

and A2.1 expression in 4.2.1 and 4.2.2 were tested in a cytolytic assay for recognition by the MDM2-specific TCR (figure 4.14).

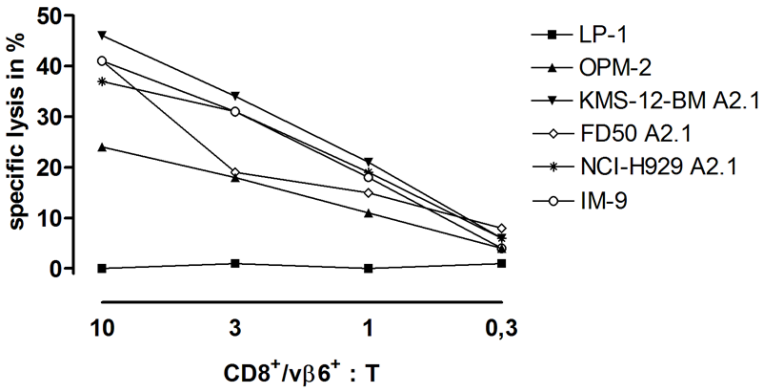

Figure 4.14 MDM2 and A2.1 expressing MM cell lines were recognized by MDM2 TCR redirected T cells *in vitro*. ^{51}Cr-assay shows the specific lysis of target cells by MDM2 TCR-transduced T cells. Indicated MM cells were loaded with 100µCi ^{51}Cr for 90min. Target cells (T) were incubated with effector CD8$^+$/vβ6$^+$ T cells (E) for 5h30min at indicated E:T ratios.

We observed a correlation between MDM2 and A2.1 expression and recognition by MDM2 TCR-transduced T cells. The A2.1 negative cell line LP-1 served as a negative control. Cells exhibiting a strong A2.1 and MDM2 expression level, as IM-9 and NCI-H929 A2.1 are efficiently lysed by effector T cells (figure 4.14). For example, 37% of NCI-H929 A2.1 and 42% of IM-9 are specifically lysed at a E:T ratio of 10:1. OPM-2 cells were less recognized (24% lysis at a E:T ratio of 10:1) although A2.1 expression was high. This result can be explained by the lower MDM2 expression in this cell line.

4.2.4 MDM2-specific TCR shows no antitumor response in mouse transfer model

After analyzing the capacity of MDM2 TCR to target MM cells *in vitro*, we were also interested in the *in vivo* efficacy of this TCR. To investigate the recognition of MM cells *in vivo* we performed a preliminary experiment with the cell line NCI-H929 A2.1 using an NSG mouse xenograft model. This cell line showed high MDM2 and A2.1 expression (4.2.1 and 4.2.2) and was therefore strongly recognized by MDM2-specific TCR –T cells (4.2.3). In the first experiment, NSG mice were injected with tumor cells (2x10^6 cells, s.c.) and transferred with human T cells (5x10^6 Mock or CD8$^+$/vβ6$^+$ T cells, i.v.) one week after tumor inoculation. When tumor size reached 1500mm^3 the animals were sacrificed and tumor and spleen were harvested for further analysis. The experimental design is shown in figure 4.15 A.

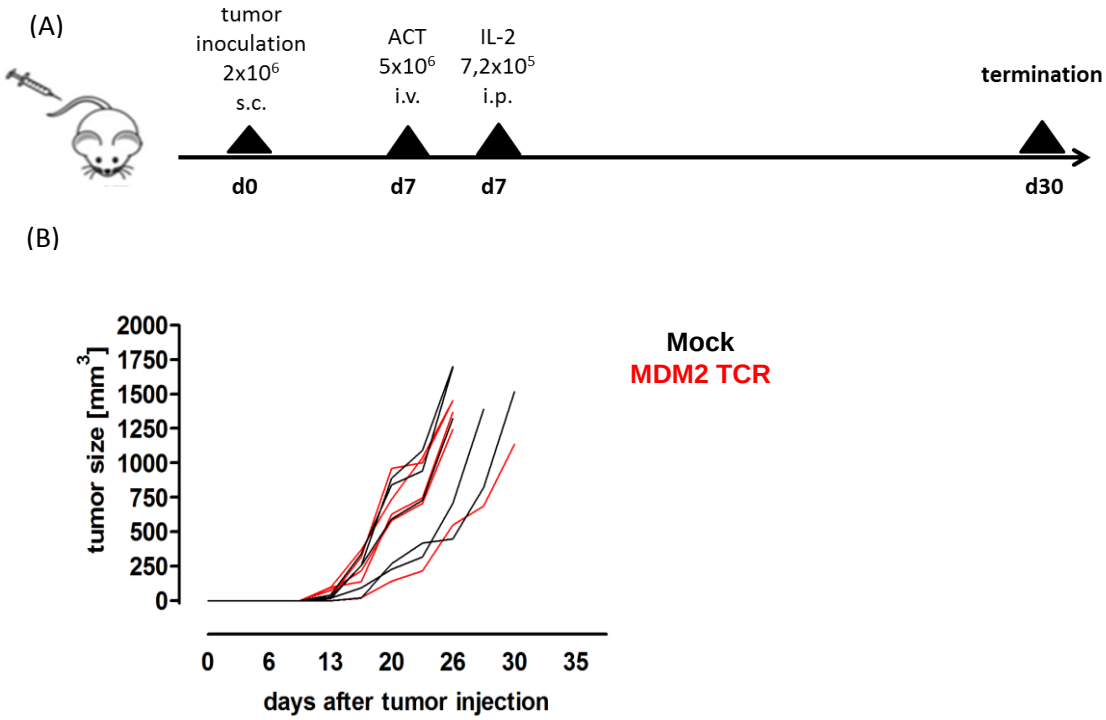

Figure 4.15 Tumor growth was not controlled by ACT of T cell transduced with MDM2 TCR. (A)) Experimental model. NSG mice were inoculated with $2x10^6$ MM cells (NCI-H929 A2.1) (s.c.) in the right flank. One week later $5x10^6$ T cells transduced with Mock or MDM2 TCR were injected (i.v.) along with $7,2x10^5$ IU IL-2 (i.p.) to boost the T cell expansion. Tumor size was measured twice a week and mice were sacrificed when tumor size reached a volume of 1000-1500mm^3. (B) Tumor growth in mice which received Mock-transduced T cells is indicated in a black line; tumor growth in mice injected with MDM2-TCR-transduced T cells is shown as a red line. Tumor volume was calculated as described in Material and Methods, n=5 per group.

Although we detected TILs which were still expressing MDM2 TCR (72% of $CD8^{+\,+}$ infiltrating T cells were positive for TCR/v$\beta6^{+}$) we could not observe tumor control in none of the mice treated with MDM2 TCR expressing T cells compared to mice treated with Mock-transduced T cells (figure 4.15 B). Both groups showed rapid tumor growth about 10 days after tumor inoculation which required the sacrifice of all mice at day 25-30 after tumor injection. Thus survival of mice was not prolonged by targeting the tumor with MDM2-specific TCR transduced T cells in this *in vivo* model. By analyzing liver, lung or gut we could not observe metastasis in this MM xenograft model.

We further analyzed *ex vivo* tumor cells and the tumor environment in more detail to understand the possible cause(s) for the lack of antitumor response observed in this tumor model.

4.3 Investigation of the tumor environment showed a tumor-escape mechanism in multiple myeloma model

We had a closer look on the tumor microenvironment to understand the circumstances which induced the lack of tumor recognition and control *in vivo*. One common way of escape mechanism of tumor cells is the down-regulation of antigens and the associated presenting molecules. Especially for the recognition of the MDM2(81-88)-peptide, which is a weak A2.1 binder, a high A2.1 expression on tumor cells is necessary to be recognized by MDM2-specific TCR transduced T cells. Another tumor-escape mechanism is the expression of inhibitory molecules. Up-regulation of PD-1, T cell immunoglobulin and mucin-domain containing-3 protein (TIM-3), lymphocyte-activation gene 3 (LAG-3) or cytotoxic CTLA-4 on TILs and the simultaneous expression of the respective ligands on the tumor cells can remarkably impair the T cell responses.

To investigate these mechanisms we first analyzed *ex vivo* tumors harvested from mice of the control group and mice treated with MDM2 TCR-transduced T cells for MDM2 and A2.1 expression. In addition the expression of inhibitory molecules on T cells and tumor cells was determined.

4.3.1 *Ex vivo* tumor cells are less recognized by the MDM2-specific TCR than parental cells due to antigen down-regulation

For analysis of the antigen expression, tumors were harvested, homogenized and lysed for detection of MDM2 protein by western blot. The investigation of A2.1 expression was performed by flow cytometry. Therefore homogenized *ex vivo* tumor cells were filtered using a cell strainer and stained. Figure 4.16 is showing the expression level of MDM2 protein and A2.1 of *ex vivo* tumor cells compared to parental cell line.

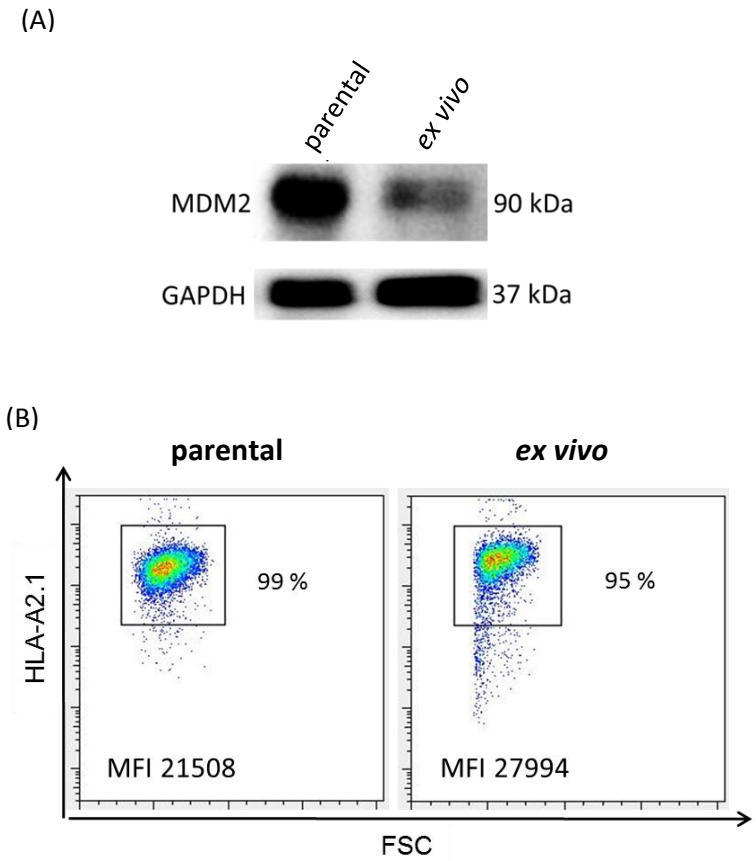

Figure 4.16 *Ex vivo* tumor cells showed a reduced MDM2 and stable A2.1 expression. Western blot analysis presents the MDM2 protein-expression level in parental and *ex vivo* tumor cells. Flow cytometry analysis was performed to determine A2.1 expression. (A) Tumors were homogenized after harvesting and erythrocytes were removed by lysis. Cells were lysed and 20µg of protein were used for SDS-PAGE and semi-dry blotting. MDM2 protein has a size of 90 kDa and internal control GAPDH shows a band at 37 kDa. (B) Tumors were treated like described in (A) and *ex vivo* tumor and parental cells were stained for A2.1 expression analysis by flow cytometry. The percentage of A2.1 positive cells as well as the MFI of the A2.1 expression is indicated.

Comparing the MDM2 expression in figure 4.16 A, we could detect a lower expression level in *ex vivo* tumor cells. This reduced expression level of MDM2 was observed in tumors harvested from mice which received Mock or MDM2 TCR-T cells (data not shown), suggesting that MDM2 antigen down-regulation is independent of the presence of T cells equipped with antigen-specific TCR. Therefore, MDM2 antigen down regulation in *ex vivo* tumor cells seems to be a general response to the tumor microenvironment. In contrast, the expression of A2.1 was not affected (figure 4.16 B). The MFI of A2.1 is even slightly higher in *ex vivo* tumor cells compared to parental cells (MFI 27994 versus 21508). These results demonstrate that tumors retain A2.1 expression at a very high level but show a reduced antigen expression in this experimental tumor model.

After determining MDM2 and A2.1 expression in harvested tumors, we investigated the effect of reduced antigen expression on the recognition of these *ex vivo* tumor cells by MDM2 TCR-T cells. For this purpose a cytolytic assay was performed (figure 4.17).

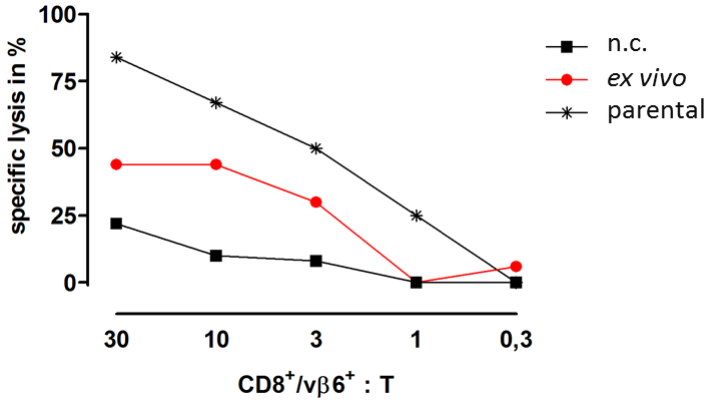

Figure 4.17 *Ex vivo* tumor cells are less recognized than parental cells by MDM2 TCR-transduced T cells. ^{51}Cr-assay shows the specific lysis of target cells by MDM2 TCR-transduced T cells. Tumors were harvested, homogenized and after lysis of erythrocytes cultured in medium over night before analysis. Target cells (T), including parental, *ex vivo* tumor cells and EA2k^{b} loaded with HIV-peptide (n.c.), were loaded with 100µCi ^{51}Cr for 90min and incubated with effector T cells transduced with MDM2 TCR (CD8^{+}/vβ6^{+}) for 5h30min at indicated E:T ratios.

Comparing the specific lysis of the parental cells and the *ex vivo* tumor cells at the highest E:T ratio 30:1 parental cells showed nearly 2-fold increase lysis (80% versus 45% specific lysis). This difference was also observed at lower E:T ratios (10:1 and 3:1). Of note, at a ratio of 1:1 recognition of *ex vivo* tumor cells is lost whereas parental cells were still lysed (30 % specific lysis). Taken this facts together we observed that *ex vivo* tumor cells were less recognized by the MDM2-specific TCR compared to the parental cell line probably due to lower antigen expression.

4.3.2 *Ex vivo* tumors showed an up-regulation of p53 expression and can be targeted by p53-specific TCR

As already described in chapter 1.2, MDM2 inhibits the expression of p53 by inducing its degradation in the proteasome. Because of this direct interaction of MDM2 and p53 proteins, we tested if *ex vivo* tumor cells also exhibited a change in p53 expression beside the altered MDM2 expression. For analysis of p53 protein expression cell lysates of parental and *ex vivo* tumor cells were used as shown in 4.3.1. Figure 4.18 exhibits the MDM2 expression which was already described in 4.3.1 and the p53 expression of parental and *ex vivo* tumor cells.

Figure 4.18 MDM2 down regulation is associated with p53 up regulation in *ex-vivo* tumors. Western blot analysis determines MDM2 and p53 expression in parental and *ex vivo* tumor cells. Tumors were harvested, homogenized and lysed for SDS-PAGE. Proteins of *ex vivo* and parental cells (20µg) were used for gel electrophoresis and semi-dry blotting. MDM2 has a molecular size of 90 kDa and p53 shows a band at 53kDa. GAPDH (37 kDa) served as an internal control.

As a consequence of MDM2 down regulation in *ex vivo* tumor cells (figure 4.18 A) we observed a stronger expression of p53 in these cells compared to parental cells (figure 4.18 B). A reduction in MDM2 expression can lead to less inhibition of p53 expression, and thus more p53 protein in these tumor cells. Our data showed that NCI-H929 A2.1 exhibit a different phenotype *in vivo* (compared to 2 dimension *in vitro* cell culture condition) by modulating their MDM2/p53 protein expression levels.

We assumed that shortly after injection of the tumor cells, MDM2 expression remains high in these cells. Then gradually the level of MDM2 is decreasing and the amount of p53 is increasing. As we did not know the exact kinetic of this antigen modulation process, we decided to target both proteins by co-transducing T cells with MDM2- and p53-specific TCRs. Figure 4.19 is showing the TCR expression of T cells retrovirally transduced with MDM2- and p53-specific TCRs and the recognition of parental and *ex vivo* tumor cells by TCR co-transduced T cells. TCR expression was analyzed by performing flow cytometry staining and functional activity of transduced cells was tested in a cytolytic assay.

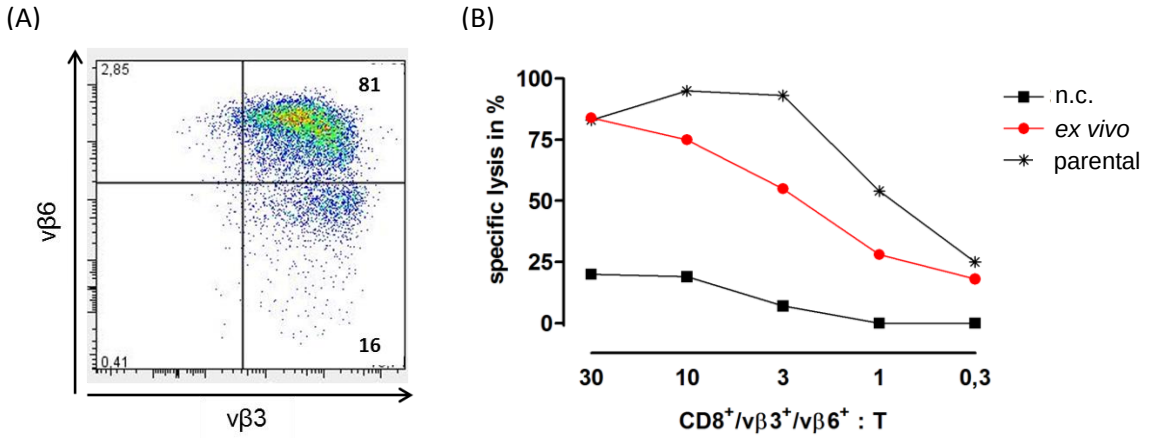

Figure 4.19 T cells transduced with MDM2- and p53-specific TCR can strongly recognize ex *vivo tumor* cells. Flow cytometry data show the MDM2-and p53-TCR expression in T cells transduced with both TCRs at day 14 after transduction and ^{51}Cr-release assay determines the effector function of TCR co-transduced T cells. T cells were transduced with MDM2 dc TCR and p53 sc TCR. (A) TCR expression levels were analyzed by flow cytometry by staining for vβ3-PE (p53 TCR) and vβ6-FITC (MDM2 TCR) at day 14 after transduction. (B) Co-transduced T cells were used as effector cells (CD8$^+$/vβ3$^+$/vβ6$^+$) in a ^{51}Cr-release assay. Target cells (T) were NCI-H929 A2.1 parental and *ex vivo* tumor cells and EA2k^b loaded with irrelevant HIV-peptide (n.c.). Target cells were loaded with 100µCi ^{51}Cr for 90min and incubated with the effector T cells for 5h30min at indicated E:T ratios.

The p53-specific TCR is a sc opt. TCR which is well established and its function has been proven already [155] and [156]. This TCR belongs to the vβ3 subfamily and can be stained for flow cytometry with anti-murine vβ3 antibody. T cells which are shown in figure 4.19 A are 100% CD8$^+$ (data not shown) and almost 100% of cells were expressing vβ3. 81% were positive for vβ3 and vβ6, and 16% of the cells were expressing vβ3 only. Thus T cells used in the cytolytic assay (figure 4.19 B) represent almost a pure vβ3$^+$/vβ6$^+$ population.

The recognition of *ex vivo* tumor cells by the co-transduced cells at an E:T ratio of 10:1 is lower than lysis of parental cells (75% versus 90%) (figure 4.19 B). At an E:T ratio of 1:1 both targets were still recognized (parental cells 60 % lysis versus 30% lysis of *ex vivo* tumor cells). Comparing the recognition of *ex vivo* tumor cells by the MDM2-specific TCR alone (figure 4.17) we observed a stronger lysis by co-transduced T cells (figure 4.19). Since also the killing of the parental cell line was stronger by co-transduced T cells compared to MDM2 TCR alone, p53 TCR seems to have an additive effect on the lysis of target cells in general. p53 TCR alone is killing *ex vivo* tumor cells as good as the MDM2 TCR alone (data not shown) and recognizes the parental cells as well. We could not detect p53 expression in parental tumor cells (figure 4.18 B) probably because of high MDM2-expression and -activity mediated p53 degradation. Most likely, degraded p53 in parental cells is highly expressed as peptide on the cell surface and therefore target cells are strongly recognized by the p53-specific TCR. These data demonstrate that transduction of T cells with MDM2- and p53-specific TCRs leads to a stronger lysis of *ex vivo* tumor cells compared to MDM2 TCR alone.

Therefore we performed an *in vivo* experiment targeting the cell line NCI-H929 A2.1 with these two antigen-specific TCRs to investigate the effect we have observed *in vitro*. After co-transduction of T cells with MDM2 and p53 TCRs the expression level of each TCR is lower than after single-transduction (data not shown) which limits their use for ACT *in vivo*. So we tested if mixing single-transduced T cells and co-transduced T cells are recognizing target cells to similar levels. T cells were transduced with MDM2- or p53-specific TCR and mixed in 1:1 ratio or simultaneously co-transduced with both TCRs and used as effector cells in a cytolytic assay. Single-transduced cells were 100% TCR/$CD8^+$ (data not shown) and co-transduced T cells showed TCR expression displayed in figure 4.19 A. The specific lysis of NCI-H929 A2.1 cells by these effector cells is shown in figure 4.20.

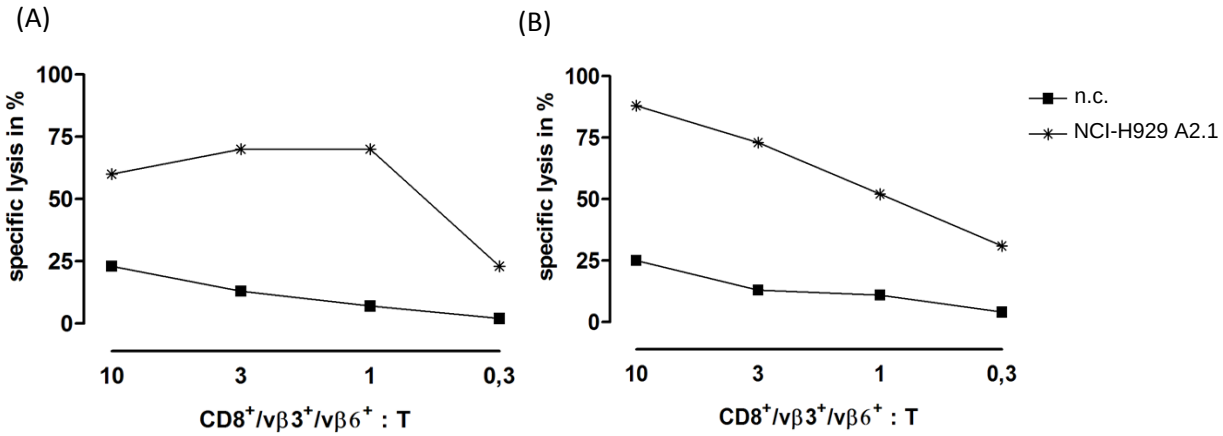

Figure 4.20 MDM2- and p53-TCR co-transduced T cells show similar recognition of target cells as mixed single-transduced T cells. ^{51}Cr-release assay shows the effector function of MDM2- and p53-TCR co-transduced T cells and mixed single-transduced T cells. EA2k^b loaded with irrelevant HIV-peptide and NCI-H929 A2.1 cells (used as target cells, T) were loaded with 100µCi ^{51}Cr for 90min. T cells were transduced with (A) MDM2- and p53-TCR (co-transduction) or (B) single-transduced with MDM2- or p53-TCR and mixed together in a 1:1 ratio. Target and effector T cells were incubated at indicated E:T ratios for 5h30min.

EA2k^b cells loaded with HIV peptide served as negative control. Figure 4.20 A shows the recognition of NCI-H929 A2.1 cell line by co-transduced T cells and figure 4.20 B the recognition by mixed single-transduced cells. Co-transduced T cells lysed 70% of the target cells at E:T ratios 3:1 or 1:1. Mixed single-transduced cells lysed 75% and 60% of the cells at the same ratios.

Since the killing capacity is comparable we decided to use single-transduced T cells for the following *in vivo* experiment. Beside the killing capacity of transduced cells also TCR expression is a crucial factor for ACT efficacy. TCR expression in co-transduced cells is lower than in single transduced cells, so separation of TCR-expressing cells would be required to increase TCR-positive T cell population for ACT. As manipulation of T cells before ACT may

affect their activity *in vivo* we performed further experiments with mixed single-transduced T cells.

For the *in vivo* experiment we inoculated mice with NCI-H929 A2.1 and injected one week later Mock- or TCRs-modified T cells and boosted T cells expansion with IL-2. Mice were subdivided into four different groups at the day of T cells injection and received T cells transduced with (i) Mock, (ii) p53-specific TCR, (iii) MDM2-specific TCR or (iv) a mix of MDM2- and p53-specific TCRs. The experimental design is described in figure 4.21 A.

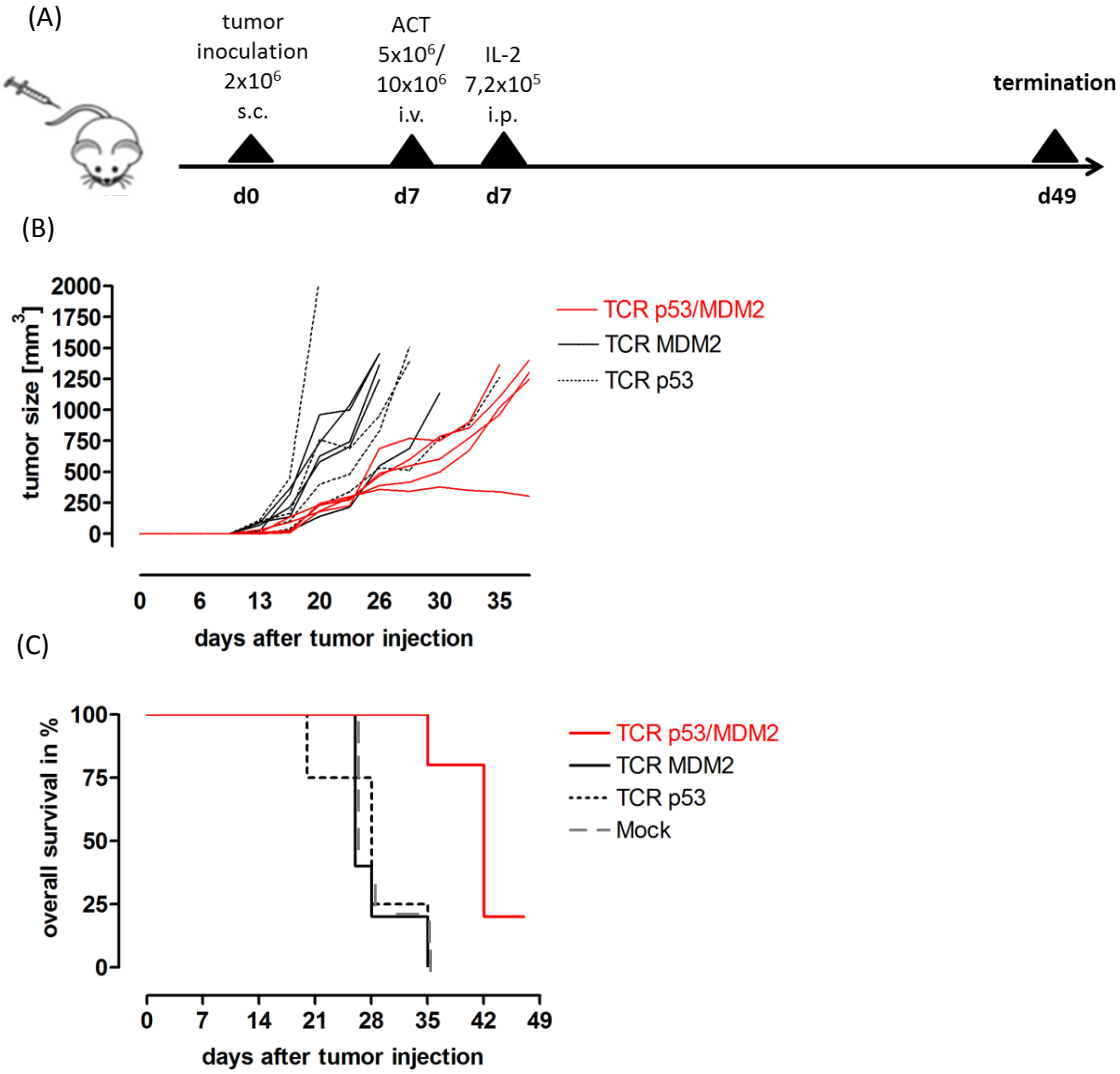

Figure 4.21 ACT targeting two antigens delayed tumor growth and prolonged mouse overall survival. (A) NSG mice were inoculated with 2x10^6 MM cells (NCI-H929 A2.1) (s.c.) in the right flank. One week later mice were infused (i.v.) with 5x10^6 T cells transduced with Mock, MDM2 TCR, p53 TCR or a mix of MDM2- and p53-TCR T cells (5x10^6 cells each). The same day 7,2x10^5 IU IL-2 were applied (i.p.) to boost the T cell expansion. (B) Tumor growth in mice which received Mock-transduced T cells is not shown here; tumor growth in mice injected with MDM2 TCR- or p53 TCR-transduced T cells is shown as black lines (solid and dashed, respectively). The red line is indicating tumor growth in mice injected with a mix of transduced T cells at 1:1 ratio. Tumor volume is calculated as described in Material and Methods. (C) Overall survival of mice is expressed as percent, n=5 per group.

The tumor growth in mice which received Mock-transduced T cells is not shown in figure 4.21 B to have a better overview. But as shown in figure 4.21 C there is no difference in terms of tumor growth between mice which were treated with Mock-transduced or MDM2 TCR-transduced T cells.

Comparing the tumor growth in mice which received p53 TCR- or MDM2 TCR-transduced T cells there is no difference in tumor growth (figure 4.21 B). Neither T-cell transfer with MDM2 TCR nor p53 TCR could induce a measureable tumor control. Only the mice which were injected with a mix of MDM2- and p53 TCR-transduced T cells showed a delay in tumor growth, including one mouse with full tumor protection.

The benefit of using two antigen-specific TCRs for targeting the tumor was observed also in terms of overall survival (figure 4.21 C). As already described above (figure 4.15 B), MDM2-TCR T cell transfer is not effective in this tumor model. Also the p53-TCR group showed a similar survival compared to the Mock group. Only mice treated with T cells expressing both antigen-specific TCRs exhibited a clear prolonged overall survival. A more striking difference could be noted at day 28 after tumor injection, where only 20-25% of mice treated with Mock-, MDM2- or p53-TCR were alive, while all mice infused with p53/MDM2 TCRs were still alive. At day 35, 80% of p53/MDM2 TCRs treated mice were still alive while all the mice from the other groups had to be sacrificed earlier.

In summary, we could not observe tumor control in mice treated with MDM2 or p53 TCR. Only the combination of both TCRs resulted in a prolonged overall survival of mice inoculated with MM. However, tumors could not be eradicated except in one mouse. Further analysis of *ex vivo* tumors and infiltrating T cells demonstrated a strong up-regulation of inhibitory molecules which may account for this partial antitumor response in this tumor model.

4.3.3 Expression of inhibitory molecules is up-regulated in *ex vivo* tumor cells and TILs

In addition to antigen down-regulation, expression of inhibitory molecules is another potential tumor-escape mechanism. Tumor cells can increase their expression of PD-L1 and PD-L2 which bind to PD-1 on T cells. Activation of this inhibitory pathway can remarkably impair antitumor T cell response.

We were also wondering whether inhibitory molecules could be detected in *ex vivo* cells in our MM model. Therefore *ex vivo* tumors and spleens from tumor-engrafted mice were analyzed for expression of different cell surface markers. To discriminate tumor cells from murine cells and TILs, cells were stained with anti-HLA-A2.1 because injected T cells were derived from A2.1 negative donors. To identify human T cells within the tumor mass and murine splenocytes, cells were co-stained with anti-human CD3 antibody. First PD-L1/L2 expression in *ex vivo* tumor cells was investigated. Figure 4.22 is showing one representative example of PD-L1 expression in parental and *ex vivo* tumor cells harvested from mice treated with p53/MDM2-TCRs (experimental setting figure 4.21).

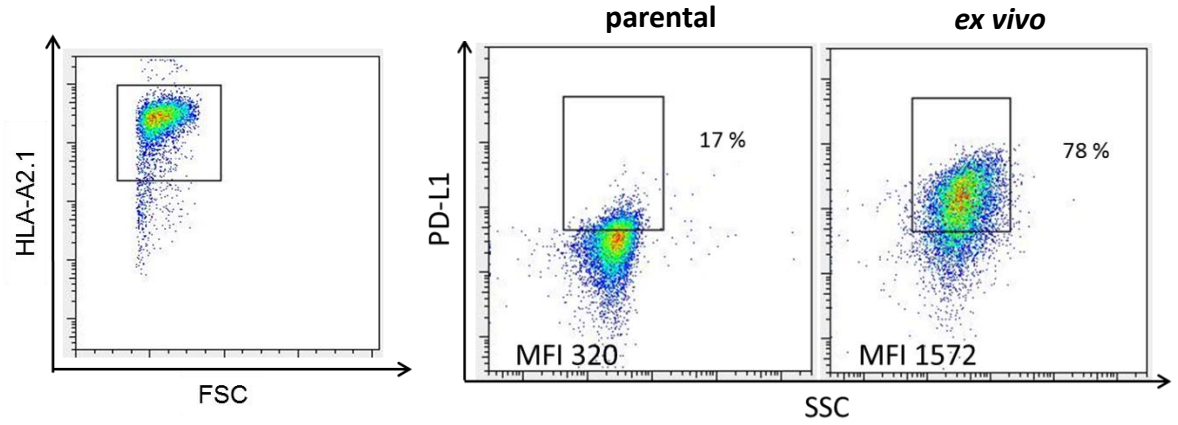

Figure 4.22 PD-L1 expression is up-regulated in ex vivo tumor cells. Flow cytometry data show PD-L1 expression on A2.1 gated tumor cells (left panel). Tumors were harvested, homogenized and erythrocytes were lysed. Parental and *ex vivo* tumor cells were stained for A2.1 and PD-L1 for flow cytometry analysis. The percentage of PD-L1 positive cells as well as the MFI of the PD-L1 expression is indicated.

Parental NCI-H929 A2.1 cells expressed PD-L1 at a weak level (17%) (figure 4.22). The expression of PD-L1 in *ex vivo* tumor cells increased up to 78% and the MFI in these cells was 5-fold higher than in the parental cells (1572 versus 320). It is important to mention that increased expression level illustrated in figure 4.22 was observed in tumors harvested from mice regardless of the TCR treatment. We analyzed tumors harvested from mice of each group and at different time points after tumor injection. The collected data from 11 mice are depicted in figure 4.23.

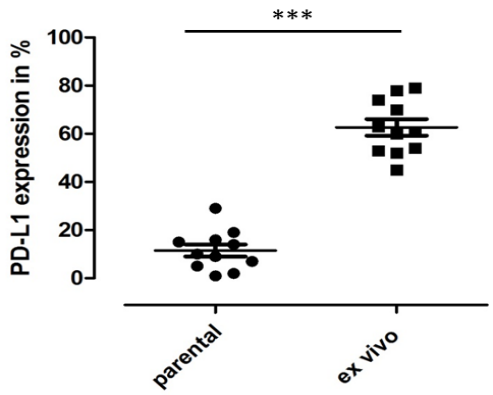

Figure 4.23 PD-L1 up-regulation is observed in all *ex vivo* tumors independently of the treatment. PD-L1 expression was investigated by flow cytometry as shown in figure 4.22. PD-L1 expression in percent of parental and *ex vivo* tumor cells of all treatment groups are summarized, n=11. Statistical analysis was performed with t test, *** means a p value < 0,001.

The mean PD-L1 expression in parental NCI-H929 A2.1 cells is 12% (+/- 3%). In *ex vivo* tumor cells the mean expression is significantly higher (63% +/- 3%). In contrast, PD-L2 and PD-1 which can be expressed on tumor cells were not detectable neither in parental nor in *ex vivo* tumor cells (data not shown).

We then analyzed PD-1 expression in TILs and spleen-infiltrating T cells to determine if the corresponding receptor for PD-L1 was also expressed. T cells recovered from tumors and spleens were stained for PD-1 expression. Figure 4.24 illustrates one representative example of PD-1 expression in TILs and spleen-derived T cells in comparison to control.

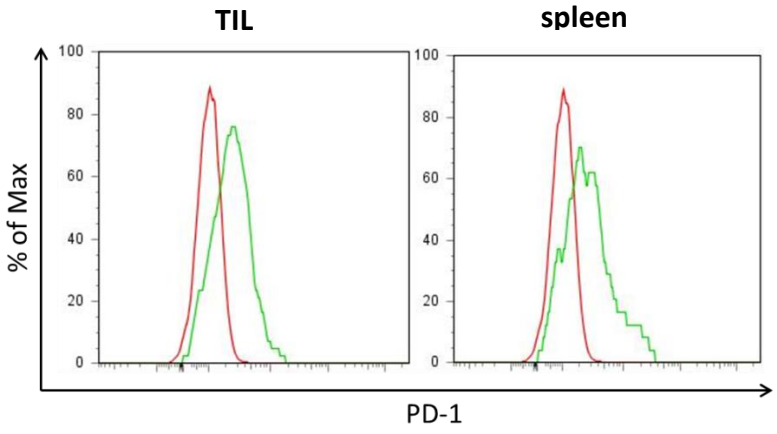

Figure 4.24 Tumor infiltrating T cells and T cells infiltrating the spleen showed enhanced PD-1 expression. Flow cytometry analysis presents PD-1 expression in T cells. Tumor and spleen were harvested, homogenized and erythrocytes were removed by lysis. Cells were stained for CD3 and PD-1 and expression was analyzed by flow cytometry. Histograms show the PD-1 expression in $CD3^+$ gated cells. PD-1 expression in TILs and spleen infiltrating T cells is indicated as green line in comparison to the parental T cell line (red line).

In TILs (left panel) and in T cells from spleen (right panel) a clear up-regulation of PD-1 was detectable compared to the parental T cell line (figure 4.24). The MFI in TILs was 658 and in T

cells from spleen 551 whereas in the parental T cell line the MFI was 153. A more global analysis of PD-1 expression in T cells infiltrating tumors and spleens from all groups was investigated and data are summarized in figure 4.25.

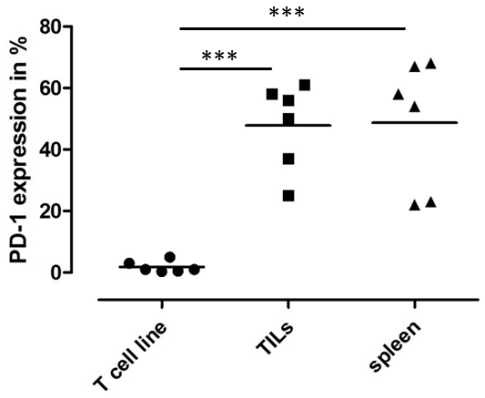

Figure 4.25 PD-1 expression is enhanced in T cells infiltrating tumor and spleen *in vivo*. PD-1 expression was investigated as described in figure 4.24. PD-1 expression in percent of T cells from tumor or spleen were collected and MDM2 TCR-T cell line was used as a control for PD-1 expression, n=6. Statistical analysis was performed with t test, *** means p< 0,001.

PD-1 expression in MDM2 TCR-T cell line is nearly undetectable (2% +/- 1%). In TILs, PD-1 expression however is 48% (+/- 6%). PD-1 expression in T cells recovered from the spleen is equal to expression level in TILs (49% +/- 9%). T cells were also tested for CTLA-4 expression but neither the T cell line nor *ex vivo* T cells express CTLA-4 (data not shown). In summary, we could detect an enhanced expression of inhibitory molecules in tumor cells and TILs *in vivo*. This microenvironment "profile" may account for the partial antitumor response of T cells in the xenograft mouse model presented in figure 4.21.

Our next step was therefore to combine adoptive T cell transfer with immune checkpoint blockers.

4.3.4 Combination of checkpoint inhibition and adoptive T cell transfer improves the antitumor response

Immune-checkpoint inhibitors (ICIs) are new classes of very effective therapeutic antibodies already used in cancer immunotherapy. Different drugs have been tested so far or will be tested in future trials targeting for example PD-1, PD-L1, CTLA-4, TIM-3, LAG-3 or TIGIT (T cell immuno-receptor with Ig and ITIM domains).

For our MM xenograft mouse model we chose the anti-PD-1 antibody nivolumab (Opdivo®) in combination with adoptive T cell transfer using two antigen-specific TCRs. The experimental design is described in figure 4.26 A.

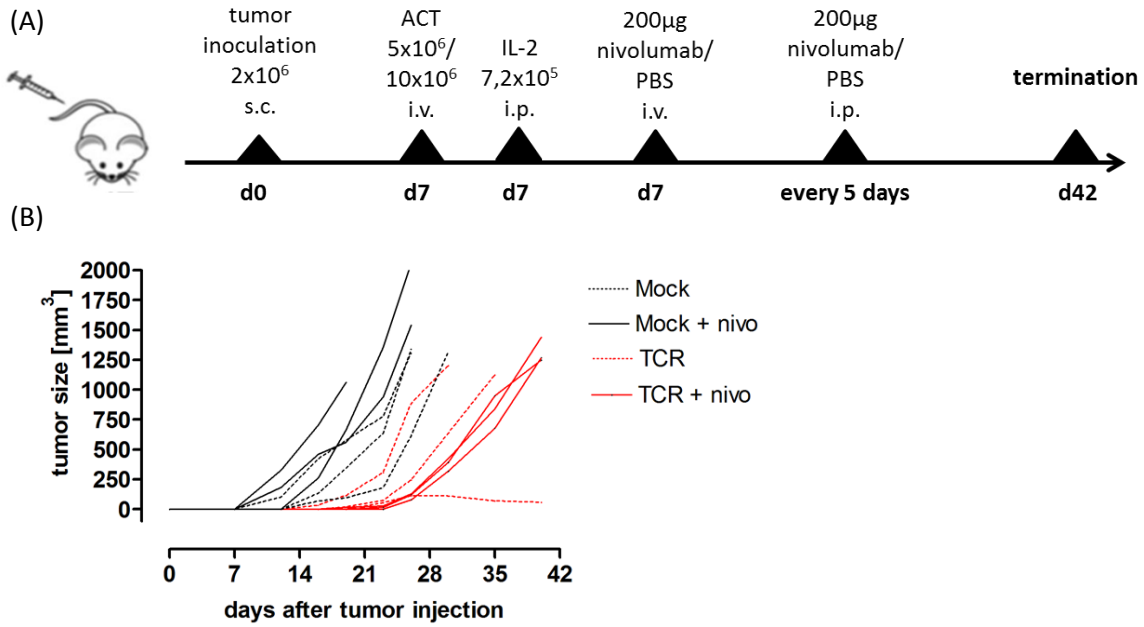

Figure 4.26 Tumor growth was slightly delayed in the combination therapy group. (A) NSG mice were inoculated with $2x10^6$ MM cells (NCI-H929 A2.1) (s.c.) in the right flank. One week later $5x10^6$ T cells transduced with Mock or a mix of T cells transduced with MDM2 or p53 TCR ($5x10^6$ T cells each) were injected (i.v.) along with $7,2x10^5$ IU IL-2 (i.p.) to boost the T cell expansion. At day 7 (post tumor inoculation) the first injection of nivolumab (200µg/mouse) was applied (i.v.) followed by repetitive injections of nivolumab (i.p) every five days (for a total of 8 injections). (B) Tumor growth in mice which received Mock-transduced T cells +/- nivolumab is shown as a black line (solid and dashed lines, respectively). The red line is indicating tumor growth in mice injected with a mix of MDM2 and p53 TCRs transduced T cells at 1:1 ratio +/- nivolumab (solid and dashed lines, respectively). Tumor volume is calculated as described in Material and Methods, n= 3 mice per group.

Because we saw no antitumor response by T cells transduced with MDM2- or p53 specific TCR alone (figure 4.21) we did not include these groups in the present experiment and compared mice which received T cells transduced with (i) Mock, (ii) Mock + nivolumab (nivo) treatment, (iii) p53/MDM2 TCR (TCR) and (iv) TCR + nivo treatment. Tumor growth in these mice is presented in figure 4.26 B. We observed a slight enhanced tumor growth in mice treated with nivolumab in the mock groups (figure 4.26 B). In mice which received p53/MDM2 TCR-transduced T cells tumor growth was also delayed compared to Mock group as already described in the previous experiment (figure 4.21). Nivolumab treatment in the p53/MDM2 TCR group was associated with a slight delay in tumor growth compared to untreated p53/MDM2 TCR group, yet T cell transfer did not result in tumor control.

We further evaluated this combination therapeutic approach using another anti-PD-1 antibody. Pembrolizumab (Keytruda®) treatment was investigated in mice injected with T cells transduced with (i) Mock + pembrolizumab (pembro), (ii) p53/MDM2 TCR (TCR) and (iii) TCR + pembro. The experimental setting of ACT combined with pembrolizumab treatment is shown in figure 4.27 A.

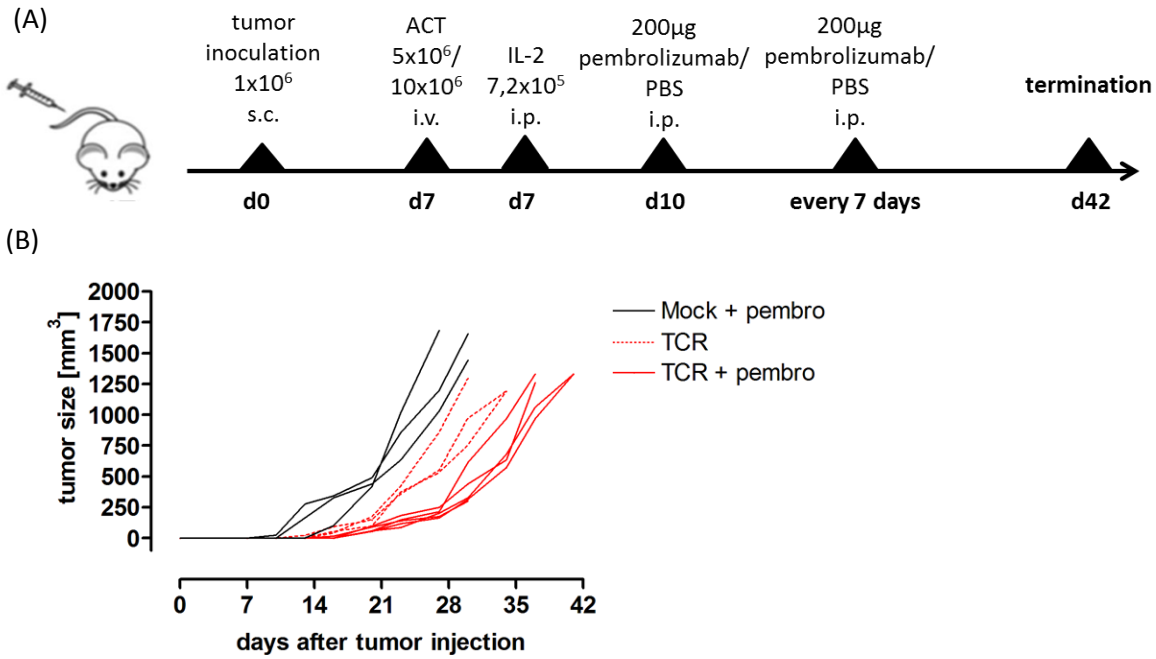

Figure 4.27 Tumor growth was delayed in mice treated with ACT and anti-PD-1 antibody. (A) NSG mice were inoculated with $1x10^6$ MM cells (NCI-H929 A2.1) (s.c.) in the right flank. One week later $5x10^6$ T cells transduced with Mock or a mix of T cells transduced with MDM2 or p53 TCR ($5x10^6$ T cells each) were injected (i.v.) along with $7,2x10^5$ IU IL-2 (i.p.) to boost the T cell expansion. At day 10 the first injection of pembrolizumab (200µg/mouse) was applied (i.p.) followed by repetitive injections (i.p) every seven days (for a total of 5 injections). (B) Tumor growth in mice which received Mock-transduced T cells + pembrolizumab (pembro) is shown as a black line. The red line is indicating tumor growth in mice injected with a mix of MDM2 and p53 TCR transduced T cells at 1:1 ratio +/- pembro (solid and dashed lines, respectively). Tumor volume is calculated as described in Material and Methods. n= 3 mice for mock + pembro or TCR groups and n=5 animals for TCR + pembro group.

The antitumor effect of combination therapy with ACT and nivolumab (figure 4.26 B) or pembrolizumab (figure 4.27 B) is comparable. Pembrolizumab treatment in mice injected with Mock-transduced T cells had no effect on the tumor growth (figure 4.27 B). Mice treated with MDM2/p53 TCR transduced T cells developed palpable tumors at later time points and tumor growth was slower compared to Mock group, confirming our previous data. The combination of MDM2/p53 TCR transduced T cells and pembrolizumab treatment had an additive antitumor effect compared to ACT alone, as observed with nivolumab therapy (figure 4.27 B). Although this combination approach led to an improved overall antitumor response, it did not result in full tumor protection.

These results strongly suggest that combination of ACT with one checkpoint inhibitor is most likely not sufficient in this tumor model. Maybe we have to target also PD-L1 on the tumor site or SLAMF7 (signaling lymphocytic activation molecule family member 7) receptor (CD319), another new target molecule for MM therapy. SLAMF7 is expressed on most primary MM cells and the cell line NCI-H929 A2.1 used in our MM model.

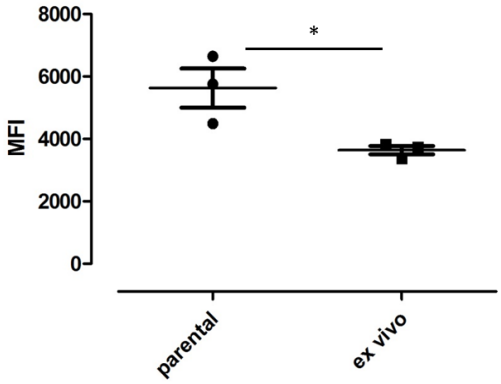

Figure 4.28 Parental and *ex vivo* tumor cells express SLAMF7. Expression of SLAMF7 was investigated by flow cytometry analysis. *Ex vivo* tumor cells were harvested and prepared as described elsewhere. Parental and *ex vivo* NCI-H929 A2.1 tumor cells were stained for SLAMF7 and expression was analysed by flow cytometry. MFI was analyzed by FlowJo software, n=3. Statistical analysis was performed with t test, * means p<0,05.

Figure 4.28 shows the expression level of SLAMF7 in parental and *ex vivo* tumors harvested from tumor-engrafted NSG mice (model described above). Parental cells expressed SLAMF7 at a high level (MFI 5632 +/- 626). This marker remains expressed in *ex vivo* tumors yet at lower levels (MFI 3640 +/- 136) compared to parental cells. In conclusion, NCI-H929 A2.1 tumor cells remain SLAMF7 positive *in vivo* suggesting their potential susceptibility to anti-SLAMF7 antibody therapy (in our xenograft model). Since we did not detect CTLA-4 expression in T cells *in vivo* (at least in this model) we did not consider the combination of nivolumab and ipilimumab.

In summary, we could observe synergistic antitumor response of ACT and checkpoint inhibition, yet to improve adoptive T cell immunotherapy combination with other immunotherapeutic approaches should be evaluated.

4.3.5 Full tumor protection is achieved with dual TCR ACT in mice engrafted with low tumor load

To demonstrate the therapeutic potential of our dual TCR ACT approach in MM, we modified the experimental setting as follow. Mice were inoculated with a lower tumor cell number and ACT was performed two days earlier compared to the previous experiments (see figure 4.29 A).

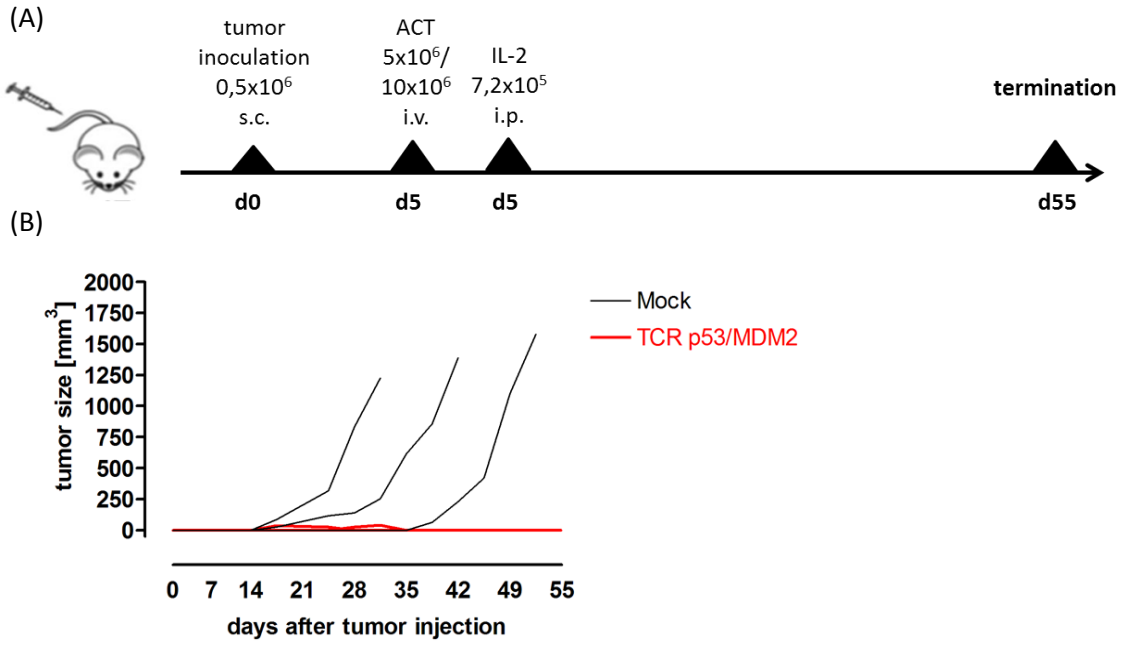

Figure 4.29 Mice treated with p53/MDM2 TCR-transduced T cells control the tumor in a modified tumor model. (A) NSG mice were inoculated with 0,5x10^6 MM cells (NCI-H929 A2.1) (s.c.) in the right flank. Five days later 5x10^6 T cells transduced with Mock or a mix of cells transduced with MDM2 or p53 TCR (5x10^6 T cells each) were injected (i.v.) along with 7,2x10^5 IU IL-2 (i.p.) to boost the T cell expansion. (B) The black line shows tumor growth of mice which received Mock transduced T cells, and in red line mice which received p53/MDM2 TCR transduced T cells. Tumor volume is calculated as described in Material and Methods, n= 3 mice per group.

In this experimental setting mice treated with p53/MDM2 TCR-transduced T cells controled the tumor until the experiment was terminated (figure 4.29 B). Between day 14 and 30 palpable tumors were observed but were rapidly eradicated and mice remained tumor-free until they were sacrified. Tumors in the Mock group showed a slower growth compared to the previous experiments because of the lower tumor load. In two mice tumors started to grow at day 14 after tumor injection and in the third animal palpable tumor was even detected at day 35.

So we could show that MM cells can be eradicated *in vivo* by p53/MDM2 TCR-transduced T cells in a model with low tumor load. We did not investigate if MDM2 TCR transduced T cells alone could control the tumor in this modified model but this experiment is a proof for the functionality of ACT in this MM tumor model. The main aim of this section is to establish an *in vivo* model were impaired antitumor T cell response in adoptive T cells transfer experiment can be improved by combined therapy with other approaches.

4.4 Investigation of primary multiple myeloma cells

In the sections 4.2 and 4.3 we tested different human MM cell lines for A2.1 and MDM2 expression and analyzed if MM could be targeted by MDM2-specific TCR in adoptive T cell therapy. For this purpose we wanted to extend this question to primary MM cells freshly isolated from bone marrow of patients. Primary MM cells behave differently from cell lines. Primary cells do not usually proliferate *in vitro* and can be maintained in culture for few days only. Because we were limited in cell numbers we focused on the analysis of MDM2 expression in these cells and expression of inhibitory molecules. Since we observed an up-regulation of inhibitory molecules in the tumor microenvironment *in vivo* models (4.3), we were also interested in primary MM cells for the expression of these molecules.

4.4.1 MDM2 expression can be detected in primary multiple myeloma cells

In section 4.2 we could show MDM2 overexpression in most of the investigated MM cell lines. Therefore we analyzed MDM2 expression in primary MM cells.

From bone marrow aspirates of MM patients, tumor cells were isolated by Ficoll centrifugation and selection for CD138 with MACS separation. Purified MM cells were lysed and analyzed for MDM2 expression by western blot. Figure 4.30 shows the MDM2 expression of eleven MM patient samples.

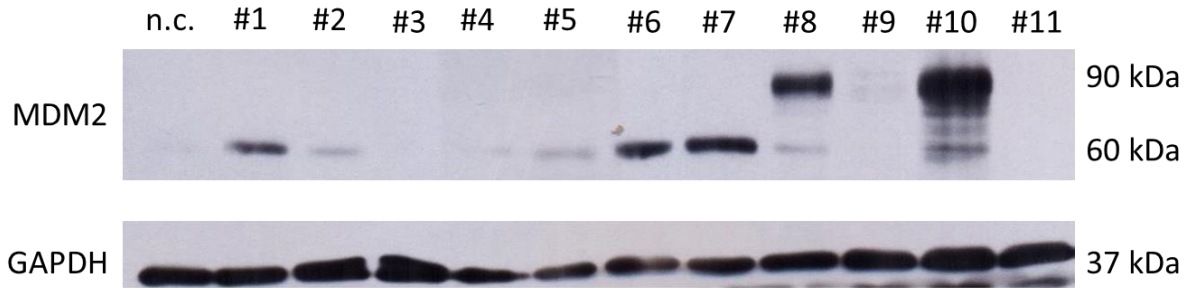

Figure 4.30 Most of the investigated primary MM cells express MDM2 protein. Western blot analysis shows MDM2 protein expression level in CD138-purified primary MM cells isolated from patient BM-aspirates. Primary cells were lysed and 30µg protein was used for SDS-PAGE and wet blotting ON on a PVDF membrane. Lysate of MDM2-low expressing cell line RPMI-8226 was used as negative control (n.c.). MDM2 protein showed two bands at 90 kDa and 60 kDa. GAPDH protein (37 kDa) was used as internal control.

In two samples we could detect a strong 90 kDa (full length) MDM2 band (#8 and #10). In samples #1, #6 and #7 a 60 kDa MDM2 cleaved form is strongly expressed. This form results from the cleavage of the full length MDM2 by caspase 3 at the C-terminal part. Interestingly, the 60 kDa cleaved form of MDM2 was not detectable in MM cell lines (figure 4.12). A faint

expression of 60 kDa MDM2 is measurable in samples #2, #4, #5, #8 and #10. Samples #3, #9 and #11 showed no detectable MDM2 expression. In total MDM2 expression could be detected in eight out of eleven samples.

4.4.2 Primary multiple myeloma cells do express T cell-associated inhibitory molecules

To determine whether the up-regulation of PD-L1 described in our MM cell line-based *in vivo* model (4.3.3) is a common strategy of tumor escape mechanism in MM patients, we tested also primary MM cells for PD-L1/L2 expression. For this purpose cells were stained immediately after isolation for flow cytometry analysis. Figure 4.31 illustrates the expression of PD-L1, PD-L2 and PD-1 in primary MM cells.

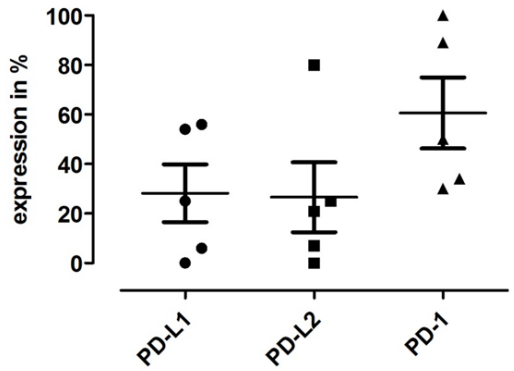

Figure 4.31 Most of primary MM cells express inhibitory molecules. Expression of PD-L1, PD-L2 and PD-1 was investigated by flow cytometry analysis. Primary MM cells were isolated from BM-aspirates of patients by Ficoll-centrifugation and CD138-MACS separation. Cells were stained for PD-L1, PD-L2 and PD-1 and expression was analyzed by flow cytometry. Expression levels are indicated in percent, n=5.

MM cells from 5 patients were analyzed for expression of inhibitory molecules (figure 4.31). The mean expression of PD-L1 was 28,2% (+/- 11,7%). PD-L2 was expressed at a mean level of 26,6% (+/- 14,1%) and PD-1 expression was the highest (60,6% +/- 14,3%). In comparison with our *ex vivo* tumor cell model (NCI-H929 A2.1), PD-L1 expression was lower in primary MM cells. But PD-1 which could not be detected in *ex vivo* NCI-H929 A2.1 cells was strongly expressed in primary tumor cells. The same goes for PD-L2 expression. Although we analyzed only few samples we could observe that expression of inhibitory molecules, in particular PD-L1, PD-L2 and PD-1, seems to be a frequent event in MM cells, suggesting a potential tumor escape mechanism.

4.5 Analysis of melanoma as another suitable cancer type for MDM2-specific TCR-based therapy

MDM2 is overexpressed in several cancer types, including soft tissue sarcoma, multiple myeloma, liposarcoma, glioblastoma and melanoma. Malignant melanoma is a common and often aggressive type of cancer with a high mortality rate. Immunotherapy with checkpoint inhibitors was a breakthrough and remains the front-line treatment option for the aggressive forms of melanoma since the approval of ipilimumab (anti-CTLA-4) in 2011 and pembrolizumab and nivolumab (anti-PD-1) later on.

So we were also interested to study melanoma as a new target for MDM2-specific TCR-based immunotherapy. We first tested melanoma cell lines for expression of A2.1 and MDM2 and the recognition of these cells by the MDM2-specific TCR *in vitro*. We further investigated the capacity of MDM2 TCR to target melanoma *in vivo* using a xenograft mouse model.

4.5.1 MDM2 and A2.1 expressing melanoma cell lines are recognized by MDM2-specific TCR

We first determined A2.1 expression levels in melanoma cell lines by flow cytometry and the corresponding MDM2 protein expression was analyzed by western blot (figure 4.32).

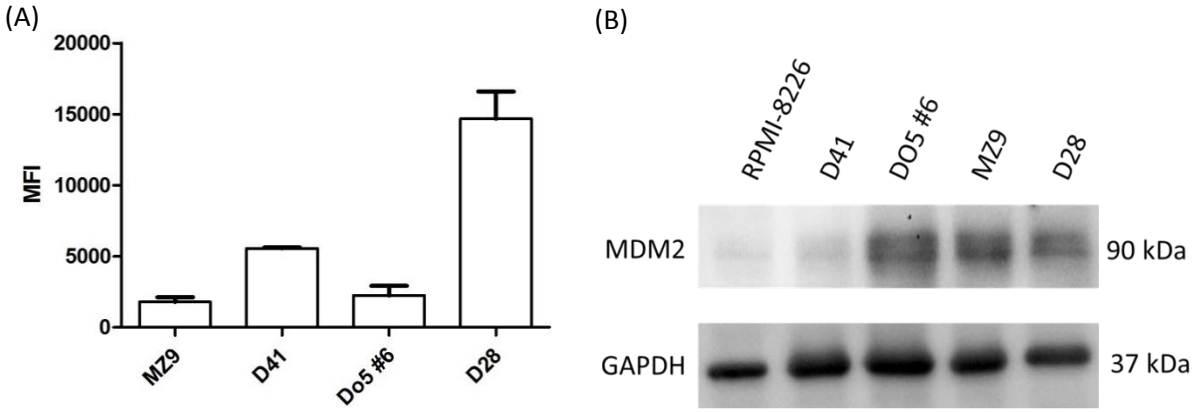

Figure 4.32 Analysis of A2.1 and MDM2 protein expression in melanoma cell lines. Flow cytometry analysis shows HLA-A2.1 expression in melanoma cells. MDM2 protein expression was determined by Western blot. (A) Melanoma cells were stained for A2.1 and expression as well as MFI were determined by flow cytometry. Mean values of three experiments are presented. (B) Melanoma cells were lysed and 20µg protein were used for SDS-PAGE and blotted semi-dry on a PVDF membrane. Lysates of MDM2-low expressing cell line RPMI-8226 were used as reference. MDM2 showed a band at 90 kDa and internal control GAPDH at 37 kDa.

Among the four tested melanoma cell lines D28 cells expressed the highest level of A2.1 (MFI 15000) (figure 4.32 A). A2.1 expression of D41 was three times lower than D28 (MFI

5000). The MFI of A2.1 in DO5 clone #6 (DO5 #6) was 3540 and 2400 in MZ9. Expression in DO5 #6, MZ9 and D41 was nearly in the same range whereas expression level in D28 was remarkably higher. MDM2-low expressing cell line (RPMI-8226) was included for comparison (figure 4.32 B). In D41 cells, a very weak expression could be measured. DO5 #6, MZ9 and D28 cells exhibited a moderate MDM2 band.

In summary, we observed MDM2 expression in three out of four tested melanoma cell lines. D28 cells had a very high A2.1 expression and moderate MDM2 protein expression. MZ9 and DO5 #6 cell lines exhibited a moderate MDM2 expression but A2.1 expression levels were much lower than in D28. D41 cells showed hardly MDM2 expression whereas the A2.1 level is higher than in MZ9 and DO5 #6.

To analyze the relationship between A2.1 and MDM2 expression levels in melanoma cell lines and their corresponding specific recognition by MDM2-specific TCR, a cytolytic assay was performed. Figure 4.33 shows the specific lysis of melanoma cell lines by MDM2-specific TCR transduced T cells.

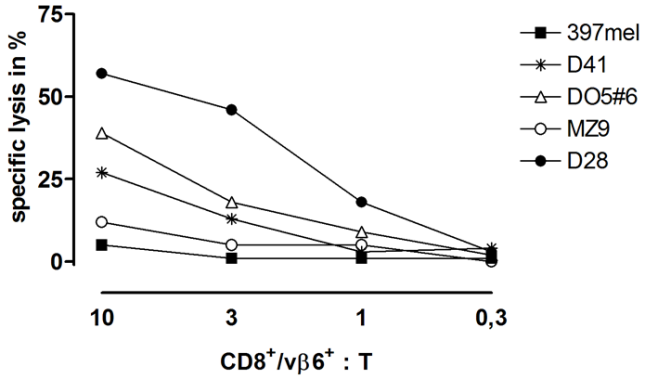

Figure 4.33 Melanoma cell lines were recognized by MDM2-specific TCR according to their A2.1 and MDM2 expression levels. ^{51}Cr-release assay shows the lysis of melanoma cells by MDM2-specific TCR. Indicated target cells (T) were loaded with 100µCi ^{51}Cr for 90min and incubated with effector T cells transduced with MDM2-specific TCR ($CD8^+/v\beta6^+$) for 5h30min at indicated E:T ratios.

The A2.1 negative MDM2 positive melanoma cell line 397mel served as a negative control. This cell line showed no specific lysis (figure 4.33). MZ9 cells which exhibited a strong MDM2 but a low A2.1 expression were hardly recognized by MDM2-specific TCR probably because of weak MHC molecule expression. DO5 #6 cells showed a similar MDM2 expression as MZ9 cell line whereas A2.1 expression was slightly higher. This resulted in a stronger lysis of DO5 #6 cells (35% at 10:1 ratio and 20% at 3:1 ratio). MDM2 expression of D41 cell line was hardly detectable but A2.1 expression was higher than in MZ9 or DO5 #6 which translated into better lysis by T cells compared to MZ9 cells (25% at a ratio 10:1) but less than DO5 #6

cells. The highest A2.1 expression was observed in D28 cells. Together with an intermediate MDM2 expression this leads to a strong recognition by MDM2-specific TCR with 55% specific lysis at 10:1 ratio and 50% at 3:1 ratio. These results implicate a strong correlation of A2.1 expression and recognition of cells by MDM2-specific TCR. A2.1 expression seems to be determinant as MDM2(81-88)-peptide is a weak binder to A2.1 molecule.

Since we observed specific lysis of melanoma cell lines by MDM2-specifc TCR *in vitro* we performed TCR transfer experiment in a xenograft mouse model to investigate the capacity of MDM2 TCR to recognize melanoma *in vivo*.

4.5.2 Targeting melanoma cells *in vivo* with MDM2 TCR transduced T cells resulted in a moderate tumor growth delay

We investigated the antitumor efficacy rate of MDM2 TCR *in vivo* in a preliminary xenograft mouse model using NSG mice inoculated with the human melanoma cell line D28. This cell line was chosen as target cells in the following experiment because it was efficiently lysed *in vitro* by MDM2 TCR. For ACT, seven days after tumor inoculation human T cell transduced with MDM2 TCR were injected. In the control group mice received Mock-transduced T cells. The experimental design is depicted in figure 4.34 A.

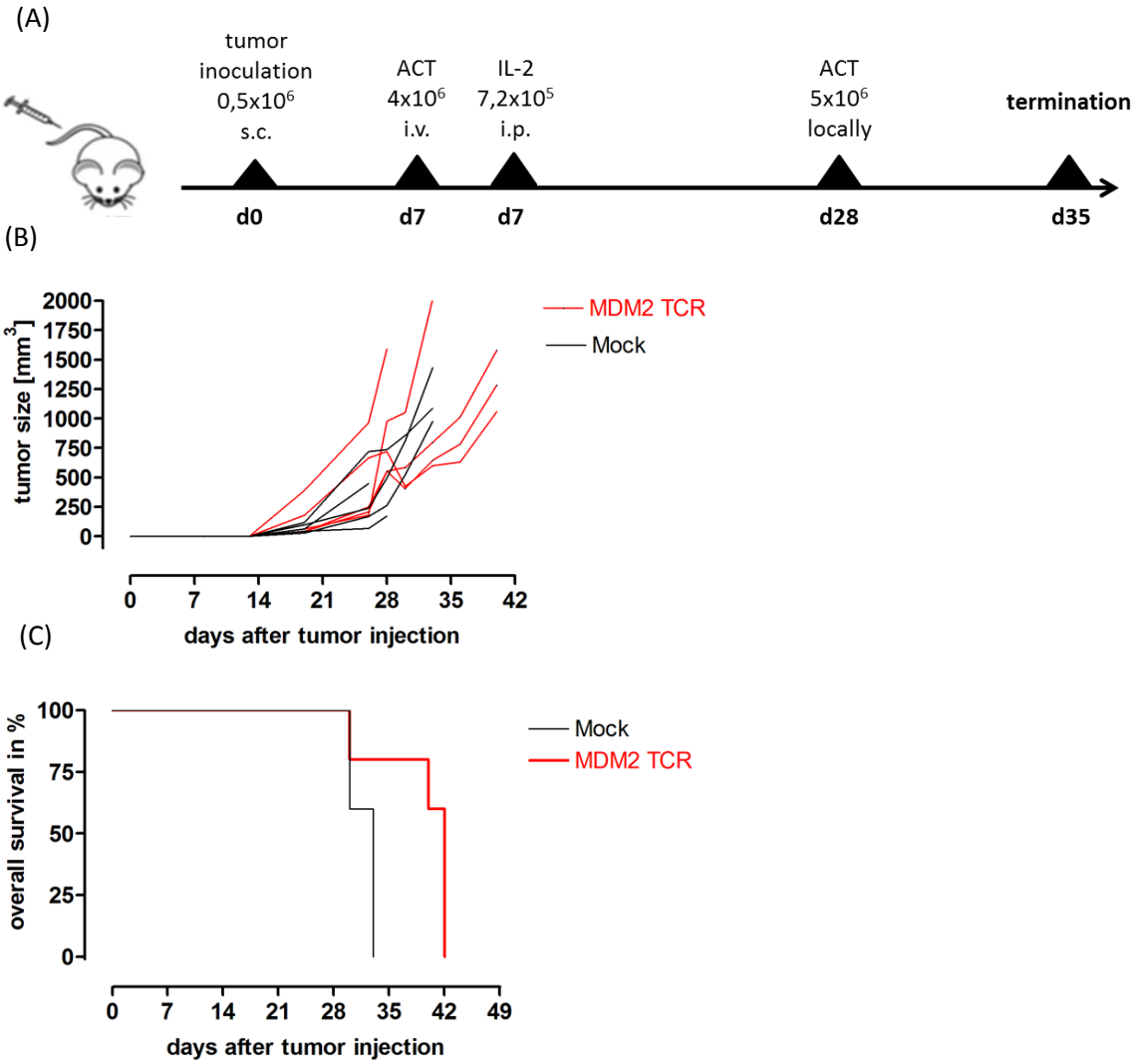

Figure 4.34 ACT slightly delayed tumor growth and prolonged overall survival. (A) NSG mice were inoculated with 0,5x10^6 melanoma cells (D28) (s.c.) in the right flank. One week later 4x10^6 T cells transduced with Mock or MDM2 TCR were injected (i.v.) along with 7,2x10^5 IU IL-2 (i.p.) to boost the T cell expansion. At day 28 a second dose of 5x10^6 T cells transduced with Mock or MDM2 TCR were injected locally in the closer environment of the tumor site. Mice were sacrificed when tumor size reached a volume of 1000-1500mm^3. (B) The black line shows tumor growth of mice which received Mock transduced T cells, and in red line mice which received MDM2 TCR transduced T cells. Tumor volume is calculated as described in Material and Methods. (C) Overall survival is indicated in percent, n=5 mice per group.

Tumor-inoculated mice started to show palpable tumors in both groups at day 14 after tumor injection (figure 4.34 B). Two mice exhibiting small tumors in the Mock group had to be sacrificed between days 25 and 28 because of illness (fur and weight loss), most likely due to tumor metastasis. The tumors in the three other mice from the Mock group showed a slow growth compared to tumors in two mice of the MDM2 TCR group. The second transfer of T cells had no effect on the tumor growth in these three Mock mice, and mice had to be sacrificed at day 33 after tumor injection. In two mice from the MDM2 TCR group, tumors showed a rapid growth. One mouse had to be sacrificed before the second T cell transfer. The tumor in the other mouse had a large volume at the time of transfer (1000 mm^3), which

precluded any potential antitumor response by the second T cell transfer. Tumors in the three other mice of MDM2 TCR group were growing slowly and had a volume of 550 to 750 mm^3. After the second T cell transfer tumor volume in one mouse remained stable for a short time, in the two other mice tumors were shrinking at day 30 to a volume of about 400 mm^3. Ultimately, all mice showed tumor growth at later time points and had to be sacrificed at day 42.

In summary, we observed a prolonged overall survival of 10 days in mice which were treated with MDM2-specific TCR transduced T cells (figure 4.34 C). The tumor cell line D28 which was used for the melanoma model exhibit growth aggressiveness. Therefore, the number of transferred T cells in the first and second injection was most likely sub-optimal to achieve a sufficient antitumor response. In mice which received two injections of MDM2 TCR transduced T cells we could detect MDM2 TCR-expressing TILs (data not shown) suggesting that the lack of antitumor response was not due to deficient homing of T cells to the tumor site. We harvested tumors from mice in both groups for further characterization and observed a reduced recognition of these cells of about 50 % compared to parental cells in a cytolytic assay using T cells transduced with the MDM2-specific TCR as effector cells (data not shown). Testing *ex vivo* tumor cells for A2.1 expression demonstrated a sustained expression, suggesting that other escape mechanisms than MHC class I down-regulation are most likely involved in this model. Other possibilities to explain the poor response *in vivo* are the down-regulation of MDM2 antigen in the tumor cells and/or up-regulation of inhibitory molecules like in our multiple myeloma model (described in 4.3). Further analysis will be required to characterize the efficacy of MDM2 TCR gene transfer in this melanoma xenograft model.

In conclusion, we could show that melanoma cell lines overexpress MDM2 and can be recognized by MDM2 TCR tranduced T cells *in vitro*. First *in vivo* data revealed a partial antitumor effect of MDM2 TCR in a melanoma mouse model, but calling for further analysis to investigate in more details immune suppressive mechanisms and their potential effect on MDM2 TCR ACT.

5 Discussion

5.1 Modification of a high-affinity MDM2 TCR for adoptive T cell therapy

Among tumor-associated antigens as potential targets for T cell based immunotherapy the oncoprotein MDM2 is a promising candidate. MDM2 is an ubiquitous self-protein which is involved in different processes of malignant transformations and frequently overexpressed in multiple tumor types, including solid and hematological malignancies [61]. MDM2 is up-regulated in tumors by (i) gene amplification, (ii) increased transcription level or (iii) enhanced translation. Especially in soft tissue tumors like liposarcomas a high frequency of MDM2 gene amplification was reported. Therefore targeting tumor cells with MDM2-specific TCR may represent a new treatment approach for cancer patients. Since non-mutated MDM2 is a self-protein this precludes the probability to find T cell expressing high-affinity MDM2-specific TCR from patient's peripheral blood due to self-tolerance. This issue was circumvented using transgenic mice. A high-affinity murine TCR recognizing the human A2.1-restricted non-mutated MDM2(81-88) peptide was isolated from a CTL clone and cloned in retroviral vectors for TCR gene transfer analysis in human T cells. Codon-optimization enhances the translation rate of transgenic TCR chains which have therefore an advantage over endogenous expressed TCR in the competition for CD3 [157]. Scholten et al. showed that codon-optimization increases the functional expression of the introduced TCR chains [138]. We also codon-optimized the sequences encoding for TCR α- and β-chains and by using a self-cleaving peptide 2A-based construct an equal expression level of TCR α- and β-chains was ensured [158]. Another risk while introducing a TAA-specific TCR in primary T cells is the formation of mixed TCR-heterodimers resulting from paring of natural and transgenic TCR chains with potential autoreactive properties. In a mouse model mimicking a clinical setting, Bendle at al. observed the formation of self-reactive TCRs as a result of mispairing of natural and transgenic TCR chains which were associated with autoimmunity [159]. To reduce mispairing, TCR sequences were modified by adding cysteine residues in the TCR constant domains to generate a second disulfide-bond between the constant TCR α- and β-chains [139]. Also codon-optimization can potentially reduce mispairing. In line with this, our results showed an enhanced TCR expression level in human T cells transduced with the opt. TCR compared to cells engrafted with the wt

TCR (figure 4.3). Analysis of transduction efficiency at day 4 showed a remarkable difference in TCR expression, which was confirmed at later time points after *in vitro* stimulation. T cells modified with the opt. TCR exhibited 100% (transgenic) TCR expression within 11 days post-transduction while wt TCR-engineered T cells showed 40% TCR expression at most (figure 4.4). Importantly the EC50 values of the opt. TCR remained unchanged (nM range).In a cytolytic assay we could show that the functional properties of the opt. TCR were not impaired (figure 4.6). In terms of recognition and killing of MDM2 expressing target cells both wt and dc opt. TCR had comparable efficacy (figure 4.7). After investigating the expression and functionality of the opt. MDM2 TCR we further analyzed mispairing occurrence in cells transduced with the dc opt. TCR versus wt TCR. One approach to investigate mispairing in TCR-engineered T cells is the knockout of endogenous TCR expression. Expression of transgenic wt or dc opt. TCRs in these knockout cells should be comparable since mispairing cannot occur in this setting. There are already several gene-editing approaches described for a successful knock-down of target genes. Beside CRISPR/Cas9 and ZFN (Zinc finger nucleases) [161] TALEN technique has been also used [160]. Gene-editing techniques for T cell therapies have been successfully reported, for example the knock-down of PD-1 together with endogenous TCR by CRISPR/Cas9 to enhance T cell reactivity and avoid mispairing. ZFN has been used to knockout the chemokine receptor CCR5 which resulted in HIV resistant cells (summarized in [162]) [161],[163],[164].

Using TALEN technique the endogenous CD3-expression in human T cells could be remarkably reduced and lentiviral transduction of CD3-knockout cells with an antigen-specific TCR enhanced transgenic TCR expression compared to T cells expressing natural TCR chains [154]. In an attempt to knock-down the natural TCR in human T cells by using TALEN-based gene-editing approach, we achieved a CD3-negative fraction of about 25%. However the subsequent transduction of MACS-selected CD3-negative cells with MDM2 TCR has been unsuccessful (data not shown). Our two step approach, in contrast to the procedure described by Berdien and colleagues, has revealed some limitations. We observed that manipulating T cells with electroporation and magnetic cell sorting for CD3 negative cells somehow drastically reduces their subsequent transduction with retroviral vectors. Another approach could be the use of lentiviral vectors for TCR transduction [154] or the “simplified” TCR gene editing protocol achieved by ZFN-based approach

combined with lentiviral delivery of a transgenic NY-ESO-1 TCR as recently demonstrated in a xenograft MM model [163]. Following this single editing protocol only the natural α-chain was disrupted by ZFN in human T cells with subsequent lentiviral transduction of NY-ESO 1 TCR α- and β-chains. These T cells recognized and killed antigen-expressing target cells with a high specificity and showed no off-target toxicity in a xenograft MM mouse model. A more elegant "2 in 1" gene-editing strategy using CRISPR/Cas9 would be the insertion of the transgenic antigen receptor into the TCR constant α locus as recently demonstrated by Sadelain group [165]. T cells were redirected with a guided-RNA targeting a sequence within the TCR constant α locus and a vector encoding CD19 CAR. The authors showed that CAR-expressing T cells with disrupted natural TCR α-chain (TARC-CAR) behave similar *in vitro* in terms of cytotoxicity and proliferation as T cells with randomly introduced CAR. However, in a mouse model of acute lymphoblastic leukemia TRAC-CAR T cells revealed a higher antitumor response and prolonged overall survival compared to control CAR T cells. This method is currently being established in the laboratory. Meanwhile, we have addressed the question of TCR mispairing by comparing TCR expression in a T cell line lacking endogenous TCR expression. Transduction of the T cell line Jurkat 76 with wt or dc opt. TCR resulted in a comparable TCR expression (figure 4.5), suggesting that differences in TCR expression between wt and dc opt. TCR constructs observed were mainly due to mispairing of wt TCR with the natural TCR chains. Yet, we cannot exclude the possibility of residual mispairing that may occur with the opt. TCR. In this line, our laboratory has designed and generated a new TCR scaffold name single-chain (sc)TCR construct based on our sc TCR p53 TCR format [166],[156].

In the MDM2 sc TCR, the variable α and variable β domains are connected via a glycine/serine rich peptide linker (Li) [167] generating a Vα-Li-VβCβ fragment co-expressed with a truncated constant α (Cα) domain (figure 4.9). Because the sc TCR showed very faint if any expression in human T cells after retroviral transduction, the TCR sequence was further codon-optimized the same way as the conventional (dc) TCR, including the addition of cysteines residues in the Cα and Cβ chains and cloned into one single 2A-based pMx retroviral vector. These molecular modifications significantly improved the expression of the sc opt. TCR to significant levels than those obtained with the wt TCR (figure 4.10). However this sc opt. TCR exhibited a higher EC_{50} value

compared to the wt TCR, indicating a lower affinity (figure 4.11). Most likely the modification of the TCR sequence changed the conformation of the TCR and resulted in a lower functionality. Since the dc opt. TCR showed a high TCR expression and a high-affinity within the nM-range and was less prone to mispairing, we therefore decided to focus our research work with this TCR construct.

Clinical studies performed in the past illustrated already the risk of using high-affinity TCR-engineered T cells for adoptive T cell therapy. In 2009 Rosenberg and colleagues observed on-target toxicity in a clinical trial with patients with metastatic melanoma [52]. Patients were treated with T cells transduced with high-reactive TCRs recognizing melanoma-melanocyte antigens. Tumor regression was observed but also destruction of normal melanocytes in eye, skin and ear. This high-affinity TCR was generated based on a TCR recognizing the antigen MART-1 and was cloned from the TILs of a resected melanoma lesion. In another clinical study Rosenberg and colleagues observed that transfer of T cells retrovirally transduced with a murine TCR recognizing CEA induced an objective response in patients with colorectal cancer but induced also a severe transient inflammatory colitis [53]. This publication represented the first successful clinical TCR trial for the treatment of colorectal cancer with objective TCR-mediated tumor regression after adoptive T cell transfer but showed the potential risk of TCR gene transfer-associated on-target (off-tumor) toxicity. The study of Morgan et al. in patients infused with MAGE-A3 TCR revealed that beside MAGE-A3, this high-avidity TCR recognized also MAGE-A9 and –A12 [54]. The authors reported tumor regression but also neuronal toxicity in treated patients most likely due to MAGE-A12 expression in human brain tissue. Recognition of MAGE-A12 by the MAGE-A3 TCR transduced T cells induced a TCR-mediated inflammatory response in the brain tissue and a neuronal cell destruction.

Based on the side effects described above it was necessary to test the safety of our high-affinity MDM2 TCR in mouse T cell transfer model since MDM2 is ubiquitously expressed in tumor and nonmalignant cells. To answer the question of on-/off-target toxicity a syngeneic mouse model is needed with murine T cells transduced with MDM2 TCR as antigen-specific effector cells and HLA-A2.1/K^b transgenic mice expressing human MDM2 as recipient animals for T cell engraftment. Unfortunately, these transgenic mice do not exist so far. Although the murine MDM2(81-88)-peptide sequence (LLGDVFGV) differs in one amino acid from the human homolog (LLGDLFGV), the murine peptide is not

recognized by the MDM2 TCR (data not shown). Our group has further evaluated the reactivity of the MDM2 wt TCR against a large panel of A2.1-positive normal cells [135],[168] and has shown that MDM2 TCR expressing T cell do not recognize or lyse normal cells, including hepatocytes, renal epithelial cells, fibroblasts, dendritic cells, PBMCs, B lymphocytes or activated T lymphocytes. At least *in vitro* any evidence of on-target/off tumor reactivity of the MDM2 TCR could be observed. *In vivo* studies analyzing the safety of the TCR however are still missing.

Here, we could show that modifications of the MDM2 wt TCR significantly enhanced the TCR expression level without damping its functionality and reduced the occurrence for mispairing. Based on these results the subsequent efficacy studies were performed with the optimized dc MDM2 TCR using xenograft mouse models.

5.2 Efficacy of adoptive T cell therapy targeting MDM2

5.2.1 Multiple myeloma tumor model

To test the antitumor functionality of the MDM2 TCR we used a xenograft MM mouse model because we observed MDM2 overexpression in MM cell lines (six out of eight cell lines) and primary tumor cells (eight out of eleven samples) (figure 4.12 and 4.30) and a strong recognition of these cells by MDM2 TCR-transduced human T cells in a cytolytic assay (figure 4.14). However first experiments to evaluate the functionality of the MDM2 TCR *in vivo* showed no antitumor response in NSG mice engrafted with the MM NCI-H929 A2.1 cell line (figure 4.15) although growing tumors were infiltrated by MDM2 TCR expressing T cells (data not shown). Further analysis of *ex vivo* tumor cells showed a reduced MDM2 protein-expression compared to the parental cell line (figure 4.16 A). Reduced MDM2 antigen expression was observed in mice infused with either MDM2 TCR- or Mock-transduced T cells, suggesting an antigen-independent tumor-escape response which was most likely due to the tumor microenvironment. Accordingly, *ex vivo* antigen-loss tumor cells were less recognized than the parental cell line by MDM2 TCR-T cells in a cytolytic assay (figure 4.17). Down-regulation of antigen and/or MHC molecule expression is a well-described tumor escape mechanism [169],[170], yet A2.1 down-regulation was not observed in the present tumor model (figure 4.16 B). We observed that reduced MDM2 expression was reversible as *ex vivo* tumor cells regained their

steady state MDM2 expression level (data not shown) after few days in culture and were *de novo* recognized by MDM2 TCR-transduced T cells. MDM2 expression could be modulated at multiple levels, including gene amplification, transcriptional and post-translational regulation. It has been recently reported that the deubiquitinase USP15 is involved in the regulation of MDM2 expression in T cells and cancer cells [171]. In this study, the authors observed a spontaneous reduction of MDM2 protein expression without a reduction of MDM2 mRNA level after knockdown of USP15 with shRNA in melanoma and colorectal cancer cell lines. Interestingly, MDM2 down-regulation was associated with an up-regulation of p53 expression. This inverse relationship of MDM2 and p53 expression levels has been also observed in our *ex vivo* MM cells (figure 4.19 B). Therefore it is tempting to assume that USP15 could also be involved in MDM2 protein regulation in MM cells as well, yet this mechanism needs to be further investigated. Another possible explanation for the reduced MDM2 expression observed in *ex vivo* tumor cells might be a clonal selection of $MDM2^{low}$ expressing cells which may have a survival advantage over $MDM2^{high}$ expressing variants *in vivo*. Harvested *ex vivo* tumor cells were a mix of $MDM2^{high}$ and a much higher ratio of $MDM2^{low}$ cells which possibly had no growth advantage in culture anymore. The up-regulation of p53 expression is a direct result of lower MDM2 protein expression since MDM2 activity inhibits p53 expression and function. It has been shown that inhibition of the binding of MDM2 to wt p53 (using Nutlin-3a for example) enhances p53 function and resulted in apoptosis of MM tumor cells [172].

To find an ideal target for TCR gene transfer-based ACT for targeting MM is a quite challenging issue. In 2015, June and colleagues published the results of a clinical trial using ACT with antigen-specific TCR-engineered T cells in myeloma patients [173]. This TCR recognizes a peptide shared by the cancer-testis antigens NY-ESO-1 and LAGE-1. Patients with antigen-positive MM cells included in this study were treated with TCR-modified T cells two days after autologous stem cell transplantation (ASCT) in combination with lenalidomide (an immunomodulatory drug). The authors reported that engineered T cells were able to proliferate, persist and traffic to the bone marrow but after a first response phase disease relapse occured. They did further analysis and found in 8 out of 10 patients a loss of persisting antigen-specific T cells in the peripheral blood whereas MM cells remained antigen-positive until relapse. However two patients

relapsed due to antigen loss of tumor cells as observed in our MM mouse model. In line with our observation and the above reported antigen-loss MM variants we decided to target MM T cell redirected with MDM2- and p53-specific TCRs. For this purpose human T cells were co-transduced with both TCRs and used as effector cells in a cytolytic assay. *Ex vivo* tumor cells were more efficiently lysed by dual TCR T cells than by single TCR modified cells (figure 4.19 B and 4.17). Therefore targeting MM *in vivo* with both antigen-specific TCRs may enhance the overall antitumor response by circumventing MDM2 antigen escape mechanism. However co-transducing cells with two TCRs leads to lower expression level of each TCR compared to single-TCR transduced cells (data not shown) which limits their use *in vivo*. For our *in vivo* studies it was important to transfer high level of TCR-expressing cells generated within a short time (to ensure less-differentiated and thus more potent effector cells). A second issue of generating T cells with two antigen-specific TCRs is the enhanced risk of mispairing. It was published that after retroviral transduction of human T cells with two TCRs not only TCR expression was reduced compared to single-transduction but also TCR function was impaired due to mispaired transgenic TCR chains[157]. In our model we used the combination of two optimized TCRs (see 5.1) consisting of conventional dc and sc TCR constructs with reduced capacity for mispairing and tested if the use of dual TCR T cells or a mix of single TCR-transduced T cells showed comparable lysis of target cells in a cytolytic assay. T cells co-transduced with two TCRs or mixed single-transduced T cells showed similar specific lysis levels (figure 4.20) which led us to use mixed single transduced T cells for our *in vivo* studies. Targeting MM *in vivo* with a combination of MDM2 and p53 TCR-modified T cells resulted in a prolonged overall survival in NSG mice compared to treatment with either MDM2 or p53 TCR alone, demonstrating a synergistic therapeutic effect, yet complete responses were not achieved (figure 4.21). Analysis of *ex vivo* tumor and TCR-expressing TILs revealed an up-regulation of PD-L1 up to 80% and PD-1 expression up to 50%, respectively (figure 4.23 and 4.25). The observed enhanced expression of inhibitory molecules may have contributed to the insufficient antitumor response. Up-regulation of PD-1 in TILs *in vitro* has been described in the context of T cell exhaustion in a chronic viral infection [174]. Stimulation of T cells via their TCR leads to a transient PD-1 up-regulation but a sustained PD-1 expression on T cells is the consequence of continuous antigen stimulation that occurs in chronic virus infections or in cancer [175]. A high PD-L1

expression in MM cells and a high PD-1 expression in T cells *in vivo* has been reported by Ray et al. in BM-samples of MM patients [176]. Activation of PD-1 on T cells via binding to PD-L1 triggers the phosphatase SHP-2 which in turn dephosphorylates TCR-proximal signaling molecules like CD3ζ, PI3K, protein kinase C Θ or zeta-chain-associated protein kinase 70 (ZAP70) [177]. De-phosphorylation of signaling molecules leads to an impaired antigen-specific T cell response. A recent study described a mechanism involved in the regulation of PD-1 in effector T cells in cancer, demonstrating that a chromatin organizer called Satb1 (special AT-rich sequence-binding protein 1) blocks the expression of PD-1 [178]. The immune-suppressive cytokine TGF-β (transforming growth factor β) which is present in a high level in the tumor microenvironment decreases Satb1 expression and activates Smad proteins. Smad proteins are transcription factors and compete with Satb1 for binding to Satb1-promoter. Thus, low expression level of Satb1 and high Smad protein levels resulted in Smad binding to PD-1 promoter, and triggering its expression. The study showed that Satb1-deficient tumor-reactive T cells lost their effector function more rapidly than wt T cells after binding to PD-L1 expressing tumors.

One approach to reverse the loss of effector function in TILs is the use of an anti-PD-1 antibody to block the interaction between PD-1 and PD-L1. Because we observed a strong up-regulation of PD-1 in TILs and PD-L1 in tumors, we decided to combine ACT with checkpoint inhibitor therapy using the anti-PD-1 antibody nivolumab in our established MM xenograft tumor model. Tumor-engrafted NSG mice were infused with a mix of T cells transduced with MDM2- or p53-specific TCR, with nivolumab or PBS (figure 4.26 A). Combining ACT and nivolumab treatment showed a slight advantage in tumor control and overall survival compared to ACT alone (figure 4.26 B). These data demonstrate the synergistic potential of ACT and checkpoint inhibitors, yet this approach did not result in complete tumor regression.

Our *in vivo* data contrasted with the work of Sanmamed et al which evaluated the combination of nivolumab and T cell transfer in NSG mice [144]. They observed a reduced tumor growth in mice treated with nivolumab compared to control animals but this experimental tumor model was different from our MM ACT model. First, they injected tumor cells and T cells at the same time and second they did not use antigen-specific TCR engineered T cells but human PBMCs. Moreover, nivolumab application was performed i.v. and not i.p. as in our model. We then carried out an experiment using the

same ACT protocol as described in figure 4.29 but injected nivolumab every 7 days i.v. instead of every 5 days i.p., yet we did not observe any benefit of nivolumab treatment. Similarly, injection of anti-PD-1 antibody every 3 days did not improve the antitumor response mediated by ACT. By slightly changing the tumor model by using another anti-PD-1 antibody we could slightly enhance the antitumor response (figure 4.27 B). Pembrolizumab was applied once a week i.p. starting three days after ACT in tumor-engrafted NSG mice (figure 4.27 A). The combination of ACT and pembrolizumab was in terms of antitumor response the more efficient treatment strategy in our model, however the combination of ACT using MDM2- and p53-specific TCR-engineered T cells and checkpoint blockade showed only moderate synergistic effect so far. We further showed complete tumor protection by TCR-engineered T cells in MM model (figure 4.29 A) by reducing the tumor load and injecting T cells early after tumor inoculation. Importantly, the full tumor control was achieved in the absence of checkpoint blockade (figure 4.29 B). This experimental model demonstrated the functionality of ACT with MDM2/p53 TCR-engineered T cells for the treatment of MM. Next, we would like to combine ACT using TCR-engineered T cells with several ICIs and/or other immunotherapeutic approaches, as monotherapies have shown limited effectiveness. Nivolumab alone was tested in a clinical trial in MM patients and in patients with B- or T-cell lymphoma [179]. Out of 27 patients, one patient showed an objective response and one had a complete response. Most of the MM patients (63%) showed a stable disease. This was the highest reported response to nivolumab in all investigated patients. Checkpoint inhibition alone is not sufficient to treat MM in patients similar to our pre-clinical mouse data. In general, checkpoint inhibitors like anti-PD-1, anti-CTLA-4 or anti-PD-L1 antibodies as monotherapy showed only poor efficacy in investigated treatments for different tumor types. The therapeutic effect of anti-PD1 antibody and anti-CTLA-4 antibody were primarily investigated in metastatic melanoma achieving high response rates and overall survival [180]. A recent study summarized selected clinical trials testing ipilimumab and nivolumab as monotherapy or in combination for the treatment of metastatic melanoma patients [141]. Ipilimumab alone had a response rate of 19%, nivolumab alone 44%. In combination therapy the response rate was about 58%. Also the combination of ipilimumab and dacarbazine (a chemotherapy drug) exhibited a moderate response rate of about 15%.

Another target for checkpoint blockade in combination therapy is PD-L1 which was also up-regulated in MM cells in our tumor model (figure 4.23). Up-regulation of PD-L1 expression in tumor cells is a frequently observed tumor escape mechanism [181]. In the present work, we observed a rapid down-regulation of PD-L1 expression in *ex vivo* tumor cells in culture (data not shown), indicating a strong influence of the tumor environment on PD-L1 expression. PD-L1 is expressed in normal cells like myeloid cells and cells of epithelial and endothelial origin to regulate the balance between T cell activation and tolerance [182]. In cancer patients this immune checkpoint pathway can be responsible for an impaired antitumor immune response. Anti-PD-L1 blockade was already used in a MM mouse model in combination with hematopoietic stem cell transplantation (HSCT) [183]. After injection (i.v.) of a murine MM cell line, mice were irradiated and infused with bone-marrow cells and splenocytes as T cell source. This model demonstrated an up-regulation of PD-1 on T cells and PD-L1 up-regulation on tumor cells which was associated with the absence of tumor control. T cells were lacking the ability to produce IL-2, IFN-γ and TNF-α but they produced the immunosuppressive cytokine IL-10. Additional treatment with anti-PD-L1 antibody showed a weak effect and an overall survival of 10%. The combination of HSCT, anti-PD-L1 and vaccination with MM cells transfected with CD80/CD137L as adjuvant for an effective T cell response showed an overall survival of about 40%. Similar to our MM model, combination of several treatments was needed to achieve an antitumor response without a complete tumor control. Therefore, our MM tumor model combining anti-PD-1 and anti-PD-L1 antibody treatment with ACT may improve antitumor response rates for MM. PD-L1 is not only binding to PD-1 on T cells but also to CD80 on APCs [184]. CD80 binds to CD28 on T cells and triggers full TCR activation by acting as co-stimulatory signal. Inhibition of this co-stimulation by PD-L1 results in an impaired T cell activation. Therapy using anti-PD-1 antibody is therefore blocking two inhibitory signaling pathways, the PD-1 PD-L1 interaction and PD-L1 CD80 interaction. Blocking PD-L1 is interesting because it is not only expressed by tumor cells but also up-regulated by cells of the tumor microenvironment. Since we used a MM xenograft mouse model and not a syngeneic model we cannot address the question regarding interaction of PD-1 expressing T cells and the host cells which are part of the environment. Although there is 75% homology (protein) in the variable domain of murine and human PD-1 [100], nivolumab is

recognizing specifically human PD-1, which excludes binding to murine cells in the tumor environment. Schreiber and colleagues analyzed the influence of PD-L1 expression in host cells in a syngeneic mouse sarcoma model and observed that tumor associated macrophages (TAMs) express PD-L1 and compose the major host cell population within the tumor microenvironment [185]. Treating mice with anti-PD-L1 antibody resulted in tumor regression whereas mice treated with control antibody showed no tumor control. To address the question of immunosuppressive influence of host cells in the tumor environment we would need a syngeneic model. The combination of nivolumab and ipilimumab is not relevant in the present work as we did not observe CTLA-4 expression in TILs in our MM model.

Another approach to inhibit interaction of PD-1 and PD-L1 to unleash the efficacy of ACT is the transfer of PD-1 KO T cells. This concept has been demonstrated in mice by disrupting PD-1 expression in CTL by CRISPR/Cas9 gene-editing approach, showing the ability of EBV-specific T cells to control EBV-associated gastric cancer in a xenograft mouse model [186]. The same approach has been used to disrupt PD-1 in primary human T cells leading to an enhanced IFN-y production and cytotoxicity in PD-1 knockout T cells *in vitro* [187]. This concept was further developed to allow multiplex gene-editing in one-shot based approach. Su and colleagues demonstrated the possibility to knock-down PD-1 as well as CTLA-4 and endogenous TCR chains and simultaneously insert CAR-encoding gene in one-shot CRISPR system by lentiviral transduction [188]. The transfer of PD-1 knockout TAA-specific TCR-modified T cells is a promising approach to circumvent intratumoral-mediated T cell exhaustion.

A further target molecule for antibody therapy in MM is CD319 which is also known as SLAMF7 (signaling lymphocytic activation molecule family member 7). SLAMF7 is a cell surface receptor and expressed on normal plasma cells and MM cells and to a lower extent on NK cells but little to no expression in normal tissue. The anti-CD319 antibody elotuzumab has two mechanisms of action against MM cells. It binds to CD16 which is the extracellular portion of SLAMF7 on NK cells and activates directly NK cells by triggering the release of granzyme B and perforin. MM cells are then destroyed by these cytotoxic granules. Elotuzumab binds to SLAMF7 directly on MM cells, a process known as tagging. The tagged MM cells also activate NK cells (summarized in [189]). We also analyzed MM cell lines used in our *in vitro* /*in vivo* experiments for SLAMF7 expression by

flow cytometry. We observed in 50% of the investigated cell lines, including NCI-H929 A2.1 used in the *in vivo* studies a strong SLAMF7 expression of nearly 100% (data not shown). Analysis of *ex vivo* NCI-H929 A2.1 tumor cells showed a persistent SLAMF7 expression (figure 4.28) making CD319 an ideal target for anti-MM therapy. Combining ACT and elotuzumab represents a potential treatment approach for MM since it was already shown that elotuzumab as monotherapy in MM patients is not effective [189]. However, combination with bortezomib, a proteasome inhibitor used as standard therapy in MM, showed an overall response rate of 70% in a phase I clinical trial. In a phase III trial elotuzumab was tested in combination with lenalidomide and dexamethasone. The overall response rate was 79% in combination with elotuzumab and 66% by treatment with lenalidomide + dexamethasone alone and an the progression-free survival of 19,4 versus 14,9 months, respectively. These results strongly suggest a synergistic effect of elotuzumab in combination with other therapies. Further experiments should test combination of nivolumab and ACT as a new therapeutic approach for MM.

A recent review summarized the current immunotherapeutic treatments and clinical trials for MM [190]. Beside elotuzumab other antibodies targeting for example CD38 (daratumumab) or CD138 have gained strong interest as potential therapeutic agents for MM. CD38 is a transmembrane receptor protein and highly expressed on malignant plasma cells, including MM, and normal B cells. CD138 is expressed on the surface of MM cells and acts as a growth factor [190]. Daratumumab showed as monotherapy an overall response rate of 35% in patients with MM and treatment with anti-CD138 antibody induced a disease control in 50% of the patients. Immunomodulatory drugs (IMIDs) such as lenalidomide and thalidomide showed especially in combination with monoclonal antibodies antitumor response. However due to the immune suppressive effect of IMIDs the combination with other immune-based approaches is limited [190]. None of these anti-MM immunotherapies showed the expected antitumor response as monotherapy. Although in combination the response rates of these different approaches are improved, MM remains an incurable disease. Therefore, combination of more potent specific therapies is needed.

In conclusion, we showed that MDM2-specific TCR-modified T cells were able to target MM cells *in vitro*, however their efficacy in a MM xenograft mouse model was rather

limited most likely due to tumor escape mechanisms. The transfer of T cells redirected with MDM2 and p53 TAA-specific TCRs enhanced the antitumor response and significantly prolonged the tumor-free survival but did not result in full tumor protection, suggesting that targeting one single antigen is not sufficient to drive a full antitumor response. Combination of ACT and ICIs was an ideal approach to target MM in our xenograft mouse model. We focused in this study on MM as a model for proving the efficacy of MDM2-specific TCR for ACT. Moreover, the benefit of combination therapy is transferable to other tumor types like melanoma. So far there are two ongoing clinical trials combining TCR-ACT and ICI (pembrolizumab) for MM and Human Papilloma virus-associated cancers.

Beside MM cell lines we also characterized primary MM cells isolated from BM-aspirates of patients. We investigated MDM2 expression by western blot analysis in primary MM cells using as a starting size, a number of 11 samples. Our analysis showed that in most of CD138-purified patient-derived MM cells express MDM2 protein (Figure 4.30). In two samples we could detect 90 kDa full length MDM2 protein and in six samples a 60 kDa cleaved MDM2 protein was expressed. The 60 kDa MDM2 isoform is a product of full length MDM2 cleaved by caspase 3 at the C-terminal end in apoptotic and also non-apoptotic human tumor cells [105]. This isoform is also believed to play a role in the regulation of p53. The 60 kDa MDM2 isoform retains is capacity to bind p53 but lost the C-terminal RING-finger domain which is responsible for the E3 ubiquitin ligase function of MDM2 [111]. Therefore, this isoform is not able to ubiquitinate p53 and mediate its degradation via the proteasome. Interestingly, the 60 kDa isoform was not detectable in our panel of tumor cells lines in their resting/steady state culture condition, but was strongly induced in *ex vivo* tumor cells (data not shown). These data suggest that primary MM have most likely lost their MDM2-mediated regulation of p53 expression by preferentially expressing the 60kDa isoform. This assumption was confirmed by our analysis of *ex vivo* MM tumor cells which were expressing the 60 kDa MDM2 isoform (data not shown) and revealed an up-regulation of p53 expression (figure 4.18).

Part of this thesis work was the understanding of potential mechanisms involved in the regulation of the expression of inhibitory molecules in MM cell lines and patient-derived primary cells. Up-regulation of PD-L1 expression in MM cells of patients has been

reported in particular after relapse or in refractory cases [191]. It was already described that MM cells from patients express high PD-L1 levels while BM-plasma cells from healthy donors do not express PD-L1 at all [192]. Expression in primary MM cells was further enhanced *in vitro* after treatment with IFN-γ, whereas cells from healthy donors showed a slight PD-L1 expression in response to IFN-γ treatment. Further analysis revealed that the MEK/ERK pathway is responsible for IFN-γ-mediated PD-L1 up-regulation in primary MM cells. In the course of this work we focused primarily on the MM cell line NCI-H929 A2.1 which under normal culture condition expresses PD-L1 at a very low level. These cells showed slight increased PD-L1 expression after IFN-γ treatment *in vitro* which was further enhanced under stress conditions (pH or glucose starvation in the culture medium) (data not shown). By treating NCI-H929 A2.1 cells with a demethylation reagent *in vitro*, PD-L1 expression could be enhanced up to the level observed in *ex vivo* tumors (figure 7.5, annex) suggesting a post-transcriptional regulation of PD-L1 expression in these cells *in vivo*. In addition a down-regulation of MDM2 expression in NCI-H929 A2.1 with this treatment was shown (data not shown). Epigenetic modifications in these cells have to be investigated in more detail.
Expression levels of PD-L1 or PD-L2 observed in our primary MM cells isolated from the BM of patients were rather low (about 27%) in contrast to high PD-1 expression of about 60% (figure 4.31). PD-1 expression in tumor cells was already described by D´Incecco et al. in non-small-cell lung cancer (NSCLC) [193]. For the lack of time we have not further investigated the possible mechanisms involved in PD-1 expression in primary MM cells.

To confirm the suitability of MDM2 as a potential MM antigen for TCR-based ACT, xenograft models using primary MM cells would be important. However, these kinds of xenograft mouse models are challenging because primary cells do not proliferate and isolation of a sufficient number of primary MM cells from one patient is often not possible. In addition tumor engraftment in mice is not always reproducible. For a proper analysis autologous T cells (from the same patient) are needed as recipient cells for MDM2 TCR-modified T cells. These types of xenograft models of ACT are very challenging and not reliable. Therefore, xenograft models based on tumor cell lines have been used in this work.

In conclusion, we could demonstrate MDM2 protein overexpression in most of our MM cell lines and primary MM cells isolated from bone marrow of patients. Analysis of expression of inhibitory molecules revealed a high PD-1 expression and low PD-L1 and PD-L2 expression on primary MM cells. The efficacy of MDM2 TCR-T cells against primary MM cells will be the subject of further experiments.

5.2.2 Melanoma tumor model

In addition to MM, we have also investigated the suitability of MDM2 as a potential target antigen for immunotherapy of melanoma. Since MDM2 is overexpressed in 56% of invasive primary melanoma cells and cells from metastatic lesions [194] we decided to target also this cancer type with MDM2 TCR. For this reason we tested a panel of melanoma cell lines for MDM2 and A2.1 expression and observed MDM2 overexpression in most of the investigated cell lines (figure 4.32 B). Considering that A2.1 expression intensity among the $A2.1^+$ tumor cells lines differed (figure 4.32 A), we analyzed the relative recognition of these cell lines by MDM2 TCR in a cytolytic assay. We observed a correlation between the efficiency of cell lysis and the expression levels of MDM2 and A2.1 (figure 4.33). For example, the D28 cell line which showed the highest A2.1 expression and strong MDM2 protein expression was the target exhibiting the strongest lysis by MDM2 TCR transduced T cells. To investigate the functionality of MDM2 TCR *in vivo* we decided to use this cell line as a model. We set up a xenograft model with D28-engrafted NSG mice infused with T cells transduced with MDM2 TCR one week after tumor inoculation, following by a second T cell transfer two weeks later (figure 4.34 A). By injecting two times antigen-specific TCR transduced T cells tumor growth could be temporarily controlled in three out of five mice with ultimately a tumor progression (figure 4.34 B). Analysis of *ex vivo* D28 tumors showed a sustained A2.1 expression but a reduced recognition by the MDM2-TCR in a cytolytic assay (data not shown). Since we did not further characterize these *ex vivo* tumor cells for MDM2 expression and up-regulation of inhibitory molecules, as we did with the MM model, we can only speculate about the potential explanation for this impaired immune response. We could demonstrate that MDM2-TCR expressing T cells were capable of infiltrating the tumor (data not shown) but were unable to control the tumor. This melanoma cell line is a fast growing cell line. Although we injected a very low number of tumor cells ($5x10^5$ cells),

the tumors were growing probably too fast to be efficiently controlled by transferred T cells. Also the up-regulation of inhibitory molecules in D28 melanoma cell line *in vivo* may have occurred as already described in melanoma cells from patients [195] which exhibited a mutation in BRAF and constitutively expressed PD-L1. These patients were the group with the worst prognosis. Another potential mechanism for impaired immune response could be antigen loss of tumor cells as observed in our MM model. It has been already described that melanoma cells down-regulate melanoma antigen upon inflammation, including gp100 or TRP-2 (tyrosinase-related protein2) after TNF-α treatment [196]. Although we did not analyze the expression of MDM2 antigen expression and cell surface inhibitory molecules in *ex-vivo* D28 tumor cells these immune escape mechanisms could be also involved in our model.

Summarized, melanoma cell lines can be targeted by MDM2-specifc TCR *in vitro* yet pilot preliminary *in vivo* studies showed partial antitumor response. This xenograft model should be further characterized.

5.3 Conclusion

We demonstrated the potential of MDM2 as a new target antigen for adoptive cell therapy for hematologic malignancies with a particular focus on MM. MDM2(81-88) is a non-mutated TAA which is overexpressed in multiple solid tumors and in leukemia. We first modified (optimized) an MDM2(81-88)-specific wt TCR to enhance TCR expression and reduce the formation of mispaired TCR heterodimers. The affinity and specific cytolytic activity of the optimized dc TCR were comparable to the wt TCR. A sc TCR was successfully generated in the lab and was further optimized in the scope of this work. However, we observed a significant decrease in the affinity for the cognate antigen. The safety of MDM2 TCR in terms of on-target/off-tumor reactivity was already confirmed *in vitro* and published earlier, however analysis of the safety of MDM2 TCR *in vivo* is still missing due to the lack of human MDM2 transgenic mice for a syngeneic mouse model. We tested the function of the optimized dc MDM2 TCR *in vitro* and observed specific lysis of MDM2 and A2.1 expressing tumor cells by transduced T cells in a cytolytic assay. First *in vivo* experiments however showed no T cell response of MDM2 TCR transduced T cells against MM cells due to tumor escape mechanisms. We observed a down-regulation of MDM2 antigen expression and up-regulation of inhibitory molecules which

resulted in a lower recognition of *ex vivo* tumor cells by MDM2 TCR expressing T cells. To circumvent these immune escape mechanisms we targeted MM tumor cells with two TAA-specific TCRs which resulted in a prolonged overall survival of mice. We next combined ACT with ICI and demonstrated a synergistic effect compared to ACT alone. However, this combination did not result in full tumor protection in this particular tumor model. What we observed in our studies has been reported in other mouse models and clinical trials with cancer patients. Our work demonstrated that MDM2 TCR-based ACT as monotherapy is not sufficient to treat MM or melanoma. ICI could enhance the antitumor reaction but did not result in fully tumor protection. A combination treatment, including ACT and other immunotherapeutic approaches, may represent a promising strategy to cure cancer patients.

6 References

[1] W. K. Decker and A. Safdar, “Bioimmunoadjuvants for the treatment of neoplastic and infectious disease: Coley’s legacy revisited,” *Cytokine Growth Factor Rev.*, vol. 20, no. 4, pp. 271–281, 2009.

[2] A. Morales, D. Eidinger, and A. W. Bruce, “Intracavitary Bacillus Calmette-Guerin in the treatment of superficial bladder tumors.,” *J. Urol.*, vol. 116, no. 2, pp. 180–183, 1976.

[3] S. S. Chang *et al.*, “Diagnosis and Treatment of Non-Muscle Invasive Bladder Cancer : AUA / SUO Guideline,” *J. Urol.*, vol. 196, pp. 1021–1029, 2016.

[4] D. A. Morgan, F. W. Ruscetti, and R. Gallo, “Selective in vitro Growth of T Lymphocytes from Normal Human Bone Marrows,” *Science (80-.).*, vol. 193, no. 4257, pp. 1007–1008, 1976.

[5] D. T. Sleijfer, R. A. Janssen, J. Buter, E. G. de Vries, P. H. Willemse, and N. H. Mulder, “Phase II study of subcutaneous interleukin-2 in unselected patients with advanced renal cell cancer on an outpatient basis,” *J.Clin.Oncol.*, vol. 10, no. 7, pp. 1119–1123, 1992.

[6] S. A. Rosenberg *et al.*, “Experience with the use of high-dose interleukin-2 in the treatment of 652 cancer patients,” *Ann Surg*, vol. 210, no. 4, pp. 474–484, 1989.

[7] M. Davies and E. A. Duffield, “Safety of checkpoint inhibitors for cancer treatment : strategies for patient monitoring and management of immune-mediated adverse events,” *ImmunoTargets Ther.*, vol. 6, pp. 51–71, 2017.

[8] G. Köhler and C. Milstein, “Pillars Article : Continuous cultures of fused cells secreting antibody of predefined specificity. Nature, 1975, 256 (5517): 495-497,” *J. Immunol.*, vol. 174, pp. 2453–2455, 2005.

[9] D. G. Maloney *et al.*, “IDEC-C2B8 (Rituximab) Anti-CD20 Monoclonal Antibody Therapy in Patients With Relapsed Low-Grade Non-Hodgkin’s Lymphoma,” *Blood*, vol. 90, no. 6, pp. 2188–2195, 1997.

[10] M. J. Leandro, J. C. W. Edwards, and G. Cambridge, “Clinical outcome in 22 patients with rheumatoid arthritis treated with B lymphocyte depletion.,” *Ann. Rheum. Dis.*, vol. 61, no. 10, pp. 883–888, 2002.

[11] G. Wei, J. Wang, H. Huang, and Y. Zhao, “Novel immunotherapies for adult patients with B-lineage acute lymphoblastic leukemia,” *J. Hematol. Oncol.*, vol. 10, no. 1, p. 150, 2017.

[12] P. van der Bruggen *et al.*, “A gene encoding an antigen recognized by cytolytic T lymphocytes on a human melanoma.,” *Sci. (New York)*, vol. 254, no. 5038, pp. 1643–1647, 1991.

[13] G. Di Lorenzo, M. Ferro, and C. Buonerba, “Sipuleucel-T (Provenge®) for castration-resistant prostate cancer,” *BJU Int.*, vol. 110, pp. 99–104, 2012.

[14] C. Guo, M. Manjili, J. Subjeck, D. Sarkar, P. Fisher, and X.-Y. Wang, “Cancer Vaccines: Past, Present, and Future,” *Adv Cancer Res*, vol. 119, pp. 421–475, 2013.

[15] L. Kranz *et al.*, “Systemic RNA delivery to dendritic cells exploits antiviral defence for cancer immunotherapy.,” *Nature*, vol. 534, no. 7607, pp. 396–401, 2016.

[16] U. Sahin *et al.*, “Personalized RNA mutanome vaccines mobilize poly-specific therapeutic immunity against cancer,” *Nature*, vol. 547, no. 7662, pp. 222–226, 2017.

[17] P. Ott *et al.*, “An immunogenic personal neoantigen vaccine for patients with melanoma,” *Nature*, vol. 547, no. 7662, pp. 217–221, 2017.

[18] and D. E. W. Steven A. Rosenberg, Beverly S. Packard, Paul M. Aebersold, Diane Solomon, Suzanne L. Topalian, Stephen T. Toy, Paul Simon, Michael T. Lotze, James C. Yang, Claudia A. Seipp, Colleen Simpson, Charles Carter, Steven Bock, Douglas Schwartzentruber, John P., “Use of Tumor-Infiltrating Lymphocytes and Interleukin-2 in the Immunotherapy of Patients with Metastatic Melanoma,” *N. Engl. J. Med.*, vol. 319, no. 25, pp. 1676–1680, 1988.

[19] L. M. Muul, P. Spiess, E. P. Director, and S. A. Rosenberg, “Identification of specific cytolytic immune responses against autologous tumor in humans bearing malignant melanoma .,” *J. Immunol.*, vol. 138, no. 3, pp. 989–995, 1987.

[20] M. Parkhurst, J. Riley, M. Dudley, and S. Rosenberg, “Adoptive transfer of autologous natural killer cells leads to high levels of circulating natural killer cells but does not mediate tumor regression,” *Clin. Cancer Res.*, vol. 17, no. 19, pp. 6287–97, 2011.

[21] P. Robbins, “Tumor-Infiltrating Lymphocyte Therapy and Neoantigens,” *Cancer J.*, vol. 23, no. 2, pp. 138–143, 2017.

[22] E. Tran *et al.*, “Cancer immunotherapy based on mutation-specific CD4+ T cells in a patient with epithelial cancer.,” *Science (80-.).*, vol. 344, no. 6184, pp. 641–645, 2014.

[23] E. Tran *et al.*, “T-Cell Transfer Therapy Targeting Mutant KRAS in Cancer,” *N Engl J Med*, vol. 375, no. 23, pp. 2255–2262, 2016.

[24] S. A. Rosenberg, “Raising the Bar : The Curative Potential of Human Cancer Immunotherapy,” *Sci. Transl. Med.*, vol. 4, no. 127, pp. 1–6, 2012.

[25] B. Savoldo *et al.*, “CD28 costimulation improves expansion and persistence of chimeric antigen receptor– modified T cells in lymphoma patients,” *J. Clin. Invest.*, vol. 121, no. 5, pp. 1822–1826, 2011.

[26] O. U. Kawalekar *et al.*, “Distinct Signaling of Coreceptors Regulates Specific Metabolism Pathways and Impacts Memory Development in CAR T Cells,” *Immunity*, vol. 44, no. 2, pp. 380–390, 2016.

[27] R. A. Morgan *et al.*, “Cancer regression in patients after transfer of genetically engineered lymphocytes.,” *Science*, vol. 314, no. 5796, pp. 126–129, 2006.

[28] M. Kalos *et al.*, “T cells with chimeric antigen receptors have potent antitumor effects and can establish memory in patients with advanced leukemia.,” *Sci. Transl. Med.*, vol. 3, no. 95, pp. 1–11, 2011.

[29] J. N. Kochenderfer *et al.*, “B-cell depletion and remissions of malignancy along with cytokine-associated toxicity in a clinical trial of anti-CD19 chimeric-antigen-receptor-transduced T cells,” *Blood*, vol. 119, no. 12, pp. 2709–2720, 2012.

[30] C. E. Rudd, A. Taylor, and H. Schneider, “CD28 and CTLA-4 coreceptor expression and signal transduction,” *Immunol. Rev.*, vol. 229, no. 1, pp. 12–26, 2009.

[31] D. M. Pardoll, “The blockade of immune checkpoints in cancer immunotherapy.,” *Nat. Rev. Cancer*, vol. 12, no. 4, pp. 252–64, 2012.

[32] F. S. Hodi *et al.*, “Improved Survival with Ipilimumab in Patients with Metastatic Melanoma,” *N Engl J Med*, vol. 363, no. 8, pp. 711–723, 2010.

[33] S. Topalian *et al.*, “Safety, Activity, and Immune Correlates of Anti-PD-1 Antibody in Cancer,” *N. Engl. J. Med.*, vol. 366, no. 26, pp. 2443–2454, 2012.

[34] F. S. Hodi *et al.*, “Combined nivolumab and ipilimumab versus ipilimumab alone in patients with advanced melanoma: 2-year overall survival outcomes in a multicentre, randomised, controlled, phase 2 trial,” *Lancet. Oncol.*, vol. 17, no. 11, pp. 1558–1568, 2016.

[35] S. Mocellin and D. Nitti, “CTLA-4 blockade and the renaissance of cancer immunotherapy,” *Biochim. Biophys. Acta - Rev. Cancer*, vol. 1836, no. 2, pp. 187–196, 2013.

[36] S. Topalian, S. Hodi, J. Brahmer, and S. et al. Gettiner, “Safety, Activity, and Immune Correlates of Anti–PD-1 Antibody in Cancer,” *N. Engl. J. Med.*, vol. 366, no. 26, pp. 339–354, 2012.

[37] J. R. Brahmer *et al.*, “Safety and activity of anti-PD-L1 antibody in patients with advanced cancer.,” *N. Engl. J. Med.*, vol. 366, no. 26, pp. 2455–65, 2012.

[38] P. Armand, “Review Article Immune checkpoint blockade in hematologic malignancies,” *Blood*, vol. 125, no. 22, pp. 3393–3401, 2015.

[39] R. E. Billingham, L. Brent, P. B. Medawar, and E. . Sparrow, “Quantitative studies on tissue transplantation immunity. II. The origin, strength and duration of actively and adoptively aquired immunity,” *Proc. R. Soc. B*, vol. 143, no. 910, pp. 58–80, 1954.

[40] Z. Dembić *et al.*, “Transfer of specificity by murine α and β T-cell receptor genes,” *Nature*, vol. 320, no. 6059, pp. 232–238, 1986.

[41] T. M. Clay, M. C. Custer, J. Sachs, P. Hwu, S. a Rosenberg, and M. I. Nishimura, "Efficient transfer of a tumor antigen-reactive TCR to human peripheral blood lymphocytes confers anti-tumor reactivity.," *J. Immunol.*, vol. 163, no. 1, pp. 507–513, 1999.

[42] H. W. Kessels, M. C. Wolkers, M. D. van den Boom, M. a van der Valk, and T. N. Schumacher, "Immunotherapy through TCR gene transfer.," *Nat. Immunol.*, vol. 2, no. 10, pp. 957–961, 2001.

[43] C. Linnemann, T. N. Schumacher, and G. M. Bendle, "T-cell receptor gene therapy: critical parameters for clinical success," *J Invest Dermatol*, vol. 131, no. 9, pp. 1806–1816, 2011.

[44] P. A. van der Merwe and O. Dushek, "Mechanisms for T cell receptor triggering.," *Nat. Rev. Immunol.*, vol. 11, no. 1, pp. 47–55, 2011.

[45] J. Lin, J. Lai, M. Biel, Y. Xu, and L. Chen, "Immunosuppressive Microenvironment in Head and Neck Cancer, Contemporary Issues in Head and Neck Cancer Management," *InTech*, vol. DOI: 10.57, 2015.

[46] K. I. Hanada, Q. J. Wang, T. Inozume, and J. C. Yang, "Molecular identification of an MHC-independent ligand recognized by a human α/β T-cell receptor," *Blood*, vol. 117, no. 18, pp. 4816–4825, 2011.

[47] J. E. Thaxton and Z. Li, "To affinity and beyond: Harnessing the T cell receptor for cancer immunotherapy," *Hum. Vaccines Immunother.*, vol. 10, no. 11, pp. 3313–3321, 2014.

[48] W. Rojas-Zuleta and E. Sanchez, "IL-9: Function, Sources, and Detection," *Methods Mol. Biol.*, vol. 1585, pp. 21–35, 2017.

[49] J. Zhu and W. E. Paul, "CD4 T cells : fates , functions , and faults," *Blood*, vol. 112, no. 5, pp. 1557–1569, 2008.

[50] D. K. Shah and J. C. Zuniga-Pflucker, "An Overview of the Intrathymic Intricacies of T Cell Development," *J. Immunol.*, vol. 192, no. 9, pp. 4017–4023, 2014.

[51] P. Delves, S. Martin, D. Burton, and I. Roitt, “Roitt´s Essential Immunology,” *Wiley-Blackwell*, vol. 12th Editi, pp. 84–95, 2011.

[52] L. A. Johnson *et al.*, “Gene therapy with human and mouse T-cell receptors mediates cancer regression and targets normal tissues expressing cognate antigen,” *Blood*, vol. 114, no. 3, pp. 535–546, 2009.

[53] M. R. Parkhurst *et al.*, “T cells targeting carcinoembryonic antigen can mediate regression of metastatic colorectal cancer but induce severe transient colitis.,” *Mol. Ther.*, vol. 19, no. 3, pp. 620–626, 2011.

[54] R. A. Morgan *et al.*, “Cancer regression and neurologic toxicity following anti-MAGE-A3 TCR gene therapy,” *J. Immunother.*, vol. 36, no. 2, pp. 133–151, 2013.

[55] G. P. Linette *et al.*, “Cardiovascular toxicity and titin cross-reactivity of affinity-enhanced T cells in myeloma and melanoma,” *Blood*, vol. 122, no. 6, pp. 863–872, 2013.

[56] J. H. van den Berg *et al.*, “Case Report of a Fatal Serious Adverse Event Upon Administration of T Cells Transduced With a MART-1-specific T-cell Receptor,” *Mol. Ther.*, vol. 23, no. 9, pp. 1541–1550, 2015.

[57] C. Bonini and A. Mondino, “Adoptive T-cell therapy for cancer: The era of engineered T cells,” *Eur. J. Immunol.*, vol. 45, no. 9, pp. 2457–2469, 2015.

[58] P. F. Robbins *et al.*, “Tumor regression in patients with metastatic synovial cell sarcoma and melanoma using genetically engineered lymphocytes reactive with NY-ESO-1,” *J. Clin. Oncol.*, vol. 29, no. 7, pp. 917–924, 2011.

[59] O. J. F. and W. J. S. Hassane M. Zarour, Albert DeLeo, “Categories of Tumor Antigens,” *Holland-Frei Cancer Med.*, vol. 6th editio, 2003.

[60] C. N. Baxevanis, P. A. Sotiropoulou, N. N. Sotiriadou, and M. Papamichail, “Immunobiology of HER-2/neu oncoprotein and its potential application in cancer immunotherapy,” *Cancer Immunol. Immunother.*, vol. 53, no. 3, pp. 166–175, 2004.

[61] J. Momand, D. Jung, S. Wilczynski, and J. Niland, “The MDM2 gene amplification database,” *Nucleic Acids Res.*, vol. 26, no. 15, pp. 3453–3459, 1998.

[62] C. De Smet *et al.*, “Genes coding for melanoma antigens recognised by cytolytic T lymphocytes,” *Eye (Lond).*, vol. 11, no. 2, pp. 243–248, 1997.

[63] M. F. Gjerstorff, M. P. Hl, K. E. Olsen, and H. J. Ditzel, “Analysis of GAGE, NY-ESO-1 and SP17 cancer/testis antigen expression in early stage non-small cell lung carcinoma,” *BMC Cancer*, vol. 13, no. 466, pp. 1–6, 2013.

[64] M. Aris *et al.*, “MART-1- and gp100-expressing and -non-expressing melanoma cells are equally proliferative in tumors and clonogenic in vitro.,” *J. Invest. Dermatol.*, vol. 132, no. 2, pp. 365–74, 2012.

[65] M. Theobald, J. Biggs, D. Dittmer, a J. Levine, and L. a Sherman, “Targeting p53 as a general tumor antigen.,” *Proc. Natl. Acad. Sci. U. S. A.*, vol. 92, no. 26, pp. 11993–11997, 1995.

[66] et al. H. Davies, G.R. Bignell, C. Cox, P. Stephens, S. Edkins, S. Clegg, “Mutations of the BRAF gene in human cancer,” *Nature*, vol. 417, pp. 949–954, 2002.

[67] A. J. Smith and L. A. Smith, “Viral Carcinogenesis,” *Prog. Mol. Biol. Transl. Sci.*, vol. 144, pp. 121–168, 2016.

[68] I. Kaplan, M. Bulut, A. Atli, M. Güneş, M. C. Kaya, and L. Çolpan, “Serum levels of carcinoembryonic antigen (CEA) in patients with bipolar disorder,” *Acta Neuropsychiatr.*, vol. 27, no. 3, pp. 177–181, 2015.

[69] S. Cascio, A. M. Farkas, R. P. Hughey, and O. J. Finn, “Altered glycosylation of MUC1 influences its association with CIN85: the role of this novel complex in cancer cell invasion and migration.,” *Oncotarget*, vol. 4, no. 10, pp. 1686–1697, 2013.

[70] J. T. Jacobsen, E. Lunde, V. Sundvold-Gjerstad, L. a Munthe, and B. Bogen, “The cellular mechanism by which complementary Id+ and anti-Id antibodies communicate: T cells integrated into idiotypic regulation.,” *Immunol. Cell Biol.*, vol. 88, no. 5, pp. 515–522, 2010.

[71] N. Vigneron, V. Stroobant, B. J. van den Eynde, and P. van der Bruggen, “Database of T cell-defined human tumor antigens: The 2013 update,” *Cancer Immun.*, vol. 13, no. 3, pp. 1–6, 2013.

[72] Y.-C. Lu and P. F. Robbins, “Cancer immunotherapy targeting neoantigens,” *Semin. Immunol.*, vol. 28, no. 1, pp. 22–27, 2016.

[73] R. Somasundaram *et al.*, “Human leukocyte antigen-A2-restricted CTL responses to mutated BRAF peptides in melanoma patients,” *Cancer Res.*, vol. 66, no. 6, pp. 3287–3293, 2006.

[74] Y. Shono *et al.*, “Specific T-cell immunity against Ki-ras peptides in patients with pancreatic and colorectal cancers.,” *Br. J. Cancer*, vol. 88, no. 4, pp. 530–6, 2003.

[75] Y. Ichiki *et al.*, “Simultaneous cellular and humoral immune response against mutated p53 in a patient with lung cancer,” *J. Immunol.*, vol. 172, no. 8, pp. 4844–4850, 2004.

[76] K. T. Hogan *et al.*, “The Peptide Recognized by HLA-A68.2-restricted, Squamous Cell Carcinoma of the Lung-specific Cytotoxic T Lymphocytes Is Derived from a Mutated Elongation Factor 2 Gene,” *Cancer Res.*, vol. 58, pp. 5144–5150, 1998.

[77] E. Strønen *et al.*, “Targeting of cancer neoantigens with donor-derived T cell receptor repertoires.,” *Science (80-.).*, vol. 352, no. 6291, pp. 1337–1341, 2016.

[78] Y.-C. Lu *et al.*, “Efficient identification of mutated cancer antigens recognized by T cells associated with durable tumor regressions,” *Clin. Cancer Res.*, vol. 20, no. 13, pp. 3401–3410, 2014.

[79] P. F. Robbins *et al.*, “Mining Exomic Sequencing Data to Identify Mutaded Antigens Recognized by Adoptively Transferred Tumor-reactive cells,” *Nat. Med.*, vol. 19, no. 6, pp. 747–752, 2013.

[80] C. A. Klebanoff *et al.*, “Central memory self/tumor-reactive CD8+ T cells confer superior antitumor immunity compared with effector memory T cells.,” *Proc. Natl. Acad. Sci. U. S. A.*, vol. 102, no. 27, pp. 9571–9576, 2005.

[81] C. Berger *et al.*, “Adoptive transfer of effector CD8+ T cells derived from central memory cells establishes persistent T cell memory in primates,” *J. Clin. Invest.*, vol. 118, no. 1, pp. 294–305, 2008.

[82] L. Gattinoni *et al.*, “Acquisition of full effector function in vitro paradoxically impairs the in vivo antitumor efficacy of adoptively transferred CD8+ T cells,” *J. Clin. Invest.*, vol. 115, no. 6, pp. 1616–1626, 2005.

[83] S. A. Rosenberg *et al.*, “Durable complete responses in heavily pretreated patients with metastatic melanoma using T-cell transfer immunotherapy,” *Clin. Cancer Res.*, vol. 17, no. 13, pp. 4550–4557, 2011.

[84] N. Labrecque, L. S. Whitfield, C. Benoist, and D. Mathis, “How Much TCR Does a T Cell Need?,” *Immunity*, vol. 15, pp. 71–82, 2001.

[85] M. de Witte *et al.*, “Requirements for Effective Antitumor Responses of TCR Transduced T Cells,” *J Immunol Ref.*, vol. 181, pp. 5128–5136, 2008.

[86] T. M. Schmitt, G. B. Ragnarsson, and P. D. Greenberg, “T cell receptor gene therapy for cancer.,” *Hum. Gene Ther.*, vol. 20, pp. 1240–1248, 2009.

[87] A. Nelson, E. Dhimolea, and J. Reichert, “Development trends for human monoclonal antibody therapeutics,” *Nat. Rev. Drug Discov.*, vol. 9, no. 10, pp. 767–774, 2010.

[88] J. K. H. Liu, “The history of monoclonal antibody development - Progress, remaining challenges and future innovations,” *Ann. Med. Surg.*, vol. 3, no. 4, pp. 113–116, 2014.

[89] M. K. Robinson, L. M. Weiner, and G. P. Adams, “Improving monoclonal antibodies for cancer therapy,” *Drug Dev. Res.*, vol. 61, no. 3, pp. 172–187, 2004.

[90] A. M. Scott, J. D. Wolchok, and L. J. Old, “Antibody therapy of cancer,” *Nat. Rev.*, vol. 12, pp. 278–287, 2012.

[91] H. Neves and H. F. Kwok, “Recent advances in the field of anti-cancer immunotherapy,” *BBA Clin.*, vol. 3, pp. 280–288, 2015.

[92] C. Engblom, C. Pfirschke, and M. J. Pittet, “The role of myeloid cells in cancer therapies.,” *Nat. Rev. Cancer*, vol. 16, no. 7, pp. 447–462, 2016.

[93] S. Spranger and T. Gajewski, “Rational combinations of immunotherapeutics that target discrete pathways,” *J. Immunother. Cancer*, vol. 1, no. 1, p. 16, 2013.

[94] A. Werner *et al.*, “Reconstitution of T cell proliferation under arginine limitation: Activated human T cells take up citrulline via L-Type amino acid transporter 1 and use it to regenerate arginine after induction of argininosuccinate synthase expression,” *Front. Immunol.*, vol. 8, no. JUL, 2017.

[95] A. Mazzoni *et al.*, “Myeloid Suppressor Lines Inhibit T Cell Responses by an NO-Dependent Mechanism,” *J. Immunol.*, vol. 168, no. 2, pp. 689–695, 2002.

[96] A. D. Fesnak, C. H. June, and B. L. Levine, “Engineered T cells: the promise and challenges of cancer immunotherapy.,” *Nat. Rev. Cancer*, vol. 16, no. 9, pp. 566–581, 2016.

[97] D. R. Leach, M. F. Krummel, and J. P. Allison, “Enhancement of antitumor immunity by CTLA-4 blockade.,” *Science (80-.).*, vol. 271, no. 5256, pp. 1734–1736, 1996.

[98] Y. Dong, Q. Sun, and X. Zhang, “PD-1 and its ligands are important immune checkpoints in cancer,” *Oncotarget*, vol. 8, no. 2, pp. 2171–2186, 2017.

[99] L. Francisco, P. Sage, and A. Sharpe, “PD-1 Pathway in Tolerance and Autoimmunity,” *Immunol. Rev.*, vol. 236, pp. 219–242, 2010.

[100] K. Ohaegbulam, A. Assal, E. Lazar-Molnar, Y. Yao, and X. Zang, “Human cancer immunotherapy with antibodies to the PD-1 and PD-L1 pathway,” *Trends Mol. Med.*, vol. 21, no. 1, pp. 24–33, 2015.

[101] J.-M. Chauvin *et al.*, “TIGIT and PD-1 impair tumor antigen – specific CD8 + T cells in melanoma patients,” *J. Clin. Invest.*, vol. 125, no. 5, pp. 2046–2058, 2015.

[102] C. Robert *et al.*, “Anti-programmed-death-receptor-1 treatment with pembrolizumab in ipilimumab-refractory advanced melanoma: A randomised dose-comparison cohort of a phase 1 trial,” *Lancet*, vol. 384, no. 9948, pp. 1109–1117, 2014.

[103] S. Jones, A. Roe, L. Donehower, and A. Bradley, “Rescue of embryonic lethality in Mdm2-deficient mice by absence of p53,” *Nature*, vol. 378, no. 6553, pp. 206–208, 1995.

[104] J. Momand, H.-H. Wu, and G. Dasgupta, “MDM2 — master regulator of the p53 tumor suppressor protein,” *Gene*, vol. 242, no. 1, pp. 15–29, 2000.

[105] R. Pochampally, B. Fodera, L. Chen, W. Shao, E. a Levine, and J. Chen, “A 60 kd MDM2 isoform is produced by caspase cleavage in non-apoptotic tumor cells,” *Oncogene*, vol. 17, no. 20, pp. 2629–36, 1998.

[106] M. E. Perry, “The regulation of the p53-mediated stress response by MDM2 and MDM4.,” *Cold Spring Harb. Perspect. Biol.*, vol. 2, no. 1, pp. 1–12, 2010.

[107] B. T. Dye and B. A. Schulman, “Structural mechanisms underlying posttranslational modification by ubiquitin-like proteins.,” *Annu. Rev. Biophys. Biomol. Struct.*, vol. 36, pp. 131–150, 2007.

[108] J. S. Thrower, L. Hoffman, M. Rechsteiner, and C. M. Pickart, “Recognition of the polyubiquitin proteolytic signal.,” *EMBO J.*, vol. 19, no. 1, pp. 94–102, 2000.

[109] L. Hicke and R. Dunn, “Regulation of membrane protein transport by ubiquitin and ubiquitin-binding proteins.,” *Annu. Rev. Cell Dev. Biol.*, vol. 19, pp. 141–172, 2003.

[110] L. Hicke, “Protein Regulation By Monoubiquitin,” *Nat. Rev. Mol. Cell Biol.*, vol. 2, pp. 195–201, 2001.

[111] R. J. Deshaies and C. A. Joazeiro, “RING domain E3 ubiquitin ligases,” *Annu Rev Biochem*, vol. 78, pp. 399–434, 2009.

[112] K. H. Vousden and C. Prives, “Blinded by the Light: The Growing Complexity of p53,” *Cell*, vol. 137, no. 3, pp. 413–431, 2009.

[113] C. A. Brady and L. D. Attardi, “p53 at a glance,” *J. Cell Sci.*, vol. 123, no. 15, pp. 2527–2532, 2010.

[114] A. O’Brate and P. Giannakakou, “The importance of p53 location: Nuclear or cytoplasmic zip code?,” *Drug Resist. Updat.*, vol. 6, no. 6, pp. 313–322, 2003.

[115] S. Sane and K. Rezvani, “Essential Roles of E3 Ubiquitin Ligases in p53 Regulation,” *Int. J. Mol. Sci.*, vol. 18, no. 428, pp. 1–20, 2017.

[116] L. D. Mayo and D. B. Donner, “A phosphatidylinositol 3-kinase/Akt pathway promotes translocation of Mdm2 from the cytoplasm to the nucleus,” *Proc. Natl. Acad. Sci.*, vol. 98, no. 20, pp. 11598–11603, 2001.

[117] Y. Ogawara *et al.*, “Akt enhances Mdm2-mediated ubiquitination and degradation of p53,” *J. Biol. Chem.*, vol. 277, no. 24, pp. 21843–21850, 2002.

[118] S. Lain and D. Lane, “Improving cancer therapy by non-genotoxic activation of p53,” *Eur. J. Cancer*, vol. 39, no. 8, pp. 1053–1060, 2003.

[119] J. Piette, H. Neel, and V. Marechal, “Mdm2: keeping p53 under control,” *Oncogene*, vol. 15, no. 9, pp. 1001–1010, 1997.

[120] X. Lu, O. Ma, T. A. Nguyen, S. N. Jones, M. Oren, and L. A. Donehower, “The Wip1 Phosphatase Acts as a Gatekeeper in the p53-Mdm2 Autoregulatory Loop,” *Cancer Cell*, vol. 12, no. 4, pp. 342–354, 2007.

[121] M. Li, C. Brooks, F. Wu-Baer, D. Chen, R. Baer, and W. Gu, “Mono- Versus Polyubiquitination: Differential Control of p53 fate by MDM2,” *Science (80-.).*, vol. 302, no. 5652, pp. 1972–1975, 2003.

[122] E. Rayburn, R. Zhang, J. He, and H. Wang, “MDM2 and human malignancies: expression, clinical pathology, prognostic markers, and implications for chemotherapy.,” *Curr. Cancer Drug Targets*, vol. 5, pp. 27–41, 2005.

[123] Y. Enokida *et al.*, “Prognostic potential of the MDM2 309T>G polymorphism in stage I lung adenocarcinoma,” *Cancer Med.*, vol. 5, no. 8, pp. 1791–1801, 2016.

[124] C. Cordon-Cardo *et al.*, “Molecular Abnormalities of mdm2 and p53 Genes in Adult Soft Tissue Sarcomas,” *Cancer Res.*, vol. 54, no. 3, pp. 794–799, 1994.

[125] A. Bouska and C. M. Eischen, “Murine double minute 2: p53-independent roads lead to genome instability or death,” *Trends Biochem. Sci.*, vol. 34, no. 6, pp. 279–286, 2009.

[126] M. Shaikh *et al.*, “Emerging role of MDM2 as target for anti-cancer therapy: A review,” *Ann. Clin. Lab. Sci.*, vol. 46, no. 6, pp. 627–634, 2016.

[127] L. T. Vassilev *et al.*, “In Vivo Activation of the p53 Pathway by Small-MoleculeAntagonists of MDM2.,” *Science (80-.).*, vol. 303, no. 5659, pp. 844–848, 2004.

[128] A. Burgess, K. M. Chia, S. Haupt, D. Thomas, Y. Haupt, and E. Lim, “Clinical Overview of MDM2/X-Targeted Therapies,” *Front. Oncol.*, vol. 6, pp. 1–7, 2016.

[129] A. G. Herman *et al.*, “Discovery of Mdm2-MdmX E3 ligase inhibitors using a cell-based ubiquitination assay,” *Cancer Discov.*, vol. 1, no. 4, pp. 312–325, 2011.

[130] M. Wade, Y. V. Wang, and G. M. Wahl, “The p53 orchestra: Mdm2 and Mdmx set the tone,” *Trends Cell Biol.*, vol. 20, no. 5, pp. 299–309, 2010.

[131] M. Pellegrino *et al.*, “Targeting the MDM2/MDM4 interaction interface as a promising approach for p53 reactivation therapy,” *Cancer Res.*, vol. 75, no. 21, pp. 4560–4572, 2015.

[132] N. Issaeva *et al.*, “Small molecule RITA binds to p53, blocks p53-HDM-2 interaction and activates p53 function in tumors.,” *Nat. Med.*, vol. 10, no. 12, pp. 1321–1328, 2004.

[133] C. Y. Zhao, V. V. Grinkevich, F. Nikulenkov, W. Bao, and G. Selivanova, “Rescue of the apoptotic-inducing function of mutant p53 by small molecule RITA,” *Cell Cycle*, vol. 9, no. 9, pp. 1847–1855, 2010.

[134] M. N. Saha, H. Jiang, A. Mukai, and H. Chang, “RITA Inhibits Multiple Myeloma Cell Growth through Induction of p53-Mediated Caspase-Dependent Apoptosis and Synergistically Enhances Nutlin-Induced Cytotoxic Responses,” *Mol. Cancer Ther.*, vol. 9, no. 11, pp. 3041–3051, 2010.

[135] T. Stanislawski *et al.*, “Circumventing tolerance to a human MDM2-derived tumor antigen by TCR gene transfer.,” *Nat. Immunol.*, vol. 2, no. 10, pp. 962–970, 2001.

[136] H. G. Rammensee, K. Falk, and O. Rötzschke, “Peptides naturally presented by MHC class I molecules.,” *Annu. Rev. Immunol.*, vol. 11, pp. 213–244, 1993.

[137] C. J. Cohen, Y. Zhao, Z. Zheng, S. A. Rosenberg, and R. A. Morgan, “Enhanced antitumor activity of murine-human hybrid T-cell receptor (TCR) in human lymphocytes is associated with improved pairing and TCR/CD3 stability,” *Cancer Res.*, vol. 66, no. 17, pp. 8878–8886, 2006.

[138] K. B. J. Scholten *et al.*, “Codon modification of T cell receptors allows enhanced functional expression in transgenic human T cells,” *Clin. Immunol.*, vol. 119, no. 2, pp. 135–145, 2006.

[139] J. Kuball *et al.*, “Facilitating matched pairing and expression of TCR chains introduced into human T cells,” *Blood*, vol. 109, no. 6, pp. 2331–2338, 2007.

[140] M. Mandalà and D. Massi, “Immunotolerance as a Mechanism of Resistance to Targeted Therapies in Melanoma,” *Handb. Exp. Pharmacol.*, vol. 10.1007/16, pp. 1–15, 2017.

[141] K. Loo and A. I. Daud, “Inhibitors of Cytotoxic T Lymphocyte Antigen 4 and Programmed Death 1/Programmed Death 1 Ligand for Metastatic Melanoma, Dual Versus Monotherapy—Summary of Advances and Future Directions for Studying These Drugs,” *Cancer J.*, vol. 23, no. 1, pp. 3–9, 2017.

[142] D. C. Deniger *et al.*, “A Pilot Trial of the Combination of Vemurafenib with Adoptive Cell Therapy in Patients with Metastatic Melanoma,” *Clin. Cancer Res.*, vol. 23, no. 2, pp. 351–362, 2017.

[143] E. K. Moon *et al.*, “Blockade of programmed death 1 augments the ability of human T cells engineered to target NY-ESO-1 to control tumor growth after adoptive transfer,” *Clin. Cancer Res.*, vol. 22, no. 2, pp. 436–447, 2016.

[144] M. F. Sanmamed *et al.*, “Nivolumab and urelumab enhance antitumor activity of human T lymphocytes engrafted in Rag2-/-IL2Rgamma null immunodeficient mice,” *Cancer Res.*, vol. 75, no. 17, pp. 3466–3478, 2015.

[145] M. E. M. Weijtens, R. A. Willemsen, E. H. Hart, and R. L. H. Bolhuis, “A retroviral vector system ‘ STITCH ’ in combination with an optimized single chain antibody chimeric receptor gene structure allows efficient gene transduction and expression in human T lymphocytes,” *Gene Ther.*, vol. 5, no. 9, pp. 1195–1203, 1998.

[146] Y. Soneoka, P. M. Cannon, E. E. Ramsdale, J. C. Griffiths, S. M. Kingsman, and A. J. Kingsman, “A transient three plasmid expression system for the production of high titer retroviral vectors,” *Nucleic Acids Res.*, vol. 23, no. 4, pp. 628–633, 1995.

[147] E. M. Shevach, J. D. Stobo, and I. Green, “Immunoglobulin and ϑ -Bearing Murine Leukemias and Lymphomas,” *J. Immunol.*, vol. 108, no. 5, pp. 1146–1151, 1972.

[148] H. G. Drexler and Y. Matsuo, “Malignant hematopoietic cell lines: in vitro models for the study of multiple myeloma and plasma cell leukemia.,” *Leuk. Res.*, vol. 24, no. 8, pp. 681–703, 2000.

[149] K. Nilsson, H. Bennich, S. G. O. Johansson, and J. Pontén, “Established immunoglobulin producing myeloma (IgE) and Lymphoblastoid (IgG) cell lines from an IgE myeloma patient,” *Clin. Exp. Immunol.*, vol. 7, no. 4, pp. 477–489, 1970.

[150] Gazdar, A, Oie, I. R. Kirsch, and F. Hollis, “Establishment and Characterization of a Human Plasma Cell Myeloma Culture Having a Rearranged Cellular myc Proto-oncogene,” *Blood*, vol. 67, no. 6, pp. 1542–1549, 1986.

[151] J. L. Fahey, D. N. Buell, and H. C. Sox, “Proliferation and differentiation of lymphoid cells: studies with human lymphoid cell lines and immunoglobulin synthesis.,” *Ann. N. Y. Acad. Sci.*, vol. 190, pp. 221–34, 1971.

[152] L. Pegoraro, F. Malavasi, B. L. Pegoraro, M. Boccadoro, and G. C. Avanzi, “The Human Cell line Line LP-1: A Versatile Model in Which to Study Early Plasma-Cell Differentiation and c-myc Activation,” *Blood*, vol. 73, no. 4, pp. 1020–1027, 1989.

[153] N. E. Sanjana, L. Cong, Y. Zhou, M. M. Cunniff, G. Feng, and F. Zhang, “A transcription activator-like effector toolbox for genome engineering,” *Nat Protoc*, vol. 7, no. 1, pp. 171–192, 2012.

[154] B. Berdien, U. Mock, D. Atanackovic, and B. Fehse, “TALEN-mediated editing of endogenous T-cell receptors facilitates efficient reprogramming of T lymphocytes by lentiviral gene transfer,” *Gene Ther.*, vol. 21, no. 6, pp. 539–548, 2014.

[155] R. H. Voss *et al.*, “Coexpression of the T-cell receptor constant α domain triggers tumor reactivity of single-chain TCR-transduced human T cells,” *Blood*, vol. 115, no. 25, pp. 5154–5163, 2010.

[156] D. Knies *et al.*, “An optimized single chain TCR scaffold relying on the assembly with the native CD3-complex prevents residual mispairing with endogenous TCRs in human T-cells.,” *Oncotarget*, vol. 7, no. 16, pp. 21199–221, 2016.

[157] S. Reuß *et al.*, “TCR-engineered T cells: A model of inducible TCR expression to dissect the interrelationship between two TCRs,” *Eur. J. Immunol.*, vol. 44, no. 1, pp. 265–274, 2014.

[158] J. H. Kim *et al.*, “High cleavage efficiency of a 2A peptide derived from porcine teschovirus-1 in human cell lines, zebrafish and mice,” *PLoS One*, vol. 6, no. 4, pp. 1–8, 2011.

[159] G. M. Bendle *et al.*, “Lethal graft-versus-host disease in mouse models of T cell receptor gene therapy.,” *Nat. Med.*, vol. 16, no. 5, p. 565–70, 1p following 570, 2010.

[160] M. J. Osborn *et al.*, “Evaluation of TCR Gene Editing Achieved by TALENs , CRISPR / Cas9 , and megaTAL Nucleases,” *YMTHE*, vol. 24, no. 3, pp. 570–581, 2016.

[161] H. Torikai *et al.*, “GENE THERAPY A foundation for universal T-cell based immunotherapy : T cells engineered to express a CD19-specific chimeric-antigen-receptor and eliminate expression of endogenous TCR,” *Blood*, vol. 119, no. 24, pp. 5697–5706, 2012.

[162] J. M. K. M. Delhove and W. Qasim, “Genome-Edited T Cell Therapies,” *Curr. stem cell reports*, vol. 3, no. 2, pp. 124–136, 2017.

[163] S. Mastaglio *et al.*, “NY-ESO-1 TCR single edited stem and central memory T cells to treat multiple myeloma without graft-versus-host disease,” *Blood*, vol. 130, no. 5, pp. 606–619, 2017.

[164] E. Provasi *et al.*, “Editing T cell specificity towards leukemia by zinc-finger nucleases and lentiviral gene transfer,” *Nat. Med.*, vol. 18, no. 5, pp. 807–815, 2012.

[165] J. Eyquem *et al.*, “Targeting a CAR to the TRAC locus with CRISPR/Cas9 enhances tumour rejection,” *Nature*, vol. 543, no. 7643, pp. 113–117, 2017.

[166] R.-H. Voss *et al.*, “Coexpression of the T-cell receptor constant α domain triggers tumor reactivity of single-chain TCR-transduced human T cells,” *Blood*, vol. 115, no. 25, pp. 5154–5163, 2010.

[167] C. R. Robinson and R. T. Sauer, “Optimizing the stability of single-chain proteins by linker length and composition mutagenesis,” *Proc. Natl. Acad. Sci. U. S. A.*, vol. 95, no. May, pp. 5929–5934, 1998.

[168] R.-H. Voss *et al.*, “Redirection of T cells by delivering a transgenic mouse-derived MDM2 tumor antigen-specific TCR and its humanized derivative is governed by the CD8 coreceptor and affects natural human TCR expression.,” *Immunol. Res.*, vol. 34, no. 1, pp. 67–87, 2006.

[169] R. D. Schreiber, L. J. Old, and M. J. Smyth, “Cancer Immunoediting: Integrating Immunity’s Roles in Cancer Suppression and Promotion,” *Science (80-.).*, vol. 331, no. 6024, pp. 1565–1570, 2011.

[170] F. Garrido, F. Ruiz-Cabello, and N. Aptsiauri, “Rejection versus escape: the tumor MHC dilemma,” *Cancer Immunol. Immunother.*, vol. 66, no. 2, pp. 259–271, 2017.

[171] Qiang Zou, Jin Jin, Hongbo Hu, Haiyan S. Li, Simona Romano, Yichuan Xiao1, Mako Nakaya, Xiaofei Zhou, Xuhong Cheng, Peirong Yang, Guillermina Lozano and S. E. U. and S.-C. S. Chengming Zhu, Stephanie S. Watowich, “USP15 stabilizes MDM2 to mediate cancer cell survival and inhibit antitumor T cell responses,” *Nat. Immunol.*, vol. 15, no. 6, pp. 562–570, 2014.

[172] M. N. Saha, H. Jiang, and H. Chang, “Molecular mechanisms of nutlin-induced apoptosis in multiple myeloma: Evidence for p53-transcription-dependent and -independent pathways,” *Cancer Biol. Ther.*, vol. 10, no. 6, pp. 567–578, 2010.

[173] A. P. Rapoport *et al.*, “NY-ESO-1 specific TCR engineered T-cells mediate sustained antigen-specific antitumor effects in myeloma,” *Nat. Med.*, vol. 21, no. 8, pp. 914–921, 2015.

[174] W. N. H. Debattama R. Sen, James Kaminski, R. Anthony Barnitz, Makoto Kurachi, Ulrike Gerdemann, Kathleen B. Yates, Hsiao-Wei Tsao, Jernej Godec,Martin W. LaFleur, Flavian D. Brown, Pierre Tonnerre, Raymond T. Chung, Damien C. Tully, Todd M. Allen, Nicole Frahm, G, "The epigenetic landscape of T cell exhaustion," *Science (80-.).*, vol. 354, no. 6316, pp. 1165–1169, 2016.

[175] E. J. Wherry *et al.*, "Molecular Signature of CD8+ T Cell Exhaustion during Chronic Viral Infection," *Immunity*, vol. 27, no. 4, pp. 670–684, 2007.

[176] D. C. and K. A. A Ray, DS Das, Y Song, P Richardson, NC Munshi, "Targeting PD1–PDL1 immune checkpoint in plasmacytoid dendritic cell interactions with T cells, natural killer cells and multiple myeloma cells," *Leukemia*, vol. 29, pp. 1441–1444, 2015.

[177] K. A. Sheppard *et al.*, "PD-1 inhibits T-cell receptor induced phosphorylation of the ZAP70/CD3zeta signalosome and downstream signaling to PKCtheta," *FEBS Lett.*, vol. 574, pp. 37–41, 2004.

[178] T. L. Stephen *et al.*, "SATB1 Expression Governs Epigenetic Repression of PD-1 in Tumor-Reactive T Cells," *Immunity*, vol. 46, no. 1, pp. 51–64, 2017.

[179] A. M. Lesokhin *et al.*, "Nivolumab in patients with relapsed or refractory hematologic malignancy: Preliminary results of a phase ib study," *J. Clin. Oncol.*, vol. 34, no. 23, pp. 2698–2704, 2016.

[180] H. Gogas, A. Polyzos, and J. Kirkwood, "Immunotherapy for advanced melanoma: Fulfilling the promise," *Cancer Treat. Rev.*, vol. 39, no. 8, pp. 879–885, 2013.

[181] C. G. D. and D. M. P. Suzanne L. Topalian, "Immune checkpoint blockade: a common denominator approach to cancer therapy," *Cancer Cell*, vol. 27, no. 4, pp. 450–461, 2015.

[182] M. E. Keir, M. J. Butte, G. J. Freeman, and A. H. Sharpe, "PD-1 and Its Ligands in Tolerance and Immunity," *Annu. Rev. Immunol.*, vol. 26, no. 1, pp. 677–704, 2008.

[183] W. H. D. Hallett, W. Jing, W. R. Drobyski, and B. D. Johnson, "Immunosuppressive Effects of Multiple Myeloma Are Overcome by PD-L1 Blockade," *Biol. Blood Marrow Transplant.*, vol. 17, no. 8, pp. 1133–1145, 2011.

[184] M. J. Butte, M. E. Keir, T. B. Phamduy, A. H. Sharpe, G. J. Freeman, and H. Sharpe, "PD-L1 interacts specifically with B7-1 to inhibit T cell proliferation," *Immunity*, vol. 27, no. 1, pp. 111–122, 2007.

[185] T. Noguchi *et al.*, "Temporally-Distinct PD-L1 Expression by Tumor and Host Cells Contributes to Immune Escape," *Cancer Immunol. Res.*, vol. 5, no. 2, pp. 1–12, 2017.

[186] S. Su *et al.*, "CRISPR-Cas9-mediated disruption of PD-1 on human T cells for adoptive cellular therapies of EBV positive gastric cancer," *Oncoimmunology*, vol. 6, no. 1, 2016.

[187] S. Su *et al.*, "CRISPR-Cas9 mediated efficient PD-1 disruption on human primary T cells from cancer patients," *Sci. Rep.*, vol. 6, pp. 1–13, 2016.

[188] J. Ren *et al.*, "A versatile system for rapid multiplex genome-edited CAR T cell generation," *Oncotarget*, 2017.

[189] H. Magen and E. Muchtar, "Elotuzumab: the first approved monoclonal antibody for multiple myeloma treatment.," *Ther. Adv. Hematol.*, vol. 7, no. 4, pp. 187–195, 2016.

[190] V. Hoyos and I. Borrello, "The immunotherapy era of myeloma: Monoclonal antibodies, vaccines, and adoptive T-cell therapies," *Blood*, vol. 128, no. 13, pp. 1679–1687, 2016.

[191] H. Tamura *et al.*, "Marrow stromal cells induce B7-H1 expression on myeloma cells, generating aggressive characteristics in multiple myeloma," *Leukemia*, vol. 27, no. 2, pp. 464–472, 2013.

[192] J. Liu *et al.*, "Plasma cells from multiple myeloma patients express B7-H1 (PD-L1) and increase expression after stimulation with IFN-γ and TLR ligands via a MyD88-, TRAF6-, and MEK-dependent pathway," *Blood*, vol. 110, no. 1, pp. 296–304, 2007.

[193] A. D'Incecco *et al.*, "PD-1 and PD-L1 expression in molecularly selected non-small-cell lung cancer patients.," *Br. J. Cancer*, vol. 112, no. 1, pp. 95–102, 2015.

[194] D. Polsky *et al.*, "HDM2 Protein Overexpression , but not Gene Amplification , is Related to Tumorigenesis of Cutaneous Melanoma," *Cancer Res.*, vol. 61, pp. 7642–7646, 2001.

[195] V. Audrito *et al.*, “PD-L1 up-regulation in melanoma increases disease aggressiveness and is mediated through miR-17-5p,” *Oncotarget*, vol. 8, no. 9, pp. 15894–15911, 2017.

[196] J. Landsberg *et al.*, “Melanomas resist T-cell therapy through inflammation-induced reversible dedifferentiation,” *Nature*, vol. 490, no. 7420, pp. 412–416, 2012.

7 Annex

7.1 Vector maps

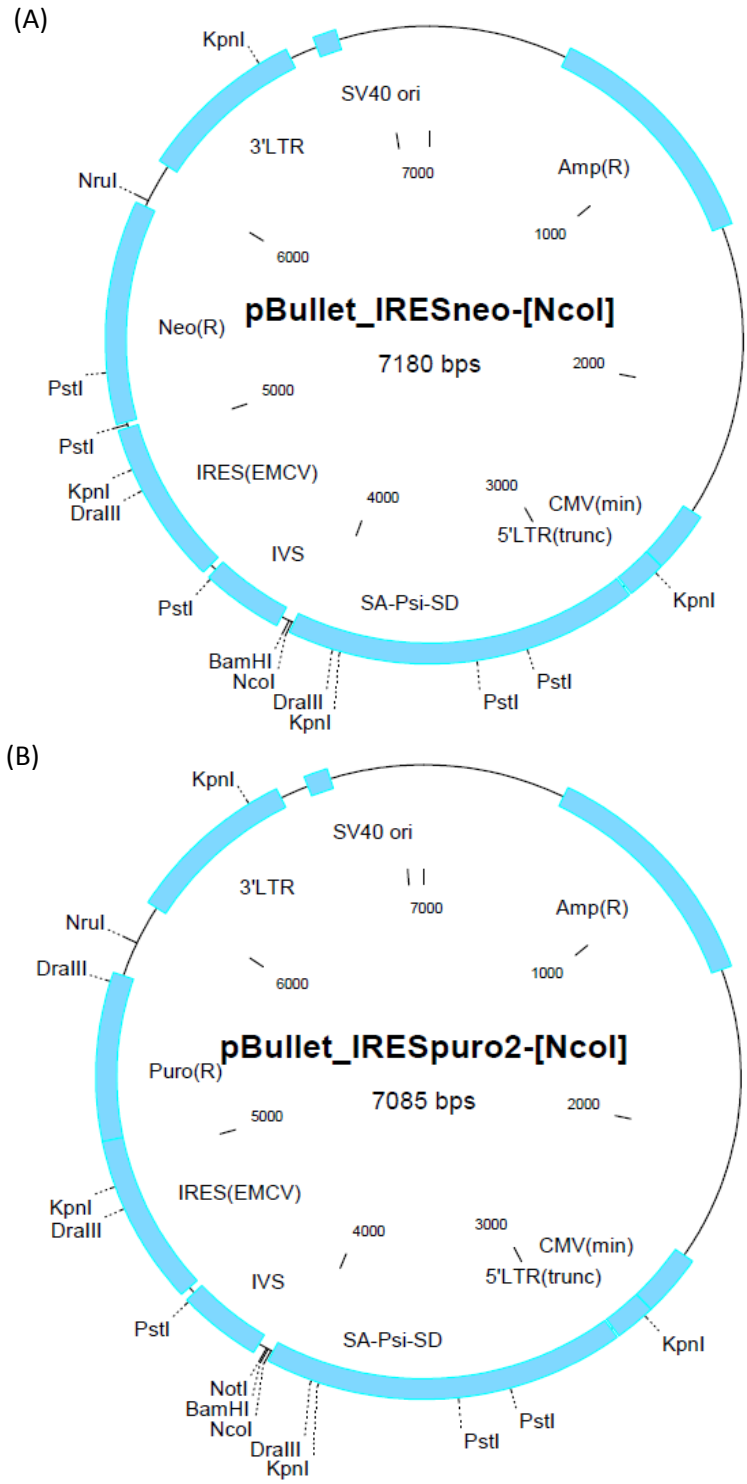

Figure 7.1 Vector maps of pBullet_IRESneo-[NcoI] and pBullet_IRESpuro2-[NcoI] plasmids. (A) The pBullet_IRESneo-[NcoI] vector was used as a plasmid-backbone for the MDM2 wt TCR β-chain. (B) The pBullet_IRESpuro2-[NcoI] vector was used as a plasmid-backbone for the MDM2 wt TCR α-chain.

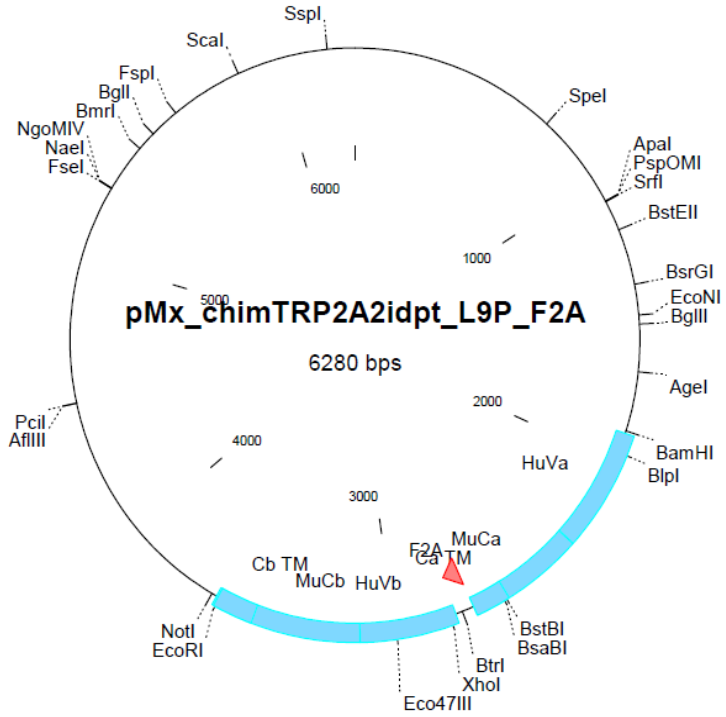

Figure 7.2 Vector map of pMx_chimTRP2A2idpt_L9P_F2A plasmid.
The pMx_chimTRP2A2idpt_L9P_F2A vector bearing another TCR was used as a plasmid-backbone for the MDM2 sc opt. TCR.

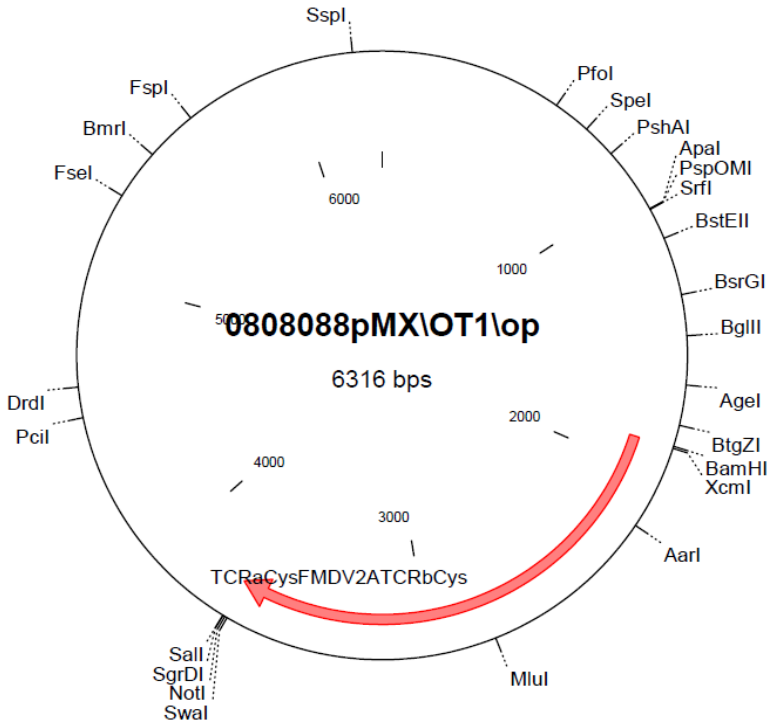

Figure 7.3 Vector map of pMx_IRESneo plasmid.
The pMx_IRESneo vector was generated by exchanging the TCRab encoding sequence (1.8kb) in the pMx_88 vector (map above) by an "IRES-Neomycin" cassette (1.5kb). For cloning purpose the full TCRab sequence could not be removed leaving a truncated TCRa sequence upstream the multiple cloning site (MCS) including NcoI, BamHI, NotI used for the subsequent cloning of the MDM2 dc opt. TCR.

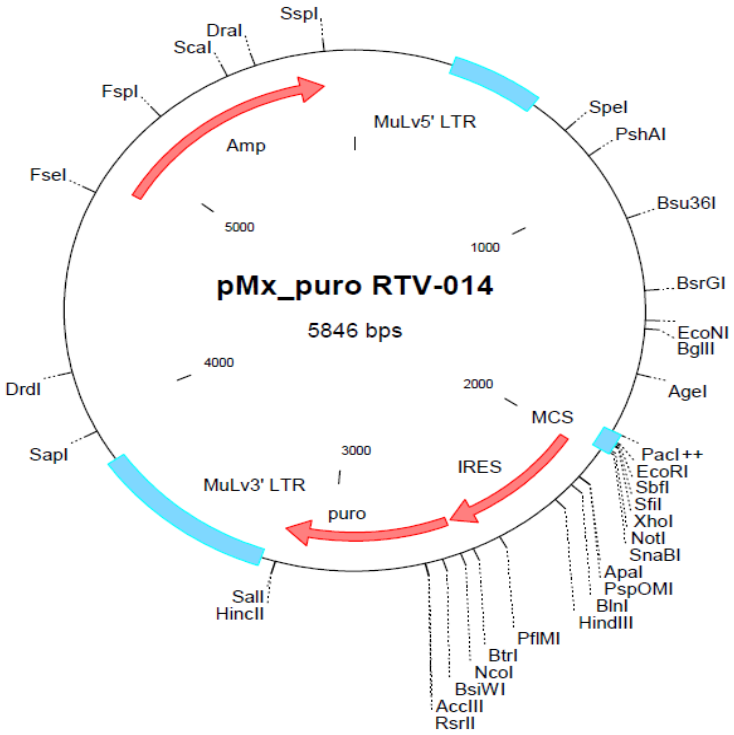

Figure 7.4 Vector map of pMx_puro RTV-014 plasmid.
The pMx_puro RTV-014 vector was used as a plasmid-backbone for the MDM2 wt TCR.

7.2 Primer

Table 7.1 Primers used for sequencing of MDM2 TCR constructs.

Primer name	Primer sequence
SE-206	5’ – TTA CAC AGT CCT GCT GAC CAC C – 3’ (22mer)
SE-221	5’ – AAA CGC ACA CCG GCC TTA TTC C – 3’ (22mer)
F-1811	5’ – GCA TCG CAG CTT GGA TAC AC – 3’ (20mer)
R-3927	5’ – GGC AGG AAC TGC TTA CCA – 3’ (18mer)
F_MDM2scP2Acys	5’ – ACC GAT CCT CAG GCT TAC AA – 3’ (20mer)
F_MDM2dcP2Acys	5’ – AGT GCC AGC AGA ACT TCA AC – 3’ (20mer)

7.3 PD-L1 expression in NCI-H929 A2.1 after 5-aza treatment

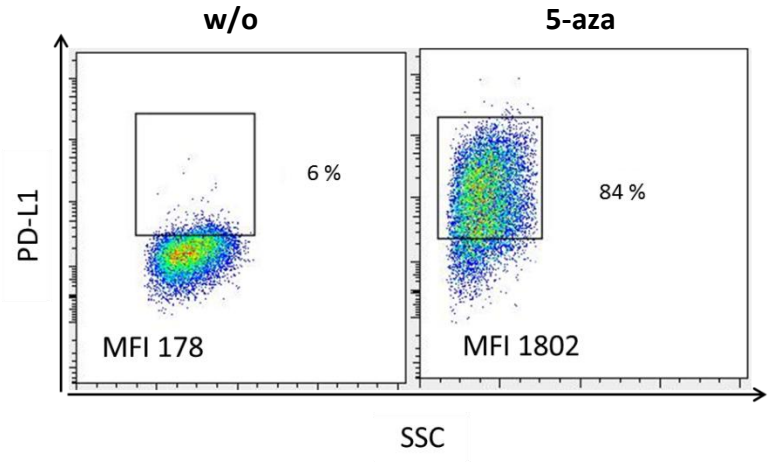

Figure 7.5 PD-L1 expression is up-regulated in NCI-H929 A2.1 after 5-aza-2'deoxy-cytidine treatment. Flow cytometry data show PD-L1 expression in NCI-H929 A2.1 untreated (w/o) and treated with demethylation reagent 5-aza-2'deoxy-cytidine (5-aza). Treated cells were cultured in the presence of 1µM 5-aza-2'deoxy-cytidine for 3d and stained together with untreated cells for PD-L1 for flow cytometry analysis. The percentage of PD-L1 positive cells as well as the MFI of the PD-L1 expression is indicated. Presented data are a representative example of PD-L1 expression out of three experiments.

Acknowledgment

Curriculum Vitae